Optimal Residential Demand Response under Dynamic Pricing in a Multi-Agent Framework

A Thesis

Submitted to the Faculty of Graduate Studies and Research

In Partial Fulfillment of the Requirements

for the Degree of

Doctor of Philosophy

in Electronic Systems Engineering

University of Regina

by

Zhanle Wang

Regina, Saskatchewan, Canada

December, 2015

UNIVERSITY OF REGINA

FACULTY OF GRADUATE STUDIES AND RESEARCH

SUPERVISORY AND EXAMINING COMMITTEE

Zhanle Wang, candidate for the degree of Doctor of Philosophy in Electronic Systems Engineering**,** has presented a thesis titled, ***Optimal Residential Demand Response under Dynamic Pricing in a Multi-Agent Framework,*** in an oral examination held on November 10, 2015. The following committee members have found the thesis acceptable in form and content, and that the candidate demonstrated satisfactory knowledge of the subject material.

External Examiner:	*Dr. Om Malik, University of Calgary
Supervisor:	Dr. Raman Paranjape, Electronic Systems Engineering
Committee Member:	Dr. Craig Gelowitz, Software Systems Engineering
Committee Member:	**Dr. Jing Tao Yao, Department of Computer Science
Committee Member:	Dr. Paul Laforge, Electronic Systems Engineering
Chair of Defense:	Dr. Hairuo Qing, Department of Geology

*Via Teleconference
**Not present at defense

ABSTRACT

Demand response (DR) is a recent effort to improve efficiency of the electricity market and the stability of the power system. A successful DR implementation relies on both appropriate policy design and enabling technology. Real-time pricing (RTP) and time of use (TOU) have been identified as two important DR policies to motivate residential customers to participate in DR programs. An efficient residential DR model should implement heterogeneous residential load forecasting, multi-criteria optimization (e.g., objectives for individual homes, utilities and aggregations of them) and intelligent distributed algorithms to evaluate the complex and large-scale power systems.

This thesis presents a multi-agent system (MAS) to evaluate optimal residential DR implementation in a distribution network, in which the main stakeholders are modeled by heterogeneous home agents (HA) and a retailer agent (RA). A heterogeneous load prediction model, a real-time electricity price model and three optimal load control models are developed to associate with the MAS. The load prediction model simulates the benchmark of individual and aggregated load profiles based on statistical information of how people use their appliances including electric vehicles (EV). Each HA has a unique load profile depending on its heterogeneous local configurations. The real-time price prediction model is defined as piecewise linear functions of power and the optimal coefficients are obtained from historical data of real-time loads and electricity prices via the norm approximation approach.

The optimal load control models are developed based on dynamic pricing of RTP and TOU. An open-loop optimal load control model under RTP (OL-LCM-RTP) is formulated into a convex programming (CP) problem to minimize electricity payment and waiting

time. A HA schedules the controllable loads based on its local information by solving the CP problem; therefore, it only requires a minimum of communication between the HA and the RA. This is greatly useful because the infrastructure for communication is still under development. In addition, the privacy of users is not sacrificed. Simulation results show that the peak-to-average power ratio (PAPR) and the standard deviation of the load profile, and electricity payments are reduced using the proposed mechanism.

A close-loop optimal load control model under RTP (CL-LCM-RTP) is developed based on the OL-LCM-RTP by further incorporating feedbacks from RA. A HA solves the CP problem to schedule the controllable loads in a round process using the global load information. The process can be quickly converged in the second round; therefore, it requires limited efforts from the communication and the coordination. It is found that this model can significantly improve the quality of the optimization based on the simulation results.

An optimal load control model under TOU (LCM-TOU) is modeled by a linear programming (LP) problem. The objective function is designed to find a trade-off among three factors: 1) the minimum electricity payment; 2) comfort levels with waiting time; and 3) to avoid peak demand rebound. We also evaluate the impacts of the participation levels of TOU programs. The simulation results show a reduced PAPR, standard deviation and the electricity payments from the HAs.

The HA, with proposed optimal control mechanisms, can be embedded into a home energy management system (EMS) to make intelligent decisions on behalf of homeowners automatically responding to DR policies. The proposed agent system can be utilized to evaluate various strategies and emerging technologies that enable DR implementation.

ACKNOWLEDGEMENTS

I sincerely acknowledge Dr. Raman Paranjape, the supervisor, for his original idea, his supervision, and his support spiritually, technically and financially. Without his help, this research truly would not have been a success.

I genuinely express my gratitude to my internal committee members: Dr. Jingtao Yao, Dr. Paul Laforge and Dr. Craig Gelowitz for the tremendous advices on my research. I am also truly grateful to Dr. Luigi Benedicenti for the advices on my study.

I am deeply grateful to Mr. Doug Wagner, Mr. Karim Naqvi and the students in my classes for great helps to enhance my teaching experiences.

I am truly grateful to Dr. Elemer Demeter, Ms. Andrea Boutin and Mr. Caleb Granat for feedbacks from the industry.

I acknowledge the SaskPower, the Faculty of Graduate Studies and Research, the Faculty of Engineering and Applied Science, and TRLabs for their research scholarship and technical support.

I am grateful and would like to express my special thanks to Mr. Zhongwei Du, Ms. Min Zhang, Mr. Diego Castro-Hernandez and Mr. Seang Cau, fellow graduate students, for their time and assistance during the research.

DEDICATIONS

To my loving family:

Ye

Carolyn and Claire

To my respected parents:

Yanzhong and Xiaoxiang

To my respected parents-in-law:

Runbao and Yuying

To my dear brother,

Yuefeng

TABLE OF CONTENTS

LIST OF TABLES

LIST OF FIGURES

NOMENCLATURES

Sets

$\mathcal{AC}$	a set of actions
$\mathcal{AG}$	a set of agents
$\mathcal{AP}$	a set of appliances in a home
$\mathcal{BAP}$	a set of background appliances
$\mathcal{CAP}$	a set of controllable appliances
$\mathcal{E}$	a set of environment characteristics
$\mathcal{GA}$	a set of generator agents
$\mathcal{HA}$	a set of home agents
$\mathcal{RA}$	a set of retailer agents
$\mathcal{RS}$	a retailer service scope set
$\mathcal{T}$	time horizon set

Variables and function

α_1, α_2	slopes in the electricity price prediction model
β_1, β_2	constants in the electricity price prediction model
λ^{ap}	dissatisfaction factor of scheduling appliance *ap*
Δt_{total}	time to charge up an EV from zero SOC
Δt^{ap}	cycle length of operating appliance *ap*
ap	an appliance
ct	constraint

$\widehat{E_B^{ap}}$	predicted electricity energy of background loads (column vector)
$\widehat{E_C^{ap}}$	predicted electricity energy of controllable loads (column vector)
L	a column vector of load
$\hat{L}$	a column vector of predicted load
l_t^{ap}	electricity load of appliance ap at time t
$\widehat{l_t^{ap}}$	predicted electricity load of ap at t
l_{TH}	load threshold in Equation 15
$occ(t)$	number of active occupants at t
P	a column vector of electricity price
p_t	electricity price at time t
$p(\cdot)$	price based on load
$pr(t \mid ap)$	probability of using an appliance $ap \in \mathcal{AP} \backslash EV$ at t.
q_{rated}^{ap}	rated power of the appliance ap
soc_0	initial SOC
t	time slot
t_0^{ap}	time of starting to operate an appliance ap
t_1^{ap}	the time when operation of the appliance must complete
w^{ap}	waiting time vector of an appliance ap

Acronyms

AEE	agent execution environment
AEP	American Electric Power
CCHT	Centre for Housing Technology
CL-LCM-RTP	closed-loop optimal load control model under RTP
CP	convex programming
CPP	critical peak pricing
DAI	distributed artificial intelligence
DER	distributed energy resources
DLC	direct load control
DR	demand response
EMCAS	electricity market complex adaptive system
EMS	energy management system
EV	electric vehicle
GA	generator agent
HA	home agent
HAN	home area network
HVAC	ventilation and air conditioning
IBR	inclining block rate
JADE	java agent development framework
LAN	local area network
LCM-TOU	open-loop optimal load control under TOU
LMP	locational margin price

LP	linear programming
MAS	multi-agent system
MINLP	mixed integer nonlinear program
OL-LCM-RTP	open-loop optimal load control model under RTP
PAPR	peak-to-average power ratio
PHEV	plug-in electric vehicles
RA	retailer agent
RPS	Renewables Portfolio Standards
RTP	real-time pricing
SOC	state of charge
TEEMA	TRlabs execution environment for mobile agents
TOU	time-of-use
VMT	vehicle miles of travelling
WMA	wholesale market agent

CHAPTER 1

INTRODUCTION

1.1 Residential Demand Response

This section is reproduce from our publication in [1] (Copyright © 2015, IEEE) and [2] (Copyright © 2013, IEEE).

Demand response (DR) is designed to reduce peak demand in response to market price and/or power availability over time [3, 4]. It provides a variety of financial and operational benefits to electricity customers, load-serving entities and grid operators [4, 5].

Power generation is always required to match the time fluctuated load and electricity cannot be stored economically. Furthermore, the dispatch of power generation units is primarily based on generation cost. Consequently, electricity generation costs are generally proportional to the amount of the load. However, this fluctuating generation cost or the wholesale electricity price due to multiple generators is mostly hidden by retailers/utilities with a flat electricity tariff for end-users. Price-based DR programs can reveal the actual electricity prices to encourage end-users to change their consumption pattern and shift electricity demand from peak-demand-periods to off-demand-periods in order to improve energy efficiency. The U.S. Department of Energy lists three types of price-based DR options: time-of-use (TOU), real-time pricing (RTP) and critical peak pricing (CPP) [5]. Another popular dynamic tariff is inclining block rate (IBR), in which the electricity price is higher when the energy consumption exceeds a certain threshold over a period of time, e.g., stepped residential rates used by BC Hydro [6].

Besides the incentive mechanisms, a successful DR implementation also relies on DR enabling technologies since it is very difficult (if not impossible) for consumers to track dynamic pricing. In a residential sector, DR enabling technologies are available in the context of a smart home. The smart home features an energy management system (EMS) that intelligently controls household loads through an association between smart meters, smart appliances, electric vehicles (EV), small home power generation units and storage facilities, etc. [2]. FIGURE 1-1 shows the diagram of a smart home [2].

Smart meters provide important information for both utilities and customers such as home load profiles and dynamic price signals. Rooftop solar panels and small wind turbines are now widely available [6]. In addition, the market of plug-in electric vehicles (PHEV) is growing fast. On one hand, this penetration tends to overwhelm the current power systems. To meet the requirement of this eco-friendly energy consumption, the current grid, especially the distribution networks need to be upgraded. On the other hand, this provides a huge volume of battery systems to store power, with the combination of DR implementation, which can reduce the energy cost for both utilities and customers. Home power generation units, storage facilities and household appliances can be connected by a home area network (HAN). A home EMS allows customers to conveniently and intelligently manage this information. The flexible demand aspect of DR applications enables time-shift electricity consumption by bringing forward or delaying the use of appliances. For instance, the EMS monitors real-time loads and price signals, and optimizes the electricity consumption by switching on/off appliances without influencing customer's comfort. In addition, the EMS can observe the home power generation and storage capacity, and then strategically consume or provide power as necessary or possible.

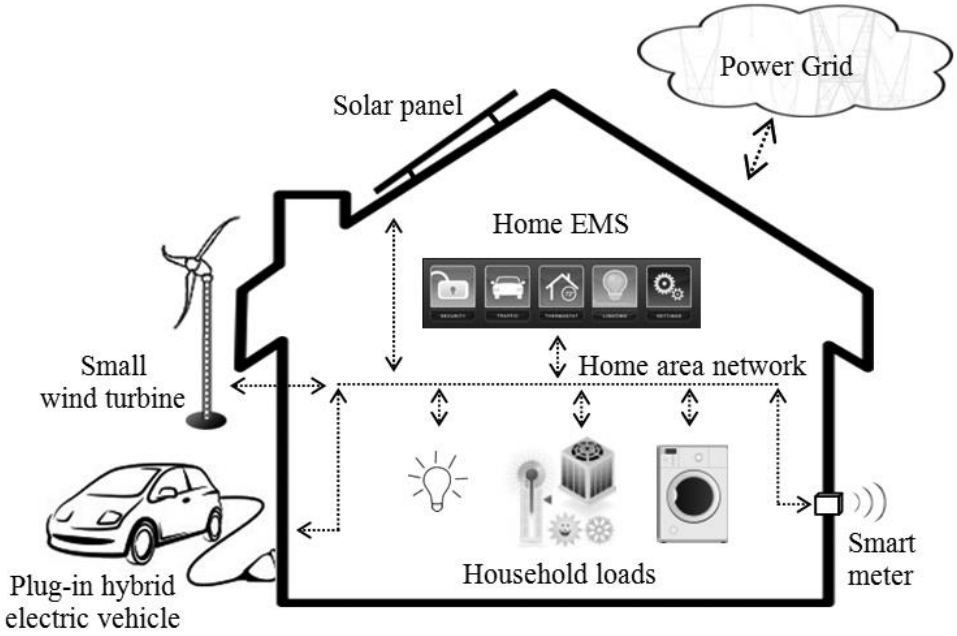

FIGURE 1-1. The diagram of a smart home

(Reprinted from our publication in [2] Copyright © 2013, IEEE)

Natural Resource Canada identifies residential energy end-use as space heating, water heating, lighting, space cooling, appliances (refrigerators, freezers, dishwashers, clothes washers, clothes dryers and ranges) and others [7]. In the context of DR application, residential loads can be generally classified as background loads and controllable loads. Background loads refer to basic electricity consumption such as lighting, which cannot be scheduled in response to DR application. By contrast, controllable loads include consumption of Heating, Ventilation and Air conditioning (HVAC), EVs, washing, drying, cooking etc. Du et al. [8] further classify controllable loads as thermostatically controlled loads and non-thermostatically controlled loads. TABLE 1-1 shows the categories of residential loads [2].

TABLE 1-1. Residential load category [2] (Reprinted from our publication in [2]

Background loads	Controllable loads	
	Thermostatically controlled	Non-thermostatically controlled
Lighting	HVACs	Dish washers
TV	Water heating	Washers, Dryers
		EVs

Developing efficient DR models to evaluate the effectiveness of DR *policies* and enabling *technology* is vital to an implementation of a DR program aiming to improve energy efficiency and power system stability. There is a trend that the smart grid moves towards to a distributed system with a large number of heterogeneous components [9]. An efficient residential DR model should implement heterogeneous residential load forecasting, multi-criteria optimization (e.g., objectives for individual homes, utilities and aggregations of them) and intelligent distributed algorithms to evaluate the complex and large-scale power systems.

1.2 Proposed Models and Methods

In this study, we consider RTP and TOU as the DR policies. RTP reveals wholesale electricity prices and provides the most precise way among others to schedule household load. TOU varies plat prices in different periods, which can be seen as a trade-off between the RTP and the easiness for tracking the dynamic prices. We propose a multi-agent system (MAS) for modeling the optimal residential DR implementation. A general wholesale electricity market scenario is modeled by the MAS, in which each component is captured by a corresponding agent: a wholesale market agent (WMA), a retailer agent (RA), a home agent (HA) and a generator agent (GA). The agents are connected by a local area network (LAN) or the Internet. Although all the agents are defined, we only focus on the power and information flow in the distribution network from a retailer/utility to end-users/homes.

A heterogeneous residential load prediction model, a price prediction model and three optimal load control models under RTP and TOU are developed, which are incorporated to the MAS. The residential load prediction model is developed based on statistical information of how people use their appliances including Vacuum, Range, Oven,

Microwave, Kettle, TV, Iron, Refrigerator, CD Player, Clock, Answering machine, Wi-Fi, PC, Printer, Light, Clothes washer/dryer, Dish washer and EV. Two EV charging models are also developed for EV electricity loads with different batteries: Lithium-Ion battery and Lead-Acid battery. The residential load prediction model captures the heterogeneous information of different homes, of which the aggregation load provides a benchmark for the optimal load control models.

The real-time price prediction model is defined as piecewise linear functions of power and the optimal coefficients are obtained from historical data of real-time loads and electricity prices via the norm approximation approach. Since the RTP is defined as piecewise linear functions with respect to load (power), the electricity payment ($\sum_t price \times load$) is a piecewise quadratic function, which is a convex function.

Under RTP, an open-loop optimal load control model (OL-LCM-RTP) and a closed-loop optimal load control model (CL-LCM-RTP) is proposed respectively. Both models are formulated as convex programming (CP) problems. The objective function minimizes the electricity payment and waiting time to find a trade-off. Using the OL-LCM-RTP, the HA schedules the controllable loads based on its local information by solving the CP problem. The CL-LCM-RTP is developed based on the OL-LCM-RTP by further incorporating feedback from the RA. The HA solves the CP problem to schedule the controllable loads in a round process using the global load information.

Experiments and numerical analysis are conducted in five scenarios under RTP. The scenario #1 simulates the benchmark without load control. A day-ahead RTP is evaluated in the scenario #2 using the OL-LCM-RTP. Since the day-ahead RTP is predetermined as a sequence price signal with respect to time. The objective function becomes linear; hence,

the model is simplified to a LP problem. The simulation results show that the day-ahead RTP can cause peak demand rebound in the lowest price time. In the scenario #3 and #4, the OL-LCM-RTP with RTP prediction is evaluated. In the scenario #3, a "dissatisfaction factor" which represents the discomfort level of users to schedule a controllable load is defined and assumed to be zero. Each HA schedules its controllable loads based its local information. The simulation results shows that the PAPR, the standard deviation and the electricity payment is reduced by 33.6%, 54.8% and 17.4% respectively. The scenario #4 further focuses on evaluating the dissatisfaction factor. Simulation results show that the electricity payment is inversely proportional to the waiting time.

The scenario #5 examines the CL-LCM-RTP, in which the HA receives feedback from the RA regarding on the load usage of the other HAs. The HAs schedule their controllable loads in a random order in a round process. The HAs have an opportunity to reschedule the controllable loads in a later round. Simulation results show that the process can be quickly converged in the second round. The PAPR, the standard deviation and the electricity payment is reduced by 39.2%, 72.7% and 19.6% respectively.

The open-loop optimal load control under TOU (LCM-TOU) is modeled by a linear programming (LP) problem. A set of random weights is introduced as a penalty function to avoid peak demand rebound. The objective function is designed to find a trade-off among three factors: 1) the minimum electricity payment; 2) comfort levels with waiting time; and 3) to avoid peak demand rebound. Experiments and numerical analysis are conducted in three scenarios under TOU. The scenario #6 simulates the reference of "without load control". Similar to the scenario #2, the LCM-TOU "without the set of

random weights" can cause a peak demand rebound at the start time of the lowest price period in the scenario #7.

The scenario #8 evaluates the LCM-TOU with a set of random weights. In addition, the impact of the participation levels of the TOU programs is examined as well. The simulation results show a reduced PAPR (by 15.5%), the standard deviation (36.6%), and the electricity payments from the HAs (by 15.4%) for a 100% participation level. However, the cost for the RA to buy the electricity energy is greater than the electricity payments collected from the HAs by $1.49. The participation levels in the range from 50% to 80% appear suitable since the quality of the observation are improved while the electricity payments from the HAs and the cost for the RA can be balanced in this range. The PAPR and standard deviation are approximately reduced by 14% and 39% respectively.

1.3 Motivations and Objectives

The existing power grid is mostly a water-fall system from power generation, to transmission system, to substation networks, and eventually delivery to the customers, where the power plants have limited real-time information about their end-users. Therefore, the grid has to maintain maximum expected peak demand capacity across the aggregated load since electricity cannot be economically stored. As this peak demand occurs infrequently, the grid is inherently inefficient. For instance, 20% of power generation capacity exists to maintain peak demand which is used in only 5% of the time [10]. Since there is a significant issue with legacy components of the electricity grid and the gap between increasing power demand and lagging investment, there has been deterioration in the system reliability.

New technologies such as EV/PHEVs and renewable resources (wind turbines and solar panels) will further deteriorate the stability and reliability of the current power system. The reason is because EV/PHEVs charging represents a significant electricity load and uncontrolled charging demand will create a much higher peak demand. The mandatory Renewables Portfolio Standards (RPS) requires increasing energy production from renewable energy sources and some states in the US have more ambitious goals, e.g., California requires 33% renewable energy by 2020 [11]. One of the challenges to integrate renewable sources is that they are not dispatchable, i.e., we cannot schedule or guarantee renewable sources in advance. Consequently, renewable penetration increases the requirements for regulation. A New England wind integration study shows that 20% of wind power penetration increases the regulation requirement from 80 MW (without wind) to 315 MW, and increases the reserve requirement from 2,250 MW (without wind) to 2,758 MW [12]. Regulation and reserve is required to maintain the stability of the power system; however, standby of this huge power generation capacity is a not economic and environmentally friendly. A possible solution is to integrate less expensive methods such as DR, EV charging/discharging and energy storage facilities to compensate for intermittent renewable sources. All these factors forces the evolution of the power system towards to a new system called the smart grid. DR is an essential component of the smart grid and an efficient design of DR plays key roles for the smart grid deployment.

The primary purpose of this research is to evaluate the two key components of a DR program, namely DR *policies* and enabling *technologies*. The second purposed is to develop optimal distributed load control mechanisms for scheduling heterogeneous

household electricity usage to improve the energy efficiency and the stability of the power system.

1.4 Contributions

We list the contributions of this study as follows.

1. We propose a MAS to evaluate benefits from DR for heterogeneous multiple HAs associated with a residential load prediction model. This model forecasts the baseline for household electricity usage including EV, which is based on statistical probability information of how people use their appliances.
2. We develop optimal load control models (OL-LCM-RTP, CL-LCM-RTP and LCM-TOU) for HAs to schedule electricity usage to observe both the individual benefit for a HA and the aggregated benefits for a RA from DR. Furthermore, the benefits of DR are emphasized from comparing with the predicted reference.
3. The proposed open-loop optimal load control mechanisms (OL-LCM-RTP and LCM-TOU) do not require coordination between HAs; therefore, they only requires a minimum of communication between the utility/retailer and multiple homes. This is greatly useful because the infrastructure for communication is still under development. Since HAs minimize electricity payments locally due to the proposed price prediction model, the privacy of users is not sacrificed.
4. The proposed closed loop control approach (CL-LCM-RTP) can significantly reduce electricity payment/cost and improve the energy efficiency. The process can be quickly converged; therefore, it only requires limited efforts in terms of communication and the coordination.

5. Since the residential load prediction model is based on statistical information, with tailoring the probabilities of using appliances to a specific area/city, the proposed MAS can be a test bed to evaluate various DR policies and enabling technologies.

1.5 Thesis Organization

This thesis is organized as follows: CHAPTER 2 is a literature review of residential load prediction models, electricity dynamic pricing, optimization models for residential DR, software techniques and their application for modeling residential DR. CHAPTER 3 proposes the design of the MAS in our study. The proposed residential load prediction model is discussed in CHAPTER 4. CHAPTER 5 presents the novel optimal load control models (OL-LCM-RTP and CL-LCM-RTP) and a numerical analysis under RTP. Following that, CHAPTER 6 discusses the LCM-TOU and numerical analysis. CHAPTER 7 concludes the thesis research with future extensions.

CHAPTER 2

LITERATURE REVIEW

Parts of this chapter are reproduced from our publications in [1] (Copyright © 2015, IEEE) and [2] (Copyright © 2013, IEEE).

2.1 Residential Load Prediction Models

An effective real-time load forecasting model is crucial for a utility to adjust its generation and to provide a baseline for evaluating DR. Previous reviews of residential electricity load prediction models identify two main types of simulation models: top-down and bottom-up [13, 14]. Top-down methods model household electricity consumption as a whole with regard to its general characteristics such as gross domestic product and unemployment rate [15]. By contrast, in the bottom-up methods, load profiles are gained from aggregation of electric consumption of various residential appliances or a variety of households.

From the bottom-up models, we identify various DR-enabled models that feature time-related end-use operations. Relying on detail household information and appliance characteristics, these DR-enabled models are constructed in four steps in general as follows.

1. Characterizing end-user's appliances (e.g., space heating, water heating, and laundry machines) or human activity patterns of using these appliances from existing data;
2. Generating the individual load profiles of these appliances;
3. Aggregating these individual load profiles from a single or multiple residential sector in a period from one day to several years;
4. Validating the model by comparing the simulation results with measured data.

A physical-based DR-enabled aggregating residential load is presented by Shao et al. [16]. Individual controllable load models are also studied e.g., air conditioning [17] and water heaters [18].

The study in [19] proposes a bottom-up approach of constructing detailed Canadian household electrical demand profiles to examine the issues of system performance, efficiency and emission reduction. The inputs of this model include a detailed appliance set, annual consumption targets and occupancy patterns. This study creates occupant driven electrical loads (lighting and appliances) at a 5-min time resolution.

Loads of lighting, appliances (refrigerators, freezers, dishwashers, clothes washers, clothes dryers and ranges) and others are created individually and then cumulated to simulate the electrical load for Canadian houses. The electrical power of the dishwasher, washer, range and dryer is calculated as follows.

$$Average\ appliance\ electrical\ power = \frac{annual\ consumption}{cycle\ duration \times cycles\ per\ year} \qquad (2\text{-}1)$$

where *annual consumption* data are from electricity use for appliances and lighting for the average Canadian household [20]. *Cycle duration* consults data from the Canadian Centre for Housing Technology (CCHT) twin house research facility. *Cycle per year* comes from standard appliance test methods of the Canadian Standards Association (CAN/CSA-C373-92, CAN/CSA-C361-92 and CAN/CSA-C360-98). The load profiles of the refrigerator, freezer and lighting are modelled based on measured refrigerator data from the CCHT. A single 105-min defrost cycle is also associated to the refrigerator and freezer. Information for "other" appliances is observed from a series of buyer's guides published

by Natural Resources Canada [21]. The time-of-use probability profiles of ranges, dishwashers, washers, lighting and other appliances are derived from [22]. The authors simulate three annual load profiles for three predefined target Canadian households: low, medium and high energy detached. These profiles are validated from a successful application in the simulation of a Stirling engine residential cogeneration system, and a consistent comparison with measured profiles from Quebec homes.

A higher resolution of 1-min synthetic electricity demand load model is presented in [23] to simulate data on occupant behaviour, presence and energy use. This model generates synthetic householder activity sequences and electricity demand profiles. Non-homogeneous Markov chains are used to model spread of electricity-dependent activities including away, sleeping, cooking, dishwashing, clothes washing, TV watching, computer using, audio listening, and other activities. These activities are then translated into power consumption using different schemes/methods based on appliance characteristics. The model parameters are estimated and validated using existing data (e.g., pilot survey of time use by Statistics Sweden). The proposed model reproduces all important features in measured demand data such as end-use composition, demand variation over different time scales in individual households, diversity among households and demand coincidence.

Rather than constructing a Markov-chain-based occupant activity simulation, another higher resolution of 1-min synthetic electricity demand load model is presented using static activity profiles [24]. In this model, not only time-of-use of appliances but also householders' activities (i.e. when people are at home and awake) are incorporated. Statistics are used to design a mean total annual energy demand and power use characteristics of appliances. Occupancy activities are represented as activity profiles using

data derived from the UK 2000 Time Use Survey, which is a comprehensive survey of how people spend their time in the UK. These activity profiles show how people use appliances (e.g., people tend to do cooking activities around meal times). These activity profiles are then linked to each appliance. In this way, appliances are used at appropriate times without the knowledge of detailed appliance usage statistics. The electric load curve is observed from aggregation of the appliance consumption. This model is validated from comparing between simulation results and measurement over the period of a year within 22 dwellings in the East Midlands, UK. In addition, an example of the model is freely downloadable enabling further incorporation into other models with appropriate modification.

Since the DR application is designed to change customers' consumption patterns such as using renewable energy and shifting peak demand by switching off/on appliances in response to dynamic prices, these bottom-up DR-enabled models are suitable in DR simulation and modeling.

2.2 Dynamic Pricing

There are two main policies to motivate customers to participate in DR programs, namely price-based DR and incentive-based DR, in which, the former one is more suitable for residential customers [25, 26]. In this section, we review some main dynamic pricing mechanism including inclining block rate (IBR), TOU and RTP.

IBR is define as a function of energy. For instance, BC Hydro uses IBR shown in FIGURE 2-1 [6]. The electricity prices vary between 7.52 ¢/kWh and 11.27 ¢/kWh based on energy consumption. If the amount of consumption in an average two-month billing period is below 1,350 kWh, customers pay the first step price (7.52 ¢/kWh); otherwise the price is 11.27 ¢/kWh in the second step (effective April 1, 2014). FIGURE 2-2 shows the electricity

payment with energy consumption. The solid blue lines show the payment linearly increases with amount of energy consumption. The slope of the first segment is the step 1 price 7.52 ¢/kWh. Once the energy exceeds the threshold, the slope becomes the step 2 price 11.27 ¢/kWh. For the purpose of optimization, these piecewise linear functions can be smoothed by a quadratic function shown by the red dash line [27].

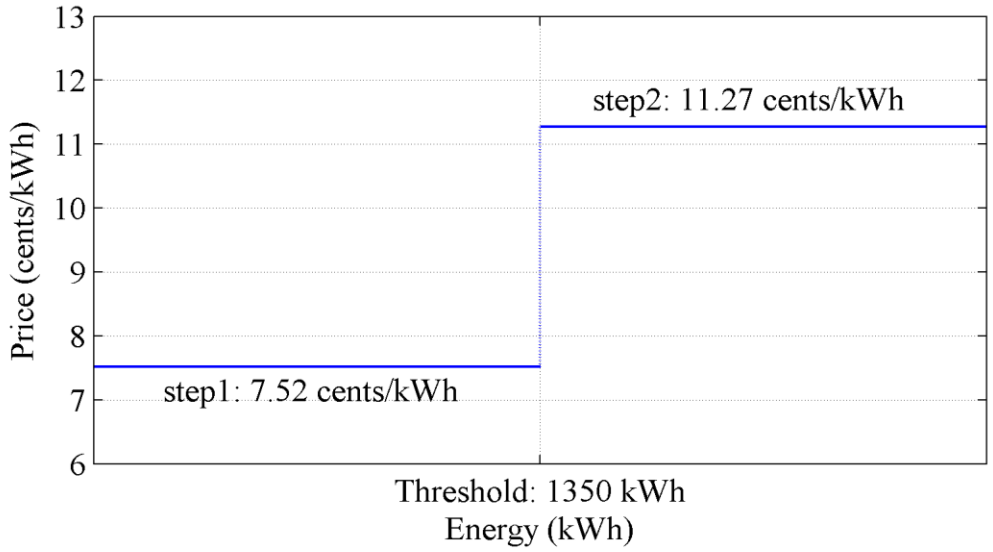

FIGURE 2-1 IBR used by BC Hydro [6]

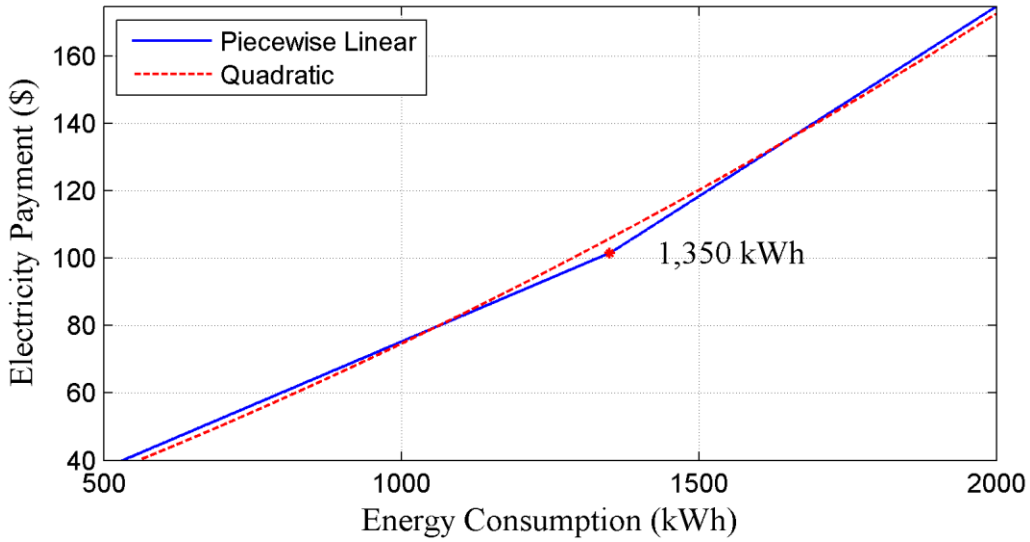

FIGURE 2-2 Electricity payment with energy consumption [27]

In TOU pricing, the electricity price is flat but different in periods. The principle is also that the generation cost is more expensive to supply higher demand. For example, the Ontario Energy Board applies TOU to customers, in which electricity price is 7.7 ¢/kWh, 11.4 ¢/kWh and 14 ¢/kWh in off-peak, mid-peak and on-peak demand period respectively (effective November 1, 2014) shown in FIGURE 2-3 [28]. The demand periods also vary among seasons, weekends and holidays. For instance, in weekdays of summers, the off-peak period is from 7pm to 6am of next day and the mid-peak period is from 11am to 4pm. The rest hours are considered as the on-peak period. Under TOU, customers pay more for electricity in peak demand periods.

TOU is predetermined by identifying the off-peak, mid-peak and on-peak demand periods from historical data and usually vary among seasons. This predetermined price structure reveals the generation cost to some extent but not in a precise manner. Also, the predetermined and preannounced electricity can cause peak demand rebound from the synchronized scheduling of multiple users. However, an appropriate design of automated DR mechanism responding to TOU can alleviate this problem [29, 30].

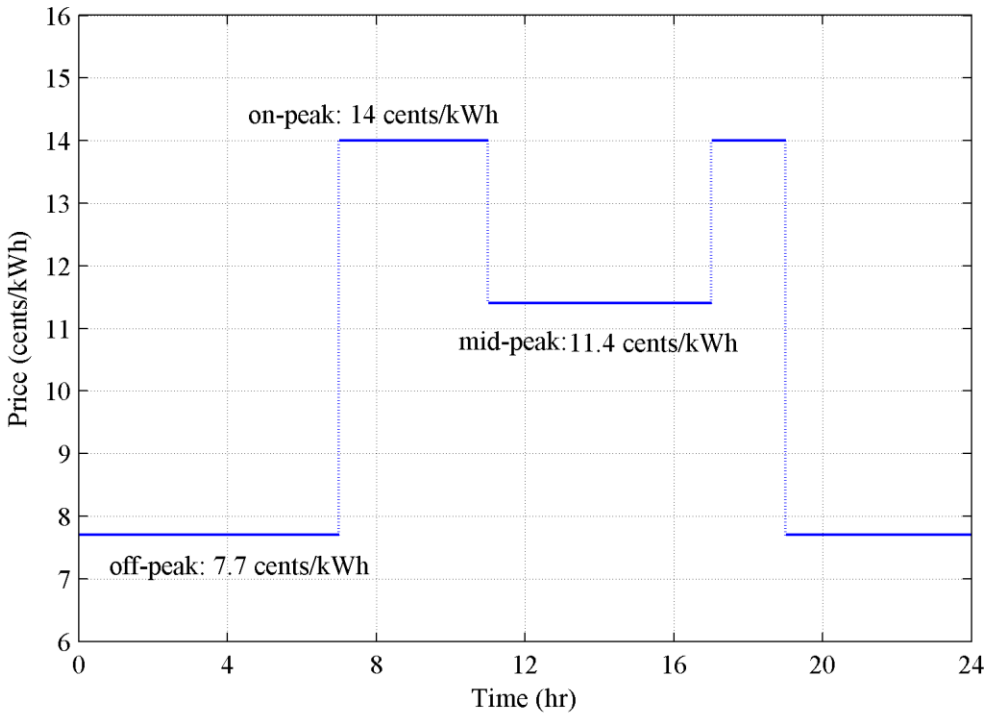

FIGURE 2-3. TOU used by Ontario Energy Board [28]

RTP applies hourly price to the customers. FIGURE 2-4 shows the electricity load and the locational margin prices (LMP) in the region of American Electric Power (AEP) in a typical day (17/12/2014) from PJM [31]. The blue solid line shows the real time load and the green dash line shows actual LMP. We can clearly see the pattern that the price is proportional to the load.

RTP can precisely reveal the generation cost to the end-users and also require a high level of participation from them. Although RTP has been adopted for large industrial and commercial customers [26, 32], it is still not available for residential customers because of the lack of communication facilities and automated-response mechanism for end-users. Also, the residential users tend to rebel the potential risks from the hourly fluctuated price structure. A day-ahead announced RTP could be alternative and a test in Ontario, Canada has shown a successful application of this scheme [33].

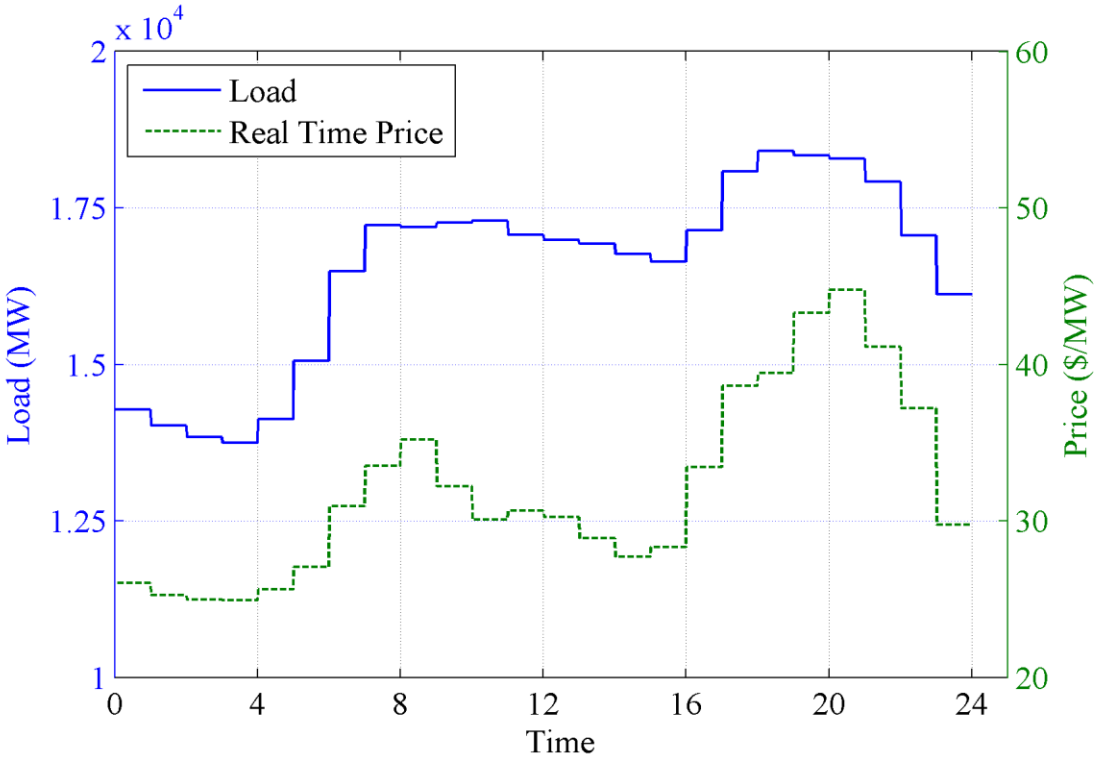

FIGURE 2-4 RTP and electricity load in the region of AEP on the day of 17/12/2014 [31]

2.3 Optimization Models for Demand Response

A variety of researchers have modelled residential DR as optimization problems under RTP and TOU. The main purpose of these studies is to develop optimization mechanisms for minimizing residential customers' electricity payment [27, 34-38] or maximizing their utilities/welfare in order to achieve generally uniform electricity load profile with a reduced PAPR [39-41]. A comprehensive view of optimization algorithms for DR application can be found in [26]. In general, the optimization model is as follows.

$$minimize \sum_{t} p(\cdot)\, l + penalty\ function$$
$$subject\ to: \text{ a set of constraints} \tag{2-1}$$

where $p(\cdot)$ is the electricity price as a function of time, load or both of them. l is the electricity load as a function of time. The first term in the objective function is the electricity bill/payment. The penalty function is usually defined as the waiting time, uncomfortable levels or both. The set of constraints are derived from physical properties of the system, e.g., rated power of an appliance, a certain amounts of energy consumption, power capacity, etc.

In [27], a single home optimal residential DR is formulated to a LP problem to minimize electricity payment and waiting time under RTP. The RTP in the study is defined as a function of both load and time primarily based on IBR or predicted prices separately. The first term (see equation 2-1) is a piecewise linear function. A price predictor filter is also proposed to forecast the price in the schedule horizon. The coefficients of the predictor filter is obtained from historical data. The price prediction is separated from the optimization model; therefore, if the price is predicted, the first term in equation 2-1 is a

sum of load with weighted coefficients. The penalty function is also defined as a linear function of electricity load. Hence, the objective function is a linear function. In addition, all the constraints are affine functions. As a consequence, the optimization model is formulated as a LP problem. DR applied for a single house is evaluated in a period of four months. A reduced PAPR is observed.

DR implementation considering a single home operating different appliances is modelled using a CP problem to minimize electricity payment in [34] for an automatic response to RTP. This study also introduces l_1-norm regularization to deal with binary decision variables for appliances operated in an on/off mode. More exactly, these binary on/off variables $x \in [0,1]$ are first relaxed to continuous values, e.g., $0 \leq x \leq 1$. The l_1-norm regularization is then incorporated into the first term of the objective function (see Equation 2-1). The l_1-norm regularization can be used to determine a sparse solution, i.e., has the most zeros in the solution for decision variables [42]; and hence, the most ones in the solution in this case. Therefore, this can be considered as a combination of an optimization method and a heuristic algorithm. By doing this, the problem can be solve significantly more efficiently than solving a mixed integer nonlinear program (MINLP) problem.

A optimization model is also proposed in a scenario of multiple houses to maximize users' utilities in [41]. The study shows that the maximization of individual household net benefits and the maximization of the welfare of the society can converge. In other words, using the proposed model, each household selfishly maximize its own benefits based on time-varying electricity prices while eventually the social welfare is also maximized. A distributed algorithm is proposed for the utility to determine this time-varying electricity

prices for the customers to compute the load schedule. The simulation results show that the set of time-varying prices exists to converge the maximization of individual benefits and the optimality of the social welfare.

Several studies have indicated that the synchronized automated response to the dynamic pricing can cause peak demand rebound at low price periods [43-45]. A coordinated DR scheme with a distributed algorithm is proposed in [43, 44] to avoid this new peak demand. A multi-stage stochastic optimization problem is formulated for a coordinated home EMS framework in [43]. The customers schedule the load based on the local information and also exchanged information with their neighbours.

To tackle the problem of peak demand rebound and also to achieve a more flattened load profile with minimum individual cost of customers, a bi-level optimization problem is designed in [44]. The upper level is aim to achieve a smooth and flattened load profile while the lower level minimizes the customer's expense. To reduce the complexity, this bi-level problem is reformulated into equivalent single-level problems, which is solved via a distributed algorithm. An EMS module solves the problem iteratively, in which the EMS module schedules the load with announced electricity prices and updates the load profile to the utility. The utility forecasts the aggregated total load profile and the EMS module asynchronously reschedules the load till the most flattened distributed load profile is obtained, where the least energy expense is also achieved. This iteration terminates when the quality of the load profile cannot be further improved. The study provides a proof of the convergence and optimality of the proposed algorithm.

The study in [45] proposes a multi-TOU and a multi-CPP to cope with this problem of peak-demand rebound, in which different groups of users see different structures of TOU

and CPP. Each home minimizes its cost individually based on the price signal from a utility. This distributed scheme also results in meeting system-wide objectives, such as reduced peak demand and generation cost. The baseline of the load profile is predicted by a bottom-up model. An optimization problem is then developed to schedule the controllable appliances, which is solved by a dynamic programming method.

The study in [46] proposes a decision-support system for residential customers to minimize the electricity expense based on TOU pricing. The system aggregates the predicted household load in a neighborhood and informs the utility. The utility uses this forecasted load to design the TOU structure and sends the prices to the customers. The customers then utilize the TOU from the utility to schedule the load to minimize the expense in a comfort zone. Through this interaction, the utility will be able to understand the consumption pattern of the customers in order to design an appropriate TOU.

The optimal load schedule based TOU is formulated as a MINLP problem in [47]. The objective is to maximize the net benefits for the residential customers under some budget limit. The MINLP is solved via Benders decomposition method to reduce the complexity. The proposed system incorporate five categories of appliances: "1) set of elastic appliances with a memoryless property; 2) set of elastic appliances with a full memory property; 3) set of elastic appliances with a partial memory property; 4) set of inelastic appliances with an interruptible operation; and 5) set of inelastic appliances with an uninterruptible operation." The weighted subtraction between utility of appliances with elastic energy consumption and energy cost is design as the objective function to maximize.

The study in [48] proposes a stochastic technique based on quadratic programming with quadratic constraints to cope with the uncertain price-elasticities of the demand. A

decision tree approach is develop to qualify the impacts of TOU on PHEV charging pattern [49]. Several TOU structures are evaluated in terms of the total PHEV fuelling costs.

Game theory as a mathematical model of interaction, competition and cooperation among self-interested agents [50] is widely applied to study DR. The study in [51] presents a two-stage (Stackelberg game in the first stage) two-level model for a smart grid retailer as an intermediary agent considering both DR for consumers and market price uncertainty. The model is reformulated to a MINLP. The dynamic prices in [52] for a DR application are determined by a game, in which a retailer agent and a customer agent are players. The retailer agent minimizes the electricity payment using a LP model while the customer agent maximizes its daily savings. Although the game theory applications for DR in [53, 54] do not use agent systems, the players in the games can be naturally modelled by autonomous agents.

In addition to the optimality of electricity expense or social welfare, the study in [55] also evaluates the fairness. This study focuses on developing electricity pricing mechanisms to achieve both optimality and fairness. A centralized optimization model is developed as a reference, in which the optimality is proved. Furthermore, to achieve fairness, the customers should be charged based on their contributions in two scenarios of staying or leaving the grid. Based on this, a billing function B_n is proposed and proved to be fair. Using this billing function, an autonomous DR game is developed and each player minimizes its electricity payment as follows.

$$minimize \sum_{h=1}^{H} B_n^h \left(x_n; x_{-n}\right) \tag{2-2}$$

where x_n is the load profile of player n and x_{-n} is the load profiles of the other players. h is the time in hour and *H* is the schedule horizon. This mechanism incorporates hourly load profile of each player; therefore it considers both the total load and the individual load flexibility.

A game-theoretic based model shows an improved market efficiency through applying TOU [54]. This study models the cost as the load profile variation and the satisfaction level with schedule the controllable load, based on which the utility function is defined. Nash equilibrium can be achieved via backward induction for single-type-users and multiple-type-users. Both the utility and customers can benefit from the scheduled demand at Nash equilibrium.

2.4 Software Agents

The concept of an agent can be traced back to the early days of research into the field of distributed artificial intelligence (DAI) in the 1970s, which include Carl Hewitt's concurrent actor model [56]. In this model, Hewitt proposed a term of "actor", which proposes the concept of a self-contained, interactive and concurrently-executing software object. An actor has an encapsulated internal state, a mail address and behaviour, and can also communicate with other actors by messaging [57].

It is very difficult to precisely define an agent. Even within the software affiliation, the word "agent" is really an umbrella term for a variety of research and development [56]. The response to this lack of definition is that some agent researchers have invented many synonyms such as softbots (software robot), personal agents and autonomous agents [56]. Nonetheless, we try to propose one definition here to make an agent clear to the audience. "An agent is referred to a component of software and/or hardware which is capable of

acting exactingly in order to accomplish tasks on behalf of its user [56].” Additionally, commonly acceptable concepts of software agents are listed as follows [56, 58, 59]:

- **Autonomy:** Agents operate without the direct intervention of humans or others, and have some kind of control over their actions and internal state [60].
- **Social Ability/Cooperation:** Agents interact with other agents (and possibly humans) via some kind of agent-communication language [61].
- **Reactivity/Proactivity:** Agents perceive and respond to their environment in a timely fashion to adapt their behaviour accordingly. The environment may be the physical world, a user via a graphical user interface, a collection of other agents, the Internet, or perhaps even all of these combined.

Software agents are difficult to define, as demonstrated, and similarly complicated to categorize. According to the overview work of Nwana [56], there are numerous ways to classify existing software agents.

Firstly, agents can be classified by their mobility: for instance, the ability of moving around a network. Agents can be categorized into the classes of either static or mobile agents. Secondly, they may be classified in terms of either deliberative agents or reactive agents. Deliberative agents derive from the deliberative thinking paradigm in which the agents have an internal symbolic, reasoning model, and these agents communicate and negotiate with other agents to achieve coordination. By contrast, reactive agents do not have any internal, symbolic models of their environment, and they behave using a stimulus/response type of action by responding to the present state of the existing environment [62].

Thirdly, agents may be categorized based on several ideal and primary attributes where agents should exhibit. The agents can be classified as collaborative agents, collaborative learning agents, interface agents and truly smart agents [56]. Truly smart agents, however, have not yet been developed. As Maes notes, "current commercially available agents barely justify the name" [63] and Foner is even more emphatic [64]. Fourthly, agents can also be classified by other characteristics, i.e. roles, or any combination of two or more attributes.

Nwana finally classified software agents into seven types to cover most currently existing agents: collaborative agents, interface agents, mobile agents, information/Internet agents, reactive agents, hybrid agents, and smart agents [56].

A MAS generally refers to a body of multiple autonomous agents that interact, cooperate, and negotiate with each other in order to satisfy their design objectives [65-67]. It provides a way of viewing the world in which an agent system can intuitively represent a real-world situation of interacting entities, and test how complex behaviors may occur [68]. Two main characteristics can be derived from the definition. Firstly, each agent is autonomous and is able to solve the problem in its domain. However, it only has incomplete information or limited capabilities for solving the whole problem and, thus, has a limited viewpoint. Secondly, through agent interaction, the system can conduct a complex problem that is beyond the capability of individual agents. Furthermore, the interaction here can be either cooperation or competition/negotiation.

If a problem domain is especially complex, huge, or/and unpredictable, then an effective way in which it can reasonably be addressed is to develop a number of functionally specific agents that are specialized for solving a specific problem aspect. For instance, it is difficult (if it is not impossible) to simulate the power system in a single model because of its large scale and enormous complexity. An ideal alternative is to model each individual component of the system. Through observing the interaction of these components, the system response can be evaluated. The advantages of this method are obvious, as discussed previously.

2.5 Agent-Based Simulation for Demand Response

A comprehensive review from the IEEE Power Engineering Society's Multi-Agent Systems Working Group identifies that a MAS can provide two novel approaches for power engineering: building flexible and extensible systems and simulation & modeling

[68]. MAS is particularly suitable for modeling heterogeneous components in the DR application for the smart grid.

The research literature includes a wide range of work using MAS to evaluate DR implementations. FIGURE 2-5 shows a typical architecture of such a MAS for observing a residential DR application. DR related components of the smart grid can be captured by various types of agents such as generator agents, home agents, and transmission and distribution agents. A MAS may include all or some of these depending on research aims. If the concept of microgrid is involved, this architecture can be duplicated and several components can interact through this structure. Through the interaction of agents and/or microgrids, various interesting insights can be developed.

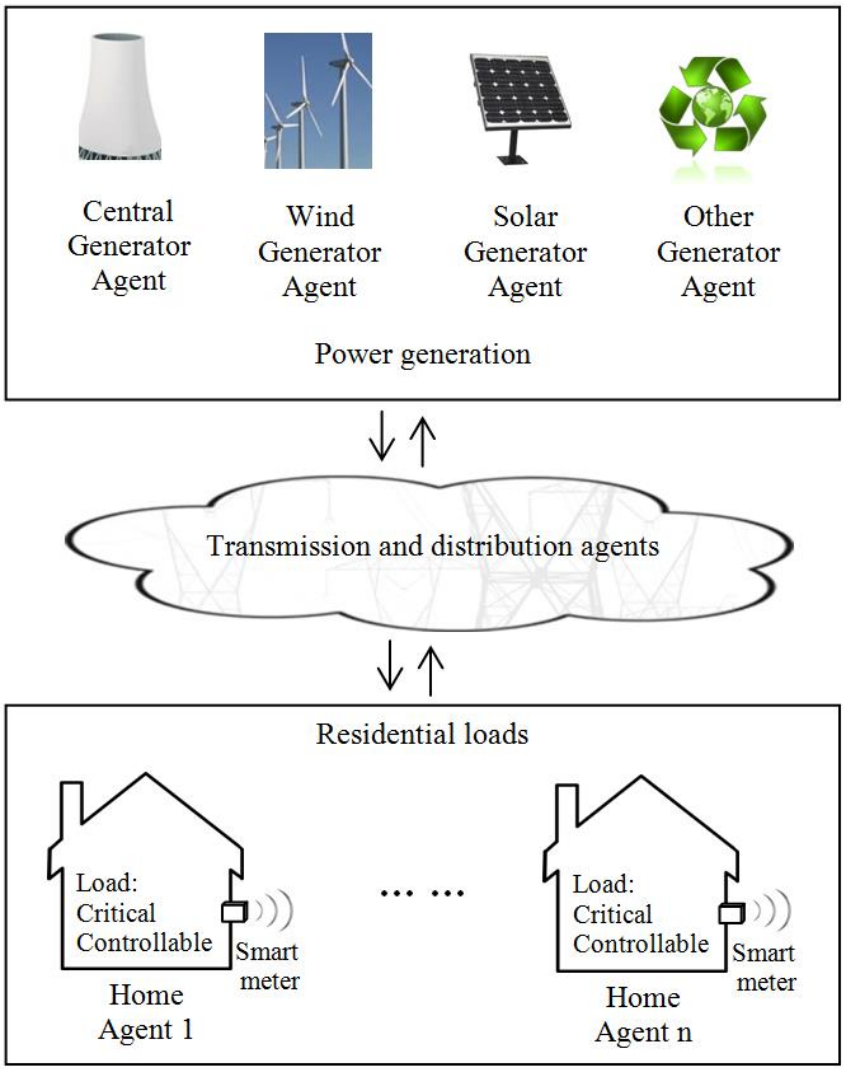

FIGURE 2-5 Typical multi-agent system architecture of residential demand response simulation

(Reprinted from our publication in [2] Copyright © 2013, IEEE)

A DR program incorporating with distributed energy resources (DER) and distributed storage is evaluated in [69] using an index-based incentive mechanism. The study in [70] proposes a ecosystem to optimize DR implementation and DER management in a residential sector using hierarchical agents. Agent-based systems are also proposed to associate DER and storage facilities with DR in order to reduce peak demand and minimize electricity payment [71]. The study in [44] proposes a MAS to solve a bi-level optimization problem using an iterative distributed algorithm to avoid peak rebounds in lower price periods and to achieve a flatten total load profile. MAS can also be found in applications for coordination of EV charging [72, 73] and microgrids control [74-76].

The study in [77] states that smart homes may no longer be modeled by passive load curves but should be considered as active participants that not only consume electricity but also generate and store it. A MAS is proposed for modeling homes as autonomous agents that make decisions to buy, sell or store electricity based on their presented loads and future loads, the generation capability and the storage capacity. In addition, the grid is modeled by a simple agent that sells/buys electricity from/to home agents. This work assumes that each household is equipped with wind turbines, solar cells and storage facilities (possibly through EV batteries). The wind power generation and power loads are represented by a data-based model. Electricity rates are calculated by an exponential function that is called a function-based model, where a real-time pricing scheme is observed. To evaluate the performance of the proposed MAS, three variables are observed: the demand deviation, the diversity factor and electricity cost. The demand deviation evaluates the mean deviations of the overall electricity demand and diversity factor characterizes the spectrum of the home peak demands. A small value of these two factors is desirable since it represents an

overall flattened aggregated demand. However, the benefit of load-shifting is not considered in their work.

A MAS is proposed in [78] to simulate households in response to dynamic pricing by scheduling household loads. Two major components of the households and the utility are captured in the MAS. The utility agent provides a price plan and then the household agents respond to the plan. A Markov gaming framework represents household agent behavior and *Q*-Learning algorithm is applied to solve the Markov problem. The rescheduling activities are classified into three types in terms of load characteristics. The detail design of the price is not given in the paper. Simulation results quantitatively evaluate the DR application.

Customers can switch on/off loads depending on their priorities and also control PHEV charge activities depending on their battery state of charge (SOC), to reduce cost and avoid overload during peak hours [79]. This paper uses a normal hourly household load curve in the U.S. as the baseline. This overall load is categorized in seven types: cooling/heating, cooking, washing/drying, refrigeration, freezing, lighting and others. Base on the actual profile, the authors evaluate the effect of PHEV charging profiles during peak hours and off-peak hours with an assumption of maximum 100 PHEV charging points. The comparison between these two scenarios shows the significance of encouraging customers to consume electricity during off-peak hours. This study identifies effectiveness of the penetration of PHEVs on reducing the energy consumption cost of the residential customers. Although the grid agent includes the battery, the wind energy and the distributed generator, their characteristics are over-simplified (e.g., wind output is assumed consistent).

An agent based intelligent EMS is proposed in [80] to facilitate power trading among microgrids and allow customers to participate in DR programs. The presented architecture simulates two generators with different levels of generation cost and two customer loads in two microgrids respectively. A priority index of DR participation is signed to customers in a continuous double auction market. Case studies are conducted in the scenarios of with and without DR. The simulation results confirm the applicability of the agent-based simulation to power management and trading in smart microgrids.

To study how to balance customer demand and renewable energy from distributed generation, five types of autonomous agents, the electricity management mechanisms, the agent communication ontology and the agent cooperation strategy are developed in [81]. The five agents are substation agent, the bus agent, the feeder agent, the load agent, and the generation agent. Besides the objective to dynamically balance the power supply and the demand, this research also desires to minimize the power cost in a distributed network and maximize the power usage from distributed generators. The distribution network is effectively balanced by satisfying the objectives through the communication and cooperation between these agents.

Recently, large-scale agent-based systems have been developed. The electricity market complex adaptive system (EMCAS) is one of them. The EMCAS simulates decisions on six different time scales, in which diverse participants in the electricity market are represented as agents [82]. The EMCAS as a commercial platform has been used in various DR research projects. Consumers use forecasted day-ahead prices to shift daily energy consumption at an hourly basis without changing the total energy consumption [83]. The study in [84] presents an agent-based model using EMCAS to study the impact of

demand price elasticity. A restructured electricity market with eight generation companies and five aggregated consumers is simulated in a month.

2.6 Summary

In this chapter, we have reviewed the literatures regarding on applications and models for residential DR implementation, which includes residential load prediction models, dynamic pricing, optimization models, and software agent & its applications for DR. In our study, we propose a multi-criteria agent-based optimization system. In general, the differences between our study and the studies in the literatures include: 1) the HAs in our study are heterogeneous with unique individual load profiles forecasted by a residential load prediction model. This prediction model forecasts household load including EV charging based on statistical information of how people operate their appliances. 2) Under the open-loop control mechanism, the HAs minimize electricity payment and waiting time using local load information and predicted electricity price to schedule controllable load/appliances; therefore, the communication among homes is at a minimum level and the privacy of information is protected. 3) The closed-loop control mechanism can significantly reduce electricity payment and cost, and improve the energy efficiency. The process can be quickly converged; therefore it only requires limited efforts the communication and the coordination. 4) Since the proposed open-loop optimal control mechanisms use distributed algorithms, these models are linearly scalable and can be implemented in parallel into a very large system. 5) We evaluate daily benefits for both individual HAs and the RA.

CHAPTER 3

MULTI-AGENT SYSTEM DESIGN

This study considers a general electricity wholesale market. Similar to other commodities, electricity can be traded in wholesale markets and retail markets. In general, retailers/utilities can *purchase* electricity from a wholesale market and *sell* it to customers in a retail market [31]. Retailers/Utilities may also own generators and sell electricity directly to end-users. We use the umbrella term of *purchase* to denote buying power from a wholesale market and/or generating power. This does not lose generality since the electricity price could be considered as generation cost if the retailer/utility generates power. This chapter is reproduced verbatim from our publications in [1] (Copyright © 2015, IEEE).

3.1 System Architecture

The general wholesale electricity market scenario is modeled by the MAS shown in FIGURE 3-1, in which each component is captured by a corresponding agent: wholesale market agent (WMA), retailer agent (RA), home agent (HA) and generator agent (GA). The agents are connected by a LAN or the Internet. Although all the agents are defined, we only focus on the power and information flow in the distribution network from a retailer/utility to end-users/homes. However, this work can be readily extended to other aspects of the power system.

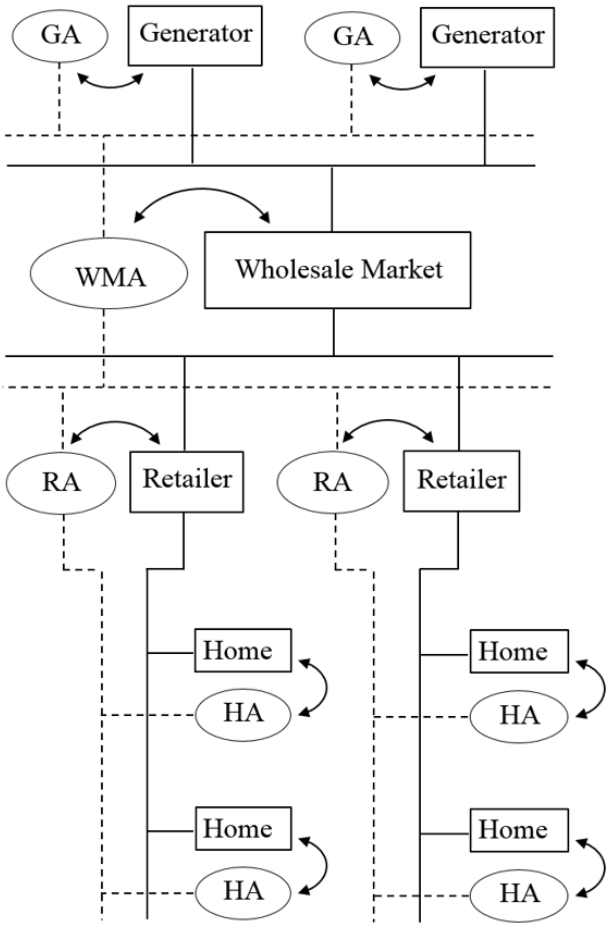

FIGURE 3-1. The multi-agent system architecture (the solid line represents power line; the dash line refers to LAN)

(Reprinted from our publication in [1] Copyright © 2015, IEEE)

Following the abstract architecture for agents in [85], the proposed MAS has a set of agents as follows.

$$\mathcal{HA} = \{HA_1, HA_2 \cdots\} \tag{3-1}$$

$$\mathcal{RA} = \{RA_1, RA_2 \cdots\} \tag{3-2}$$

$$\mathcal{GA} = \{GA_1, GA_2 \cdots\} \tag{3-3}$$

$$\mathcal{AG} = \mathcal{HA} \cup \mathcal{RA} \cup \mathcal{GA} \cup WMA \tag{3-4}$$

where $\mathcal{HA}$ and $\mathcal{RA}$ is a set of HAs and RAs respectively. $\mathcal{GA}$ is a set of GAs. The union of these agents forms the multi-agent set $\mathcal{AG}$. We also define a retailer scope set $\mathcal{RS}$.

$$\mathcal{RS} = \{RA, HA_1, HA_2, \cdots\} \tag{3-5}$$

which contains a RA itself and all the HAs whom the RA delivers electricity to.

All agents perceive their environment, which is characterized by a set $\mathcal{E}$.

$$\mathcal{E} = \{e_1, e_2, \cdots\} \tag{3-6}$$

Autonomous agents are capable of perceiving their environment, upon which they take actions. Let $\mathcal{AC}$ denotes the set of actions.

$$\mathcal{AC} = \{a_1, a_2, \cdots\} \tag{3-7}$$

Time t is discretized into time slots. Let $\mathcal{T}$ denotes the set of time slots in sequence.

$$\mathcal{T} = \{1, \cdots, T\} \tag{3-8}$$

where $T \geq 1$ is a time horizon of the environment for the simulation, during which period an agent can take actions. For instance, if the time horizon $T = 24\ hours$ and the time slot $t = 1hr$, the set has 24 elements in it.

These definitions are used in the following design of agent simulation.

3.2 Home Agent

The environment of a HA includes real-time prices P, real-time load L, real-time constraint set ct, dissatisfaction factor set λ^{ap}, and direct load control (DLC) signals DLC.

$$\mathcal{E}_{HA} = \{P, L, ct, \lambda^{ap}, DLC\} \tag{3-9}$$

where P and L is defined as a column vector of the electricity price and the household load in each time slot in Equation (3-10) and Equation (3-11) respectively. ap represents an appliance in a home. λ^{ap} is a set of factors to reflect dissatisfaction levels of a customer to schedule the appliance ap. DLC represents load control signals from a RA. ct is a set of constraints; for instance, total electricity demands at any given time (slot) in a home cannot exceed a certain capacity Q_{HA}^{max}. Other constraints are discussed in CHAPTER 5 and CHAPTER 6 in detail.

$$P = < p_1, \cdots, p_T > \tag{3-10}$$

where the element p_t in the price vector P is the electricity price at time t.

$$L = < \sum_{ap \in \mathcal{AP}} l_1^{ap}, \cdots, \sum_{ap \in \mathcal{AP}} l_T^{ap} > \tag{3-11}$$

where the household load L is the aggregation of all the appliances in a home. $\mathcal{AP}$ is a set of the appliances in a home. l_t^{ap} is the load of the appliance $ap \in \mathcal{AP}$ at time $t \in \mathcal{T}$. $\sum_{ap \in \mathcal{AP}} l_t^{ap}$ is the aggregated appliance loads at time t.

HAs have three types of actions.

$$\mathcal{AC}_{HA} = \{predict\ load, control\ load, predict\ price\} \tag{12}$$

where *predict load* and *predict price* refers to forecasting real-time household loads and real-time electricity prices respectively. The *control load* action schedules the load.

FIGURE 3-2 shows the architecture of a HA. A HA predicts an individual appliance load, and if the load is controllable (e.g., EV charging), the electricity demand is scheduled by the *control load* action. If the load of the appliance is not controllable (e.g., lighting), otherwise, it is connected to the power line immediately. The objective of the control load action is to determine an optimal set of $\mathcal{AC}_{HA}^{\star}$ to minimize electricity payment based on predicted real-time prices and/or DLC request. The optimal $\mathcal{AC}_{HA}^{\star}$ is essentially a sequence of operational signals for all controllable loads under certain constraints.

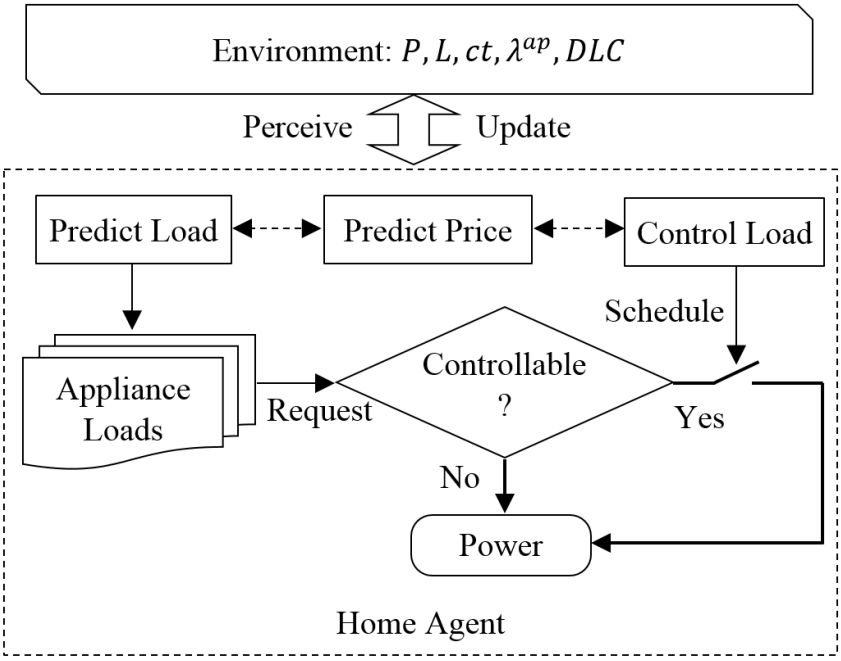

FIGURE 3-2. Home Agent. The HA is a model of a smart home, which includes load and price prediction and load control.

3.3 Retailer Agent

The characteristics of a RA's environment include real-time electricity prices P, service scope $\mathcal{RS}$, aggregated loads $\sum_{HA\in\mathcal{RS}} L_t^{HA}, \forall\, t \in \mathcal{T}$, available power Q_{RA} and the max-power capacity Q_{RA}^{max}.

$$\mathcal{E}_{RA} = \left\{P, \mathcal{RS}, \sum_{HA\in\mathcal{RS}} L_t^{HA}, Q_{RA}, Q_{RA}^{max}\right\} \tag{3-13}$$

The actions for a RA are as follows.

$$\mathcal{AC}_{RA} = \{aggregate\ load, predict\ wholesale\ price, purchase, sell, DLC\} \tag{3-14}$$

FIGURE 3-3 shows the RA architecture. A RA *aggregates* power demand of the HAs in its service area and *purchases* power from an electricity wholesale market. The RA then *sell* power to the HAs in a retail market. Under certain conditions such as transmission constraints, abundant renewable energy and power shortage, the RA may request DLC, which is a set of time sequences $\mathcal{T}_{DLC}$.

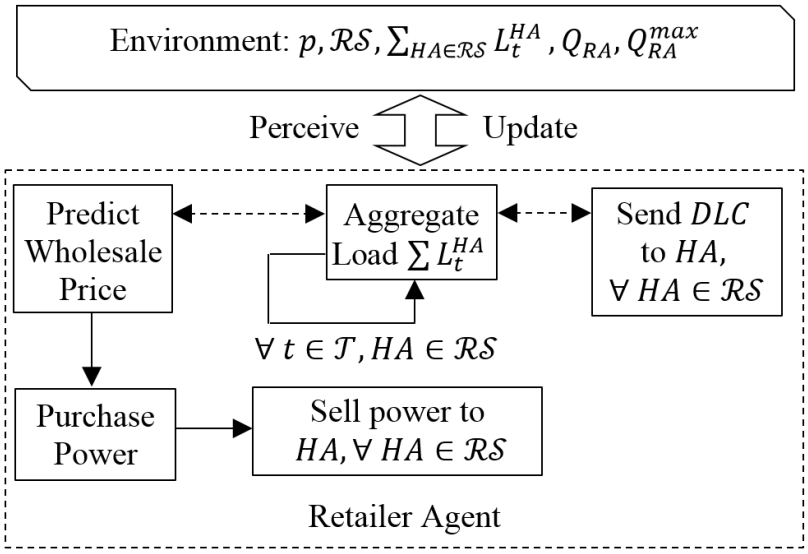

FIGURE 3-3. Retailer Agent. The RA is a model of an electricity retailer or a utility, which includes wholesale electricity price prediction, load aggregation, purchase and sell/delivery power, and direct load control.

3.4 Wholesale Market Agent and Generator Agent

This study focuses on optimal residential DR in a distribution network; therefore WMA and GA are only briefly introduced. RAs requests energy from the WMA, and GAs bids capacity to the WMA. The generation capacity with the lowest price will be assigned first in the market. Finally, the market reaches a steady state and a locational marginal price is achieved based on transmission constraints to different locations.

3.5 Common Features of Agents

In order to execute a MAS, an agent execution environment (AEE) is required. For instance, java agent development framework (JADE) provides an environment to develop agent systems compatible with FIPA protocols [86]. The TRlabs execution environment for mobile agents (TEEMA) is adopted as the platform in this work because of its familiarity to the authors [87, 88]. TEEMA provides standard libraries to support various types of operations for agents such as addressing, naming, messaging, mobility, security and logging [89]. Either of these tools can be used to implement this system.

CHAPTER 4

RESIDENTIAL LOAD PREDICTION MODEL

We develop a residential load prediction model, which incorporates 19 appliances/loads including Vacuum, Kitchen Range, Oven, Microwave, Kettle, TV, Iron, Refrigerator, CD Player, Clock, Answering machine, Wi-Fi, PC, Printer, Light, Clothes washer/dryer, Dish washer and EV. In this model, we define the appliances other than EV as conventional appliances. The load prediction mechanism for the conventional appliances and the EV is discussed in turn. This chapter is reproduced verbatim from our publications in [1] (Copyright © 2015, IEEE), [30] (Copyright © 2015, IEEE) and [90] (Copyright © 2014, IEEE).

4.1 Load Prediction for Conventional Appliances

An individual appliance load is defined as follows.

$$l_t^{ap} = q_{rated}^{ap}, \qquad \forall\, ap \in \mathcal{AP}, t \in [t_0^{ap}, t_0^{ap} + \Delta t^{ap}] \tag{4-1}$$

$$l_t^{ap} = 0, \qquad \forall\, ap \in \mathcal{AP}, t \in \mathcal{T} \backslash [t_0^{ap}, t_0^{ap} + \Delta t^{ap}] \tag{4-2}$$

where l_t^{ap} is the load of an appliance ap at a time slot t. q_{rated}^{ap} is the rated power of the appliance. t_0^{ap} is the time of starting to operate an appliance ap (shown in Equation 4-3). Δt^{ap} is a cycle length of operating the appliance. An appliance may operate multiple cycles (e.g., refrigerator) in the horizon T. The power of an appliance is zero when it is not used and we also assume that the appliance standby power is zero (shown in Equation 4-2).

$$t_0^{ap} \leftarrow pr(t \mid ap, [occ(t)]), \forall\, ap \in \mathcal{AP} \backslash EV \tag{4-3}$$

where $pr(t \mid ap, [occ(t)])$ is the probability of using an appliance $ap \in \mathcal{AP} \backslash EV$ at a time slot t. $occ(t)$ represents the number of active occupants at t in a home. Usually, an occupant is required to start an appliance; however, some appliances (e.g., refrigerator) operate on their own cycle. This option is shown by the square bracket around $occ(t)$. Except parameters for the EV, the values of $pr(t \mid ap, [occ(t)])$, $occ(t)$, Δt^{ap}, and q_{rated}^{ap} are derived from statistical information in the downloadable model of [91, 92].

FIGURE 4-1 show the process for the load prediction. The mechanism for predicting an appliance's initial operating time t_0^{ap} is that the model generates a random number following a uniform distribution between 0 and 1, and compares this random number with the scaled probability of running an appliance at time t (shown by the right side of Equation 4-3). If the random number is less than or equal to the probability, the appliance will be running in a cycle Δt_{ap}; otherwise, it will not. Electricity consumption of all appliances is then aggregated. This process is repeated in the horizon T.

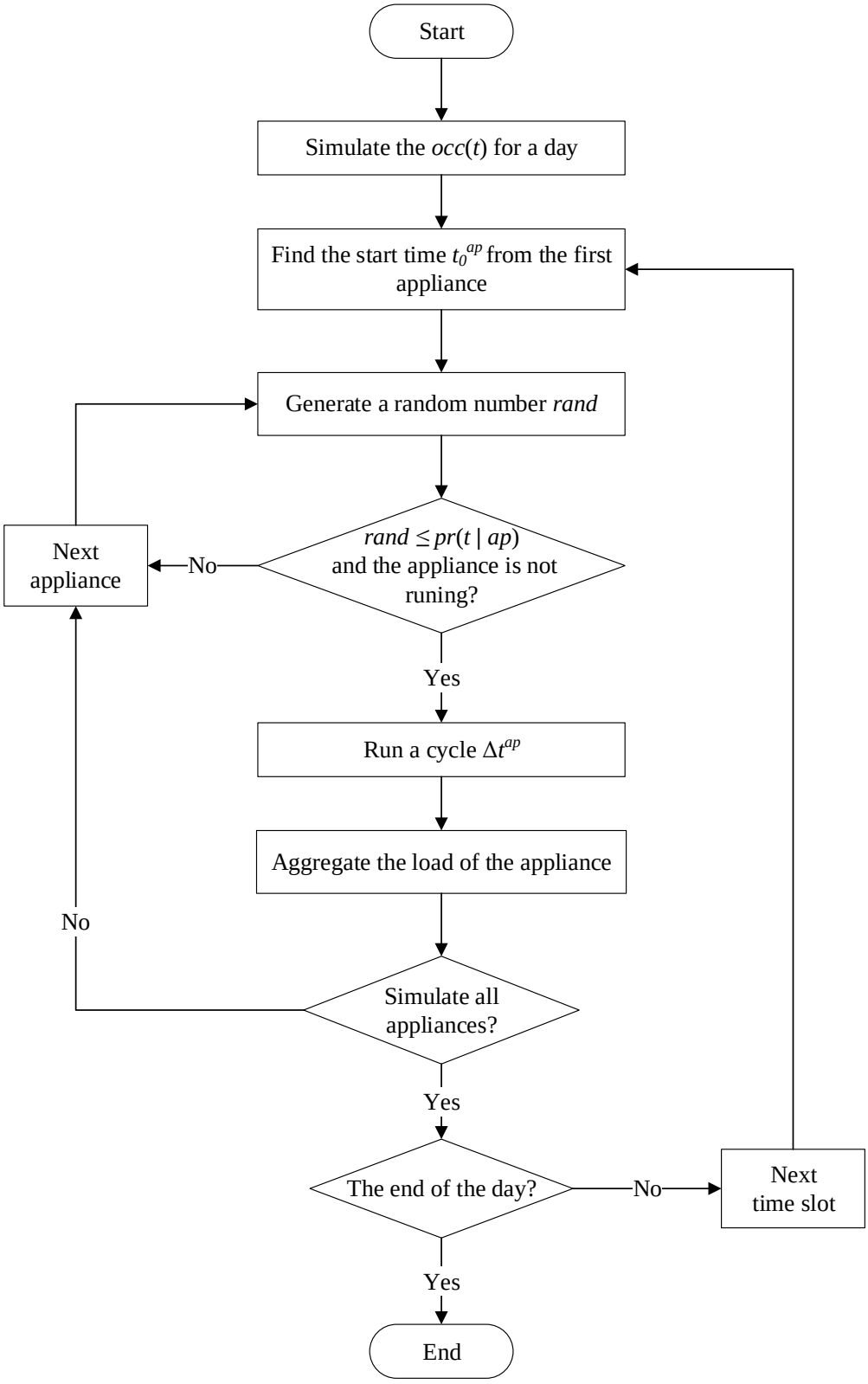

FIGURE 4-1 The flow chart for the load prediction process

The parameters for EV charging are discussed in the section 4.2.

Lastly, we divide the set of appliances $\mathcal{AP}$ into two sets: $\mathcal{BAP}$ and $\mathcal{CAP}$, which represents a set of background appliances and controllable appliances respectively.

The predicted load is shown in Equation 4-4.

$$\hat{L} =< \widehat{l_1^{ap}}, \cdots, \widehat{l_T^{ap}} > \tag{4-4}$$

Predicted energy is defined as follows.

$$\widehat{E_B^{ap}} = \sum_t \widehat{l_t^{ap}}, \forall\, ap \in \mathcal{BAP}, t \in [t_0^{ap}, t_0^{ap} + \Delta t^{ap}] \tag{4-5}$$

$$\widehat{E_C^{ap}} = \sum_t \widehat{l_t^{ap}}, \forall\, ap \in \mathcal{CAP}, t \in [t_0^{ap}, t_0^{ap} + \Delta t^{ap}] \tag{4-6}$$

where $\widehat{E_B^{ap}}$ and $\widehat{E_C^{ap}}$ is the predicted electricity energy of background loads and controllable loads. It is noted that both $\widehat{E_B^{ap}}$ and $\widehat{E_C^{ap}}$ are column vectors (e.g., $\widehat{E_B^{ap}} =< \widehat{E_{B,1}^{ap}}, \cdots, \widehat{E_{B,T}^{ap}} >$).

4.2 Load Prediction for Electrical Vehicle Charging

We now discuss the parameters for EV charging with Lithium-Ion Battery and Lead-Acid respectively. Unless we state otherwise, we consider $ap = EV$ in this section. The parameters of initial charging time t_0^{ap} and the time when the EV must be fully charged are independent on the type of EV and its battery. By contrast, the parameters of charging demand q_{rated}^{ap} and charging cycle Δt^{ap} dependant on the type of EV and its battery. Therefore, we discussed the initial charging time and the time when the EV must be fully charged in general and then address the charging demand and charging cycle based on EVs with the two types of batteries.

Assuming people plug-in and charge EVs immediately after arriving home, the probability distribution of initial charging time is the same as home-arrival time. This probability of initial charging time is formulated as a normal distribution $t_0^{ap} \sim \mathcal{N}(\mu_{t0}, \sigma_{t0})$ as follows.

$$g\left(t_0^{ap}, \mu_{\mathrm{t0}}, \sigma_{\mathrm{t0}}\right) = \frac{1}{\sigma_{\mathrm{t0}}\sqrt{2\pi}} e^{-\frac{(t-\mu_{\mathrm{t0}})^2}{2\sigma_{\mathrm{t0}}^2}} \tag{4-7}$$

where μ_{t0} is the average home arrival time and σ_{t0} is the standard deviation.

To characterize this observation, we sample the actual probability density of home arrival time (shown by the blue bars in FIGURE 4-2) 2000 times that are enough to determine this distribution, in which the probabilities of the range from 1hr to 10hr are taken out as outliers [93]. The average value μ_{t0} and standard deviation σ_{t0} is determined as 17hr and 2.8 hours respectively. The simulated normal distribution is shown by the red line in FIGURE 4-2. EVs must be fully charged in order to be used the next day. The home-departure time is also assumed to be normally distributed with $\mu = 7hr$ and $\sigma = 1\ hour$.

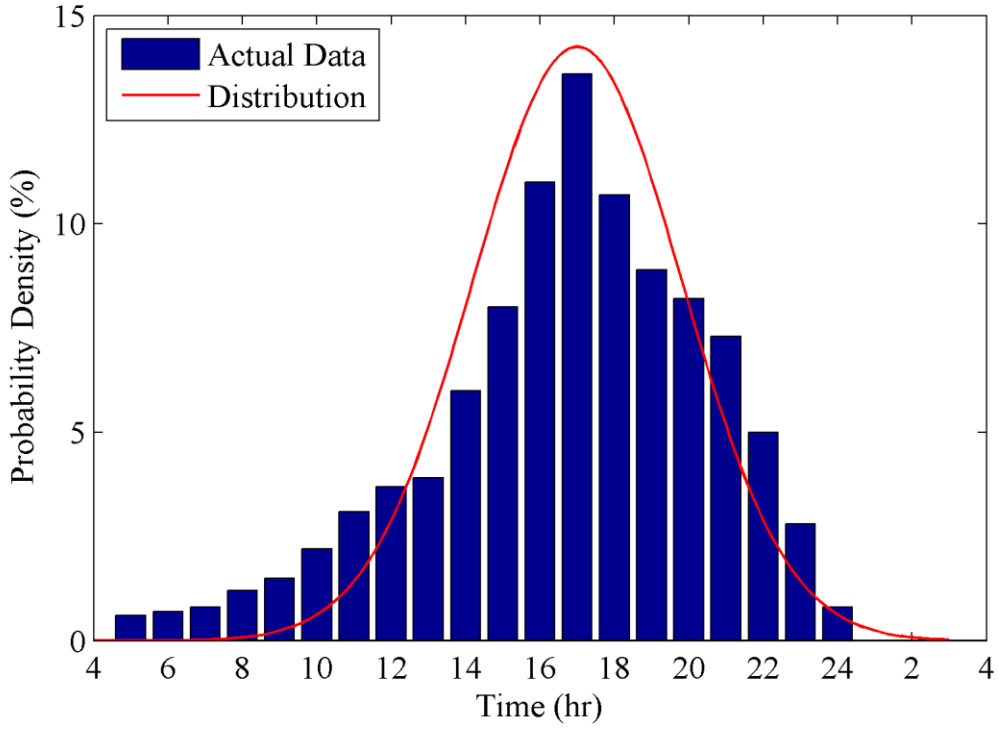

FIGURE 4-2. Actual probability density of home arrival time and simulated normal distribution [93]

(Reprinted from our publication in [30] Copyright © 2015, IEEE)

We now discuss the parameters of charging demand q_{rated}^{ap} and charging cycle Δt^{ap}, which dependant on the type of EV and its battery. Important EV charging characteristics are introduced as follows [94].

- Demand. The power demand of EV charging varies with the SOC.
- Capacity. Capacity is the total charge that fully charged battery can provided. It can be defined by either Ampere-hour or kWh.
- State of charge (SOC). SOC is defined as Remain Capacity/Rated Capacity.

4.2.1 EV with Lithium-Ion Battery

FIGURE 4-3 shows SOC and demand with charging time of a Nissan Altra-EV with a Lithium-Ion Battery [95]. The rated charging power can be assumed constant as $q_{rated}^{ap} = 6.6\ kW$.

The cycle length Δt^{ap} depends on the initial SOC soc_0 when people plug-in EV, which can be identified as a normal distribution $soc_0 \sim \mathcal{N}(\mu_{soc}, \sigma_{soc})$ from driving patterns [90]. Since available EV travel range is proportional to its SOC [95]; the average soc_0 can be calculated as follows

$$\mu_{soc} = \frac{MaxRange - VMT}{MaxRange} \tag{4-8}$$

where *MaxRange* is the available driving range of a fully charged vehicle (122 miles in this case). *VMT* is vehicle miles of travelling per vehicle shown by blue bars in FIGURE 4-5 [96]. The red dash line represents the results of linear regression assuming that the *VMT* is linearly depends on the year, i.e., the *VMT* increase linearly with time of years. The red bar shows the predicted *VMT* (64.7 miles) in the year of 2015. Similarly, σ_{soc} can be calculated from the standard deviation of *VMT*.

The cycle length $\Delta t^{ap}, \forall ap = EV$ can be calculated as follows.

$$\Delta t^{ap} = \Delta t_{total}(1 - soc_0), \forall\ ap = EV \tag{4-9}$$

where Δt_{total} is the time to charge up an EV from zero SOC.

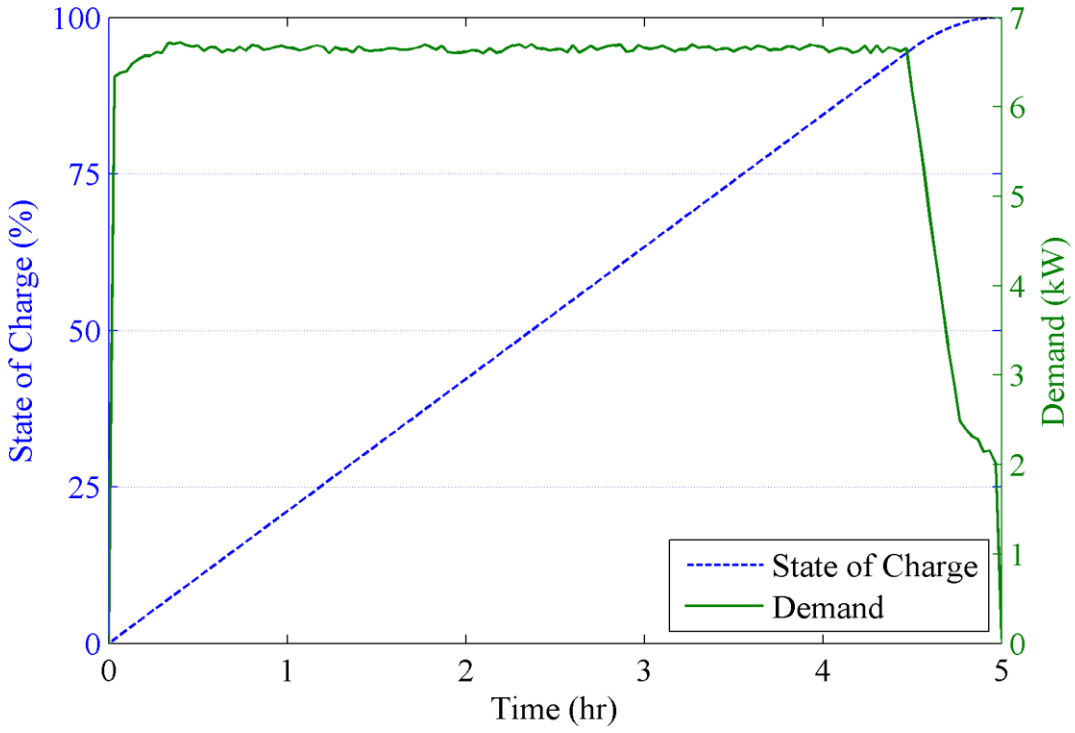

FIGURE 4-3 State of charge and rated charging demand of Nissan Altra-EV with Lithium-Ion Battery [95]

(Reprinted from our publication in [30] Copyright © 2015, IEEE)

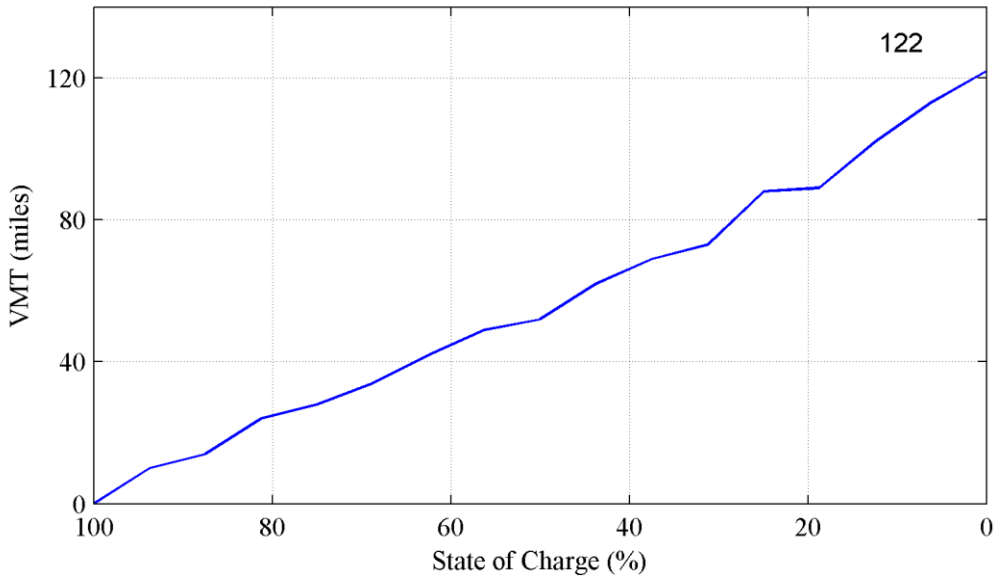

FIGURE 4-4 VMT V.S. SOC of Nissan Altra-EV with Lithium-Ion Battery [95]

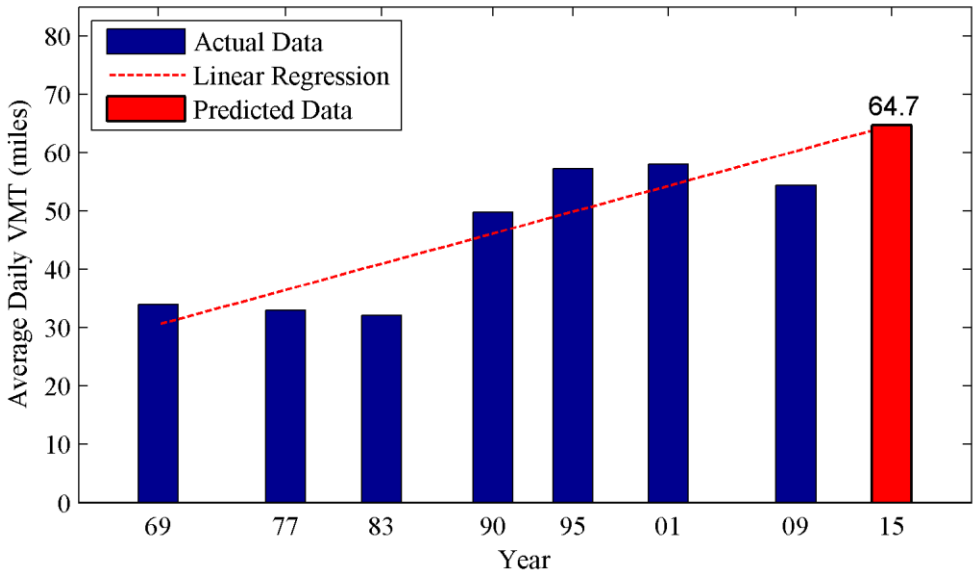

FIGURE 4-5 Average daily vehicle miles of traveling (actual data and prediction with linear regression)

4.2.2 EV with Lead Acid Battery

The method to identify the initial SOC soc_0 is the same as the EV with Lithium-Ion battery. However, unless the constant rated demand of EV with Lithium-Ion battery, the rated demand of EV with Lead-Acid battery is dependent on charging point. FIGURE 4-6 shows SOC and demand with charging point of GM EV1 Panasonic Lead Acid Battery [97].

Therefore, we need determine the charging point to find the rated power. The charging point can be determined based on the initial SOC. The mathematic expression of SOC (blue solid line in FIGURE 4-6) with respect to the charging points is simplified as follows.

$$soc(x) = \begin{cases} 0.43x & \forall\ 0 \le x < 211 \\ 0.036(x - 211) + 90.3 & \forall\ 211 \le x \le 480 \end{cases} \tag{4-10}$$

where $soc(x)$ is the 100 times of SOC. Its inverse function is as follows.

$$x(soc) = \begin{cases} 2.33\ soc & \forall\ 0 \le sox < 91 \\ 27.78\ soc - 2298.33 & \forall\ 91 \le soc < 100 \end{cases} \tag{4-11}$$

The initial charging point x_0 can be found by substituting the initial SOC (soc_0) to Equation 4-11; and therefore the rated charging power can be found using the function of demand with respect to the charging points as follows.

$$p(x) = \begin{cases} 0.0043\ x + 5.8 & \forall\ 0 \le x < 162 \\ -0.0424\ (x - 163) + 0.5 & \forall\ 162 \le x < 282 \\ 1.5 & \forall\ 282 \le x < 402 \\ -0.0192\ (x - 402) + 1.5 & \forall\ 402 \le x < 480 \end{cases} \tag{4-12}$$

where $p(x)$ is the demand and x is the charging point in minute (0~480).

This is visualized in FIGURE 4-7.

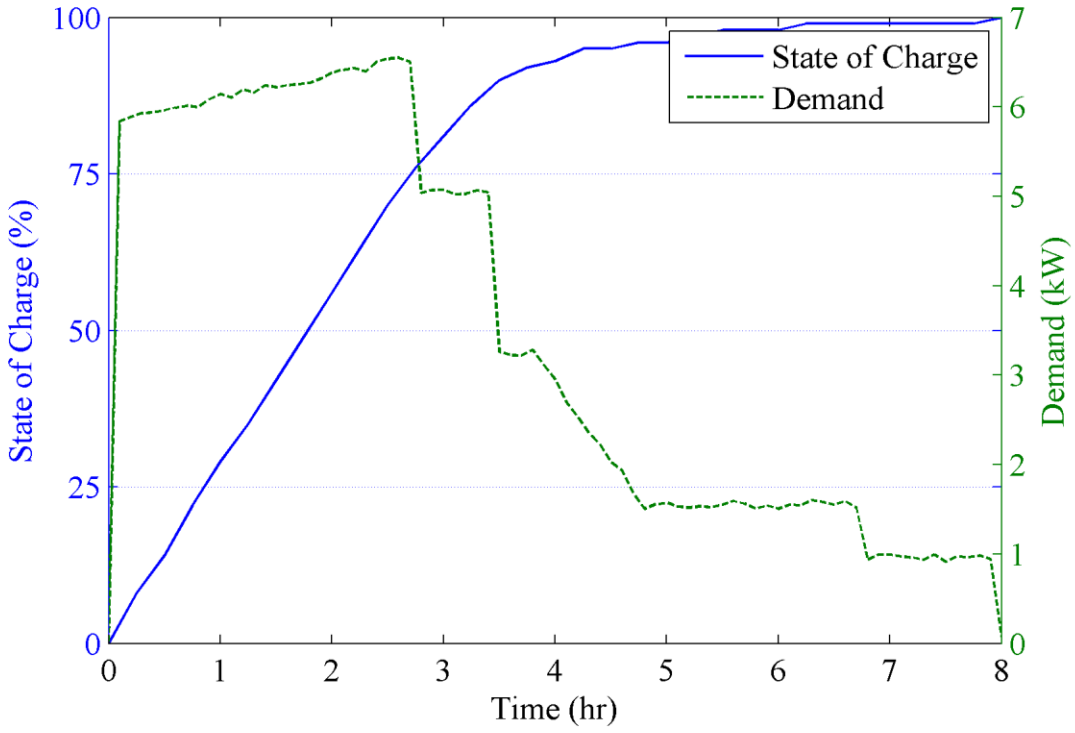

FIGURE 4-6 State of charge and rated demand of GM EV1 Panasonic Lead Acid Battery

(Reprinted from our publication in [90] Copyright © 2014, IEEE)

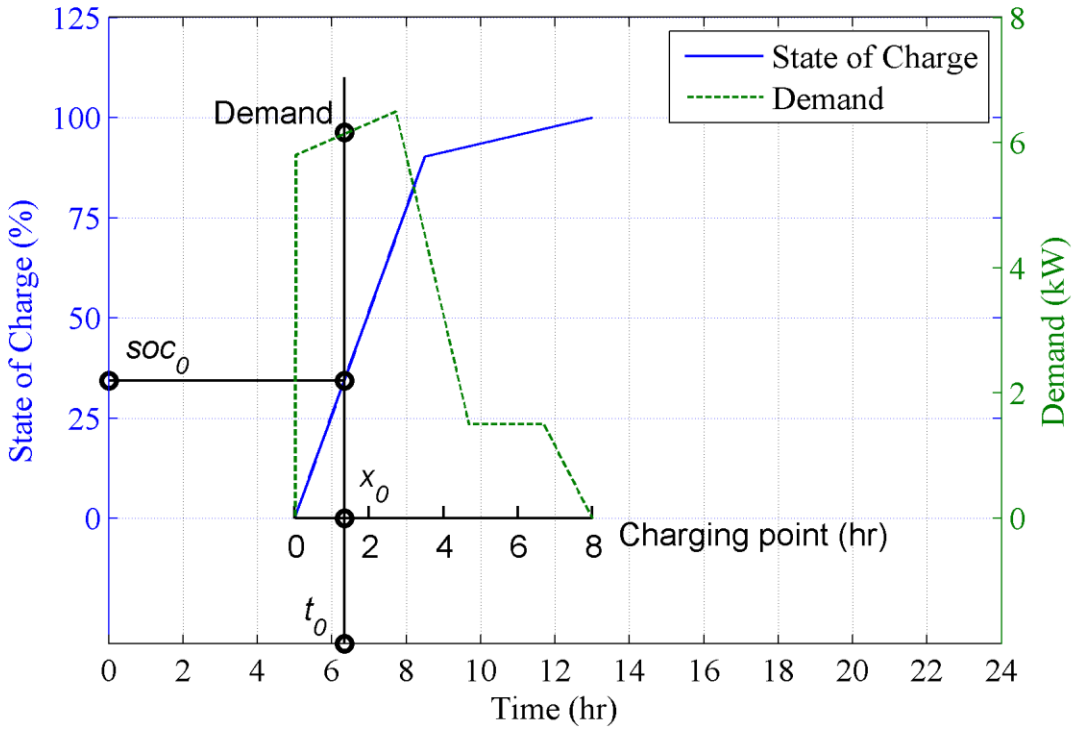

* t_0 is the start time of charging

FIGURE 4-7 Visualization of the method to find the charging rated power from the initial SOC for EV charging in a day

(Reprinted from our publication in [90] Copyright © 2014, IEEE)

4.3 Discussion

In this chapter, we have discussed the proposed residential load prediction model to forecast the electricity load profile for heterogeneous HAs. This load prediction model simulates the benchmark based on statistical information of how people use their appliances including EVs. Each HA has a unique load profile depending on its heterogeneous local configurations.

To evaluate the variation of the load prediction model, we conduct 10 runs of a simulation to predict/estimate the load. The hourly mean value, stand deviation and coefficient of variation (CV) are calculated among the 10 simulations. The CV is defined as the ratio of the standard deviation to the mean. The maximum CV is 21.4% at 0hr and the minimum value is 5.2% at 4hr. The average of CV is 10.7%. These great similarity among multiple simulations show that the load prediction model is robust and stable. FIGURE 4-8 shows the load profiles of the simulation results. We use the simulation results in the first run as the benchmark/reference in this study and continuously use these reference data in the application of the proposed optimal control mechanisms.

TABLE 4-1 The hourly statistical information among 10 simulations

Time (hr)	Mean (kW)	Standard Deviation (kW)	Coefficient of Variation (CV)
0	33.0	7.1	21.4%
1	24.8	4.5	18.0%
2	19.6	2.7	13.8%
3	16.8	1.3	7.7%
4	15.8	0.8	5.2%
5	17.7	1.7	9.5%
6	28.3	2.1	7.3%
7	57.0	4.8	8.5%
8	61.9	4.6	7.4%
9	56.2	4.7	8.3%
10	49.5	8.5	17.1%
11	51.0	5.9	11.6%
12	63.4	7.3	11.4%
13	61.8	7.6	12.3%
14	67.5	8.9	13.2%
15	79.7	10.6	13.4%
16	119.1	10.9	9.2%
17	151.0	13.2	8.7%
18	160.0	12.8	8.0%
19	150.4	11.0	7.3%
20	134.3	15.2	11.3%
21	119.5	9.0	7.5%
22	91.6	6.0	6.6%
23	58.2	7.0	12.1%

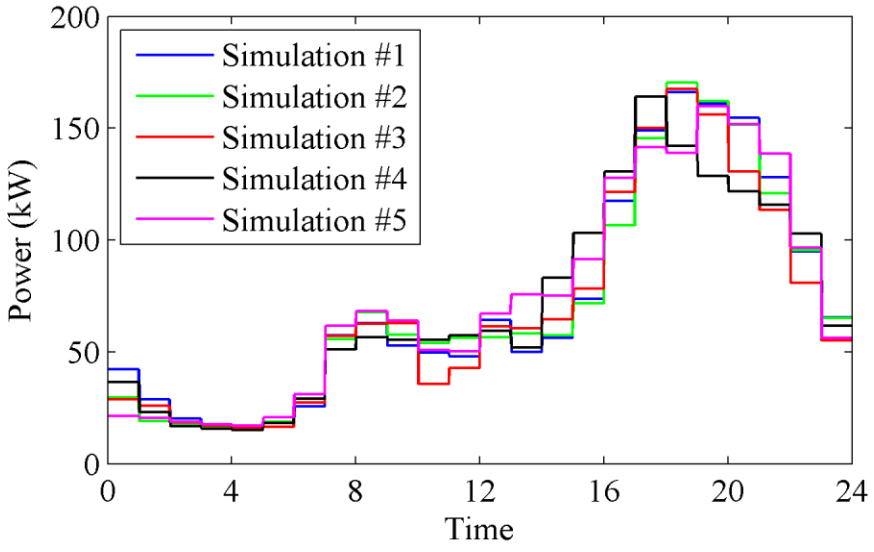

(a)

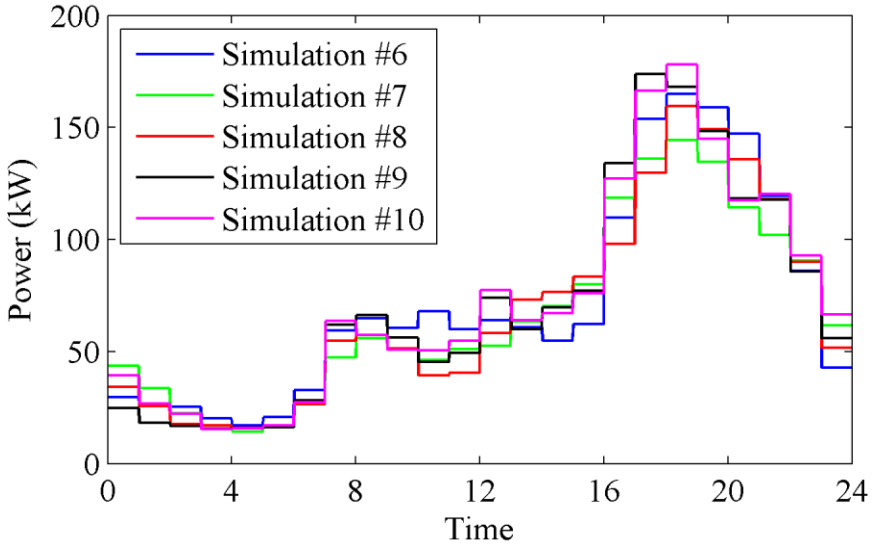

(b)

FIGURE 4-8 Comparison of load profiles among multiple simulations. (a) simulation #1~#5; (b) simulation #6~#10

CHAPTER 5

OPTIMAL DR IMPLEMENTATION UNDER RTP

5.1 Real-Time Price Prediction Model

This section is reproduced verbatim from our publications in [1] (Copyright © 2015, IEEE).

The power generation cost increases as the demand increases. RTP reveals this relationship and encourages customers to redistribute the electricity usage, which would reduce peak demand and result in a more flat load profile. The autonomous HA on behalf of customers is able to intelligently respond to RTP.

The electricity demand is highly variable and also the electricity cannot be economically stored; therefore, a mix of power generation plants/units (e.g., hydro, nuclear, coal, oil, gas, peaking hydro, etc.) is used to meet the demand [98]. Each type of plants also have a number of units. These plants/units are dispatched mainly based on their generation cost [98]. In addition, once the demand exceeds the base load, the generation cost of the units (e.g., gas and peaking hydro) to meet the peak demand increases faster. These characteristics of the composited generation cost with respect to the mix of the generation units to meet the demand can be captured by step functions (shown by the blue lines in FIGURE 5-1).

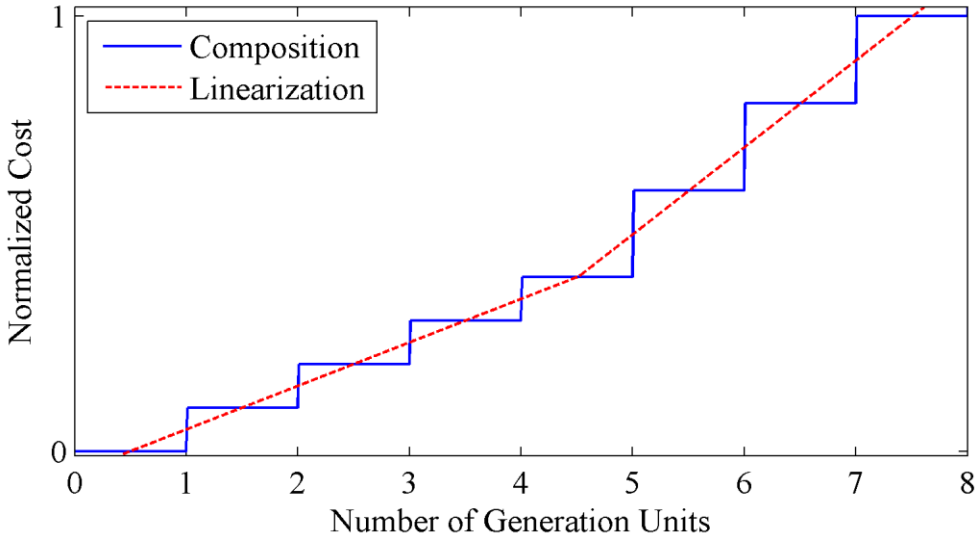

FIGURE 5-1 Normalized composited generation cost with respect to the mix of the generation units

(Reprinted from our publication in [1] Copyright © 2015, IEEE)

We define piecewise linear functions in Equation 5-1 as the price prediction model to linearize (see red dash line in FIGURE 5-1) these steps.

$$p(l_t) = \begin{cases} \alpha_1 l_t + \beta_1, & \forall\, l_t \le l_{TH}, t \in \mathcal{T} \\ \alpha_2 l_t + \beta_2, & \forall\, l_t > l_{TH}, t \in \mathcal{T} \end{cases} \tag{5-1}$$

where α_1 is the increasing slope of electricity price in the first step ($l_t \le l_{TH}$) and α_2 is the slope in the second step where $l_t > l_{TH}$. β_1 and β_2 are constants. Also, $\alpha_1 < \alpha_2$ implies the electricity price increases faster after the load exceeds the threshold l_{TH}.

FIGURE 5-2 shows the actual electricity load and locational marginal price (LMP) in the wholesale market in the region of Duquesne Light (DUQ) and American Electric Power (AEP) of the US in the year of 2014 [31]. We can see that the LMP has the same range and pattern increasing with the electricity load. However, the load in the region of DUQ (approximately from 1×10^3 MW to 2.8×10^3 MW) is much less than the region of AEP (approximately from 1×10^4 MW to 2.2×10^4 MW). Therefore, the electricity price does not directly depend on the absolute demand as long as the transmission constraint is satisfied. In our study, we use the load and price data in the region of AEP as samples; however, the load is normalized and scaled in order to fit our simulation. For instance, to predict the electricity price based individual household load, the load range is normalized and scaled from 0 to 8.5 kW, which is the range of power load in a typical home with an EV in place.

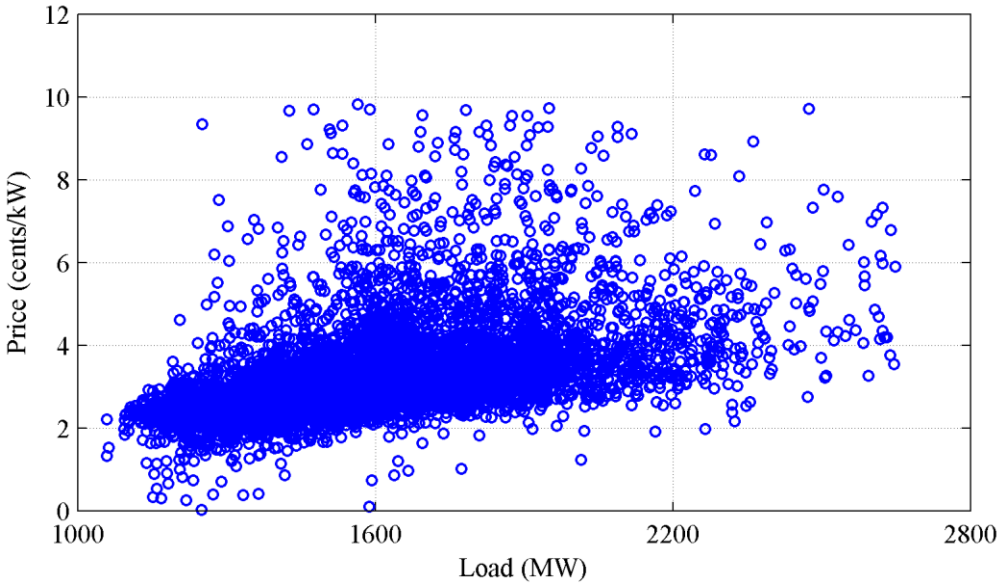

(a)

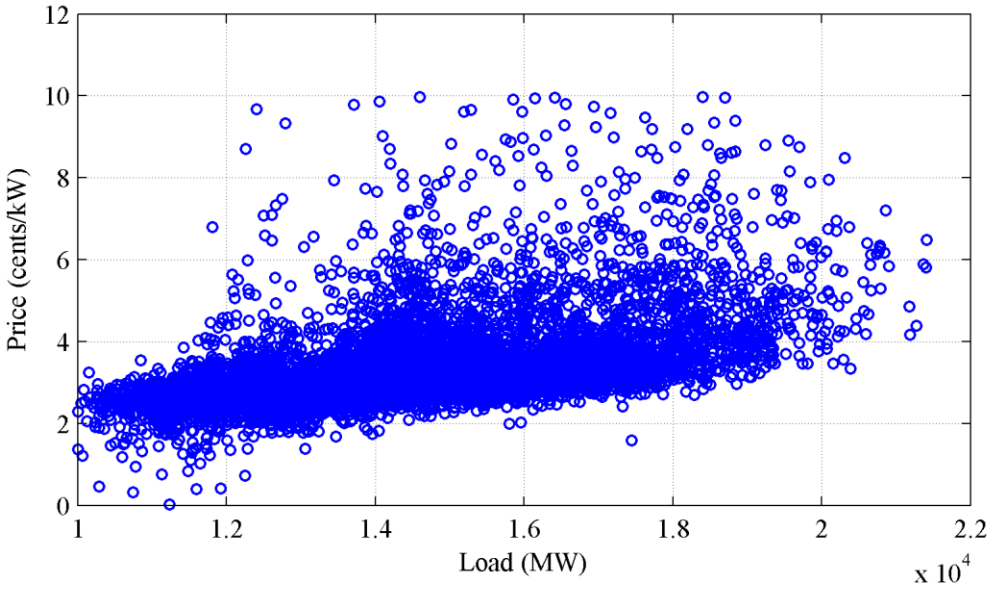

(b)

FIGURE 5-2 Actual electricity load and locational marginal price (wholesale) in regions of the US in the year of 2014. (a) the region of DUQ (b) the region of AEP [31].

The norm approximation approach is used to determine the optimal coefficients in Equation 5-1. Let $A \in \mathbb{R}^{m\times 2}$ and $b \in \mathbb{R}^{m}$ denotes actual data.

$$A = \begin{bmatrix} \dot{l_1} & 1 \\ \cdots & \cdots \\ \dot{l_m} & 1 \end{bmatrix} \tag{5-2}$$

$$b = < \dot{p_1}, \cdots, \dot{p_m} > \tag{5-3}$$

where $\dot{l_i}$ and $\dot{p_i}$ are known load and prices respectively. *i* and *m* is the index and the number of samples respectively.

Let $x \in \mathbb{R}^2$ denotes the unknown coefficients.

$$x = \begin{cases} < \alpha_1, \beta_1 >, & \forall\, l_i \le l_{TH} \\ < \alpha_2, \beta_2 >, & \forall\, l_i > l_{TH} \end{cases} \tag{5-4}$$

Then, the coefficients that lead to a best fit of known data can be calculated by the following [42].

$$minimize\ \|Ax - b\| \tag{5-5}$$

where $\|\cdot\|$ is a norm on $\mathbb{R}^m$.

For $l_i \le l_{TH}$, we use the squared l_2-norm approximation in Equation 5-6, which is also known as a least square problem. It has a closed from solution in equation 5-7 [42].

$$minimize\ \|Ax - b\|_2^2, \qquad \forall\, l_i \le l_{TH} \tag{5-6}$$

$$x^\star = (A^T A)^{-1} A^T b, \qquad \forall\, l_i \le l_{TH} \tag{5-7}$$

For $l_i > l_{TH}$, we also use the least square approximation; however, with a constraint.

$$minimize \ \|Ax - b\|_2^2, \qquad \forall \ l_i > l_{TH} \tag{5-8}$$

$$subject \ to: x[1] \ l_1 + x[2] = c \tag{5-9}$$

where $x[1]$ and $x[2]$ is α_2 and β_2 respectively. c is the $p(l_{TH})$ from the approximation of the first step. This can be solved using Newton's method [42] (p.525-p.531). FIGURE 5-3 shows an example of the prediction results. The blue circles are the real-time LMP corresponding to the real-time load. The blue solid line shows the prediction in the first step and the red dash line shows the second step.

In this study, we do not intend to explore this norm approximation technique. One can divide the data into several groups; use one of them to train the parameters and evaluate the degree of error using other groups.

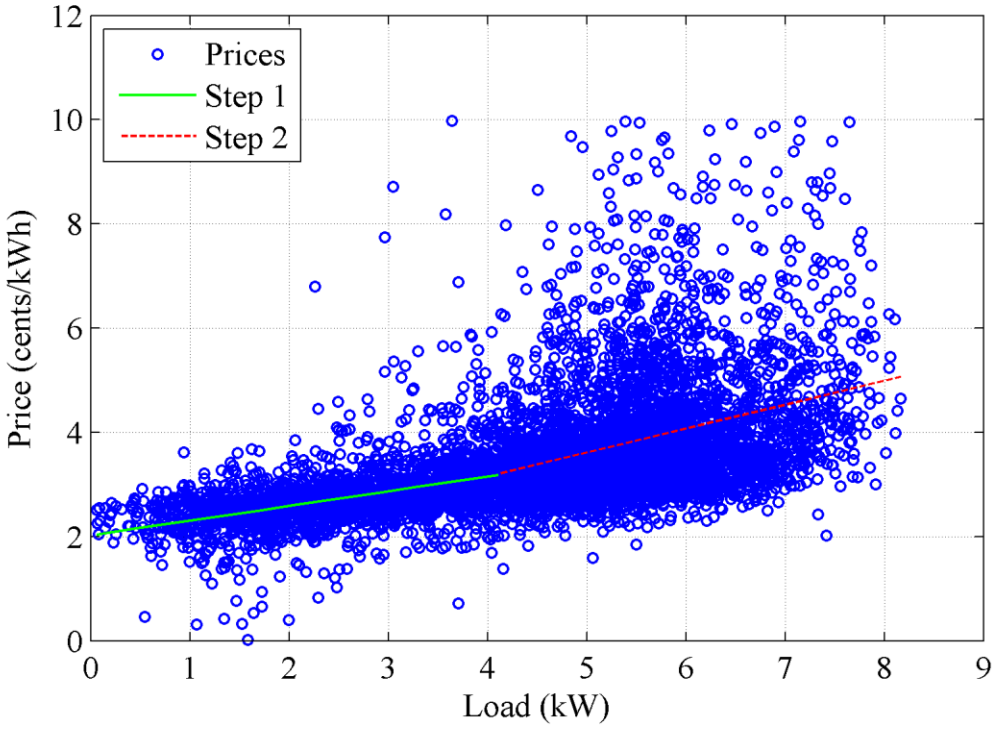

FIGURE 5-3 An example of norm approximation

(Reprinted from our publication in [1] Copyright © 2015, IEEE)

5.2 Open-Loop Load Control Model under RTP

This section is reproduced verbatim from our publications in [1] (Copyright © 2015, IEEE).

The OL-LCM-RTP provides the ability for a HA to make intelligent decisions to minimize electricity payments, which is modeled by a CP problem.

$minimize$

$$\sum_{t\in\mathcal{T}} p\left(\sum_{ap\in\mathcal{AP}} l_t^{ap}\right)\left(\sum_{ap\in\mathcal{AP}} l_t^{ap}\right)+\sum_{t\in\mathcal{T}}\sum_{ap\in\mathcal{CAP}} \lambda^{ap}\, w^{ap} l_t^{ap} \tag{o1}$$

$subject\ to$:

$$0 \le l_t^{ap} \le q_{rated}^{ap}, \forall\ ap \in \mathcal{CAP}, t \in [t_0^{ap}, t_1^{ap}\,] \tag{c1}$$

$$l_t^{ap} = 0, \forall\ ap \in \mathcal{CAP}, t \in \mathcal{T}\backslash[t_0^{ap}, t_1^{ap}] \tag{c2}$$

$$\sum_{ap}\sum_{t} l_t^{ap} = \widehat{E_C^{ap}}, \forall\ ap \in \mathcal{CAP}, t \in [t_0^{ap}, t_1^{ap}] \tag{c3}$$

$$\sum_{ap\in\mathcal{CAP}} l_t^{ap} + \sum_{ap\in\mathcal{BAP}} \widehat{l_t^{ap}} \le Q_{HA}^{max}, \forall\ t \in \mathcal{T} \tag{c4}$$

In the objective function, the electricity price $p\left(\sum_{ap\in\mathcal{AP}} l_t^{ap}\right)$ is defined in Equation 5-1, which is a piecewise linear function with load. The electricity payment $\sum_{t\in\mathcal{T}} p\left(\sum_{ap\in\mathcal{AP}} l_t^{ap}\right)\left(\sum_{ap\in\mathcal{AP}} l_t^{ap}\right)$ is a piecewise linear function times its independent variable load, which is a piecewise quadratic function. Each quadratic function is convex; furthermore, we have $\alpha_1 < \alpha_2$ and the convexity is preserved. The second term is a linear function of load l_t^{ap}, where λ^{ap} is a vector of dissatisfaction factors and w^{ap} is a waiting time vector define as follows.

$$w^{ap} = t - t_0^{ap} \tag{5-10}$$

For instance, if the EV plug-in time $t_0^{ap} = 17hr, \forall\ ap = EV$, the waiting time vector along with time is shown as follows.

w^{ap}	0	1	2	3	...
t	17hr	18hr	19hr	20hr	…

Since we minimize $\sum_{t\in\mathcal{T}}\sum_{ap\in\mathcal{CAP}} \lambda^{ap}\, w^{ap} l_t^{ap}$, an earlier operating time is more preferable. This term penalizes the scheduling levels to find a trade-off between the minimum electricity payment and comfort levels with waiting time.

The decision variables are $l_t^{ap}, \forall ap \in \mathcal{CAP}, t \in \mathcal{T}$. In the objective function, $l_t^{ap}, \forall ap \in \mathcal{BAP}$ are not decision variables; however, they are required to calculated electricity payment.

The first constraint is a relaxation of an binary constraint, in which $l_t^{ap} \in \{0, q_{rated}^{ap}\}$, which results in that the optimization problem can be solve much more efficiently. t_0^{ap} is the appliance usage requesting time and t_1^{ap} is the time when operation of the appliance must complete. $[t_0^{ap}, t_1^{ap}]$ is a possible operational range of the controllable appliance ap. For instance, an EV can be charged from the home-arrival time to home-departure time. We assume that the controllable loads can only be delayed.

The second constraint (c2) sets the load of an appliance to zero when it is not operating. Although, operating a controllable appliance could be delayed, it completes sooner or later in the operational range; therefore, it consumes the same energy as predicted. This fact is accomplished in the third constraint (c3). The (c4) constraint is that the max-power capacity of a home cannot be violated at any given time.

The objective function is a piecewise quadratic function with preserved convexity plus a linear function; therefore, the objective function is convex. In addition, all the constraints are affine functions. Therefore, the proposed optimization problem is a CP problem. If the HA receives DLC signals, the CP problem has one more constraint (c5) assuming the DLC is to request a load reduction.

$$l_t^{ap} = 0, \forall\, ap \in \mathcal{CAP}, t \in \mathcal{T}_{DLC} \quad \text{(c5)}$$

With the constraint (c5), the new CP problem is not guaranteed to be feasible, since if the schedule does not have sufficient flexibilities, a HA may not able to accept the DLC request. If the CP problem is infeasible, the HA needs to determine the maximum power that can be shifted from the $\mathcal{T}_{DLC}$.

5.3 Closed-Loop Load Control Model under RTP

The CL-LCM-RTP is developed based on the OL-LCM-RTP by incorporating feedbacks from the RA. The objective function is modified from the OL-LCM-RTP. The constraints remain the same and are duplicated here for the audience's conveniences.

$minimize$

$$\sum_{t\in\mathcal{T}} p\left(\sum_{ap\in\mathcal{AP}} l_t^{ap} + \sum_{HA\_i}\sum_{ap\in\mathcal{AP}} l_t^{ap}\right)\left(\sum_{ap\in\mathcal{AP}} l_t^{ap}\right) + \sum_{t\in\mathcal{T}}\sum_{ap\in\mathcal{CAP}} \lambda^{ap}\, w^{ap} l_t^{ap} \qquad \text{(o2)}$$

$subject\ to$:

$$0 \le l_t^{ap} \le q_{rated}^{ap}, \forall\ ap \in \mathcal{CAP}, t \in [t_0^{ap}, t_1^{ap}\,] \qquad \text{(c1)}$$

$$l_t^{ap} = 0, \forall\ ap \in \mathcal{CAP}, t \in \mathcal{T}\backslash[t_0^{ap}, t_1^{ap}] \qquad \text{(c2)}$$

$$\sum_{ap}\sum_{t} l_t^{ap} = \widehat{E_C^{ap}}, \forall\ ap \in \mathcal{CAP}, t \in [t_0^{ap}, t_1^{ap}] \qquad \text{(c3)}$$

$$\sum_{ap\in\mathcal{CAP}} l_t^{ap} + \sum_{ap\in\mathcal{BAP}} \widehat{l_t^{ap}} \le Q_{HA}^{max}, \forall\ t \in \mathcal{T} \qquad \text{(c4)}$$

In the objective function, $\sum_{HA\_i}\sum_{ap\in\mathcal{CAP}} l_t^{ap}$ is the feedback of the load information from the RA and $HA_{\_i}$ is the set of HAs except the current HA. The HAs schedule their controllable loads based on global information. The new background load becomes the sum of the background load of the HA itself and the aggregated load of the other HAs. The RA informs a HA with the other HAs' load information, which is collected for billing purpose anyways. FIGURE 5-4 shows the diagram of the mechanism of CL-LCM-RTP.

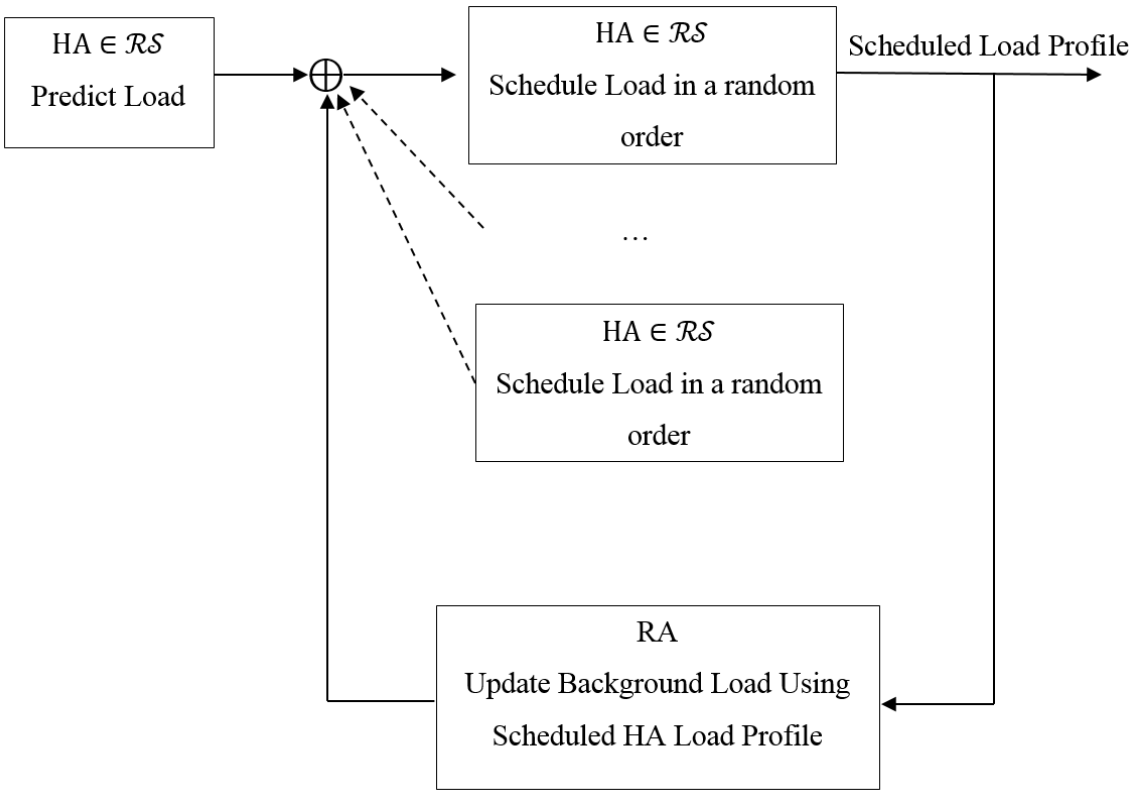

FIGURE 5-4 The diagram of the closed-loop optimal control mechanism (the dash line represents that the HA feedbacks to the system indirectly through the RA)

The closed-loop load scheduling is a round process and FIGURE 5-5 shows the algorithm. The HAs schedule their controllable loads in turn in a random order and update the load information to the RA in each round. In the first round, the RA informs the first HA with prior load information (e.g., the load profile predicted without DR application) and continuously updates the load information. In other words, the RA has more and more precise information regarding on the global load profile and therefore the latter HAs get more accurate load data. Once the first round is completed, the process goes to the next round. The HAs can reschedule the load based on the updated global load profile. The HAs continually optimize their load schedule. If the new scheduled load can reduce the electricity payment, then the HA will use the new schedule; otherwise, the HA stays the old one. This process terminates till nobody is willing to reschedule its controllable loads.

Round repeat

for $HA \in \mathcal{RS}$ in a random order

1: Input: The predicted load profile of the HA plus the global load information from the RA

2: Solving the closed-loop CP problem

3: Calculate the electricity payment

if this is the first round

Save the electricity payment for the HA in this round

else

if the electricity payment < the one from the last round

Update the load profile for the HA

Update the RA with the scheduled load profile

else

keep the load profile from the last round

4: Output: Scheduled load profile for the HA

Next round till no HA is willing to reschedule the controllable load

FIGURE 5-5 The closed-loop optimal load control algorithm

5.4 Experiments and Numerical Analysis

This section presents simulation results and numerical analysis for five scenarios:

#1: Without load control. The HAs do not take actions to control load. This is the reference scenario in this study.

#2: OL-LCM-RTP with day-ahead RTP. The RA announces real-time prices one day ahead and will charge the HAs with the announced prices.

#3: OL-LCM-RTP with $\lambda^{ap} = 0$. The HAs are able to predict electricity prices. The HAs are charged by actual wholesale electricity prices based on the aggregated load. This scenario assumes the dissatisfaction factor λ^{ap} is zero.

#4: OL-LCM-RTP with $\lambda^{ap} > 0$. This scenario is designed to study the impacts of the dissatisfaction factor λ^{ap} on load scheduling.

#5: CL-LCM-RTP with $\lambda^{ap} = 0.1$. This scenario studies the effect of cooperation and coordination to improve the energy efficiency. In addition, the impacts of EV penetration levels and flexible charging periods are evaluated as well.

The scenarios from #1 to #3 and part of the scenario #4 are reproduced verbatim from our publications in [1] (Copyright © 2015, IEEE).

The CP problem and the LP problem can be solved efficiently by the interior point method [42]. To solve them, we used the CVX, a package for specifying and solving convex programs [99, 100].

5.4.1 Experimental Configurations

In these five scenarios, we consider one RA and 100 HAs in a distribution network. We assume that the RA can obtain sufficient power from a wholesale market and all

transmission constraints are satisfied. We also assume that the retail market is budget balanced, i.e., the RA does not make profits. The power capacity of each HA is $Q_{HA}^{max} = 24\ kW$. The simulation period is one day. The time slot $t = 1hr$ and time horizon $H = 24\ hours$. The coefficients for the price prediction model are list in TABLE 5-1. The OL-LCM-RTP uses the coefficients for the single HA load. The CL-LCM-RTP uses the coefficients for the aggregated load from the 100 HAs since the new background load is aggregated from all the HAs.

20 HAs are equipped with an EV, which represents a 20% EV penetration to the power system. Among the appliances, Dish Washers, Tumble Dryers and EVs are identified as controllable load. In the first three scenarios, we assume $\lambda^{ap} = 0$. In the scenario #4, the dissatisfaction factor is studied. Detail parameters of the controllable loads are summarized in TABLE 5-2. Parameters of background load can be found in the downloadable EXCEL sheet [91].

The results of electricity payments of HAs are grouped in terms of ownership of EVs, which makes the results comparable, since EV charging represents a significant demand.

TABLE 5-1 Coefficients of the Price Prediction Model (Reprinted from our publication in [1] Copyright © 2015, IEEE)

Coefficients	α_1	β_1	α_2	β_2
Single HA load	0.282	2.025	0.459	1.317
Aggregated load from 100 HAs	0.015	1.776	0.025	0.911

TABLE 5-2 Parameter Characteristics of the Controllable Loads (Reprinted from our publication in [1] Copyright © 2015, IEEE)

	q_{rated}^{ap}	t_0^{ap}	t_1^{ap}
Dish washer	1.1 kW	Determined by Equation (4-3)	t_0^{ap} + 4 hours for breakfast/lunch; 6hr for dinner
Dryer	2.5 kW	Determined by Equation (4-3)	t_0^{ap} + 24 hours
EV	6.6 kW	Normal distribution with $\mu = 17hr$ and $\sigma = 2.8\ hour$	Normal distribution with $\mu = 7hr$ and $\sigma = 1\ hour$

5.4.2 Scenario #1: Without Load Control

This scenario is the reference in this study. The HAs do not take any actions to control load. FIGURE 5-6 shows the simulation results in this scenario. The wholesale electricity price is shown by the red dash line. The blue dash-dot line shows the equivalent flat electricity rate in the retail market assuming a budget-balanced market.

We now discuss the method of calculating the equivalent flat rate. The energy consumption was 1,716.9 kWh. To purchase this amount of energy from the wholesale market, the retailer spent \$62.77 based on the wholesale price. The HAs are charged by the flat rate. To keep the budget balanced, the equivalent flat rate is calculated as follows: $\$62.77/1{,}716.9\ kWh = 3.66\ ¢/kWh$.

The individual HA's electricity bills are shown by the blue circles in FIGURE 5-9. The average electricity payments of the HAs that own an EV was \$1.27. The maximum and minimum electricity bill was \$1.66 and \$0.97 respectively. The electricity payment of the HAs without an EV was \$0.47 (average), \$0.96 (maximum) and \$0.21 (minimum).

The peak-to-average power ratio (PAPR) was 2.32 and the standard deviation of the load profile was 47.7 kW. The usages of controllable loads are as follows: 25 usages of Dish Washer, 33 usages of Dryers, and 20 usages of EVs. In addition, there were 24 HAs who did not use controllable loads in the simulation day. The same predicted energy consumption was used for the other scenarios to make them comparable and reproducible.

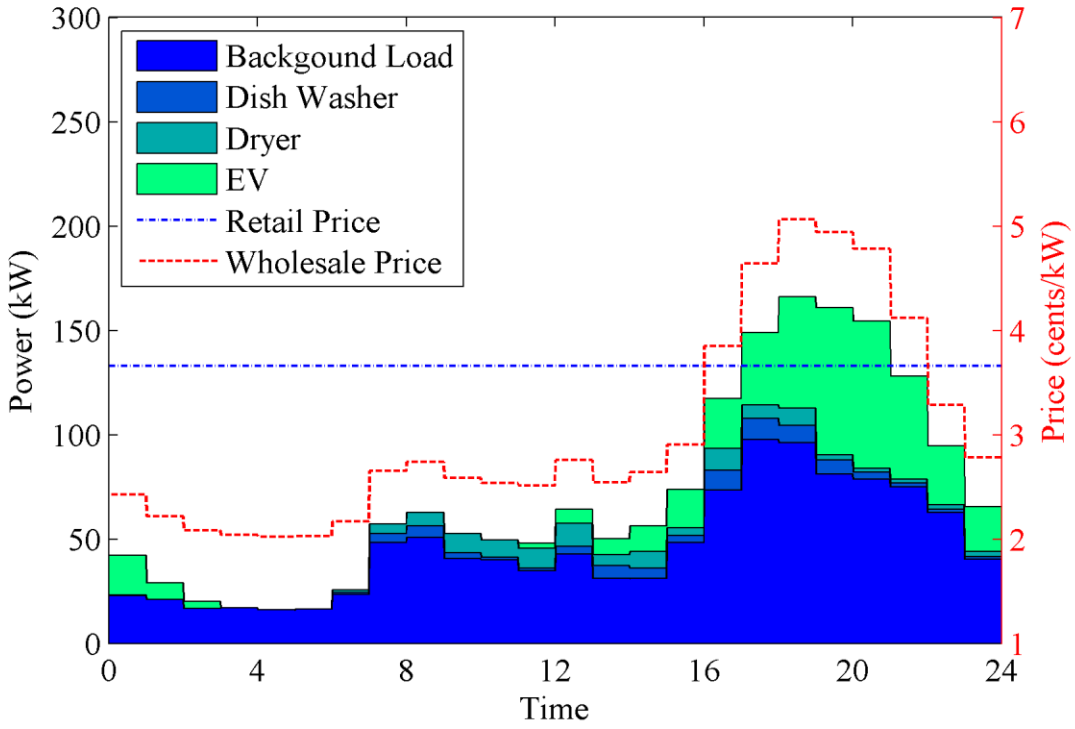

FIGURE 5-6 Load profile of aggregation of 100 HAs, retail electricity prices and wholesale electricity prices in the scenario #1

(Reprinted from our publication in [1] Copyright © 2015, IEEE)

5.4.3 Scenario #2: Open-Loop Load Control with Day-Ahead RTP

This scenario considers a situation where the RTP is announced one day ahead and the HAs can manage electricity consumption accordingly. This means that the RA will charge the HAs based on the announced price regardless of the actual wholesale price in the next day.

The HAs scheduled the controllable loads based upon the day-ahead announced real-time price by using the OL-LCM-RTP. The CP problem became a LP problem since the electricity price was provided with respect to time rather than a function of load.

FIGURE 5-7 shows the simulation results. The blue dash-dot line shows the day-ahead announced electricity price that acts as the retail electricity price to charge the HAs. The aggregated load generated a much higher new peak demand in the lowest price period. The red dash line shows the actual wholesale electricity price based on the scheduled load profile. The PAPR and the standard deviation was increased to 3.54 and 50.7 kW respectively.

In addition, the total electricity payment from the HAs was \$51.56. However, to purchase the electricity energy from the wholesale market using the actual wholesale price, the retailer needs \$64.25. Apparently, this market cannot be budget-balanced.

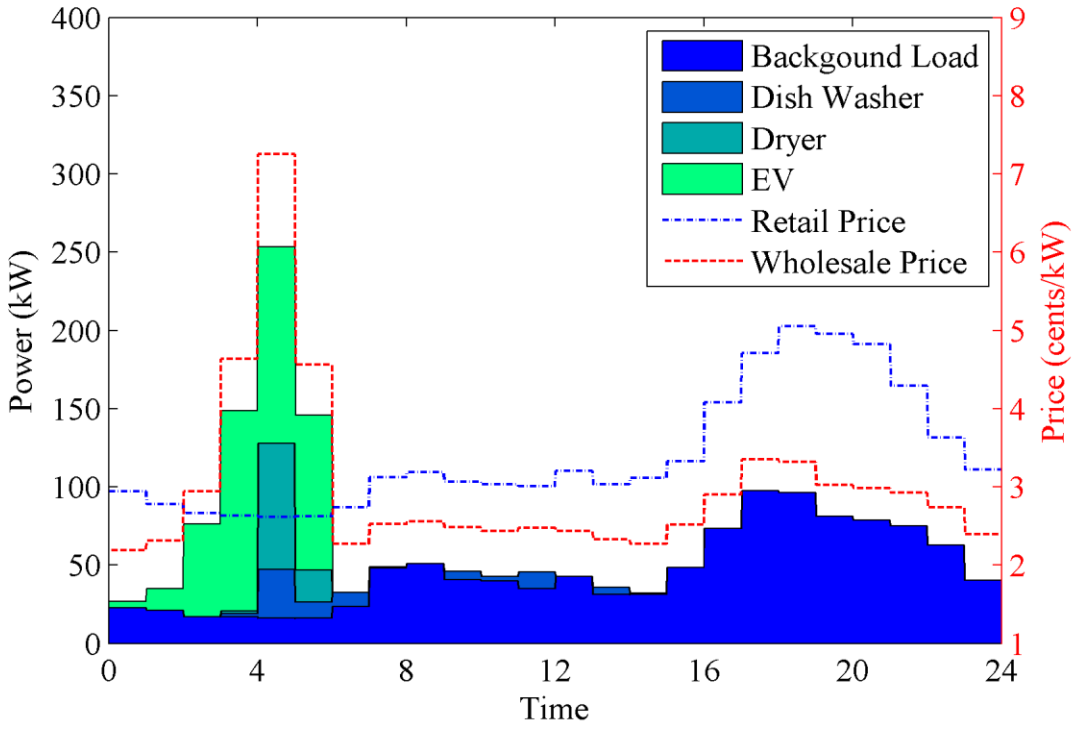

FIGURE 5-7 Load profile of aggregation of 100 HAs, retail electricity prices and wholesale electricity prices in the Scenario #2

(Reprinted from our publication in [1] Copyright © 2015, IEEE)

5.4.4 Scenario #3: Open-Loop Load Control under RTP with $\boldsymbol{\lambda^{ap} = 0}$

In this scenario, the HAs have ability to predict electricity prices using the price prediction model. The RA charged the HAs by the actual wholesale electricity price, i.e., the wholesale price was the same as the retail price. The simulation was conducted using a MacBook Pro with a 2.4 GHz Intel Core i5 processor and 8 GB of RAM memory. The computational time for solving the CP problem is about 0.4 seconds for a single HA.

The HAs scheduled the controllable loads to minimize the electricity payment. FIGURE 5-8 shows the simulation results. Both the RA and the HA benefited from a reduced electricity payment of $51.82. The PAPR was reduced to 1.54. The standard deviation was also decreased to 21.60 kW.

FIGURE 5-9 shows daily electricity bills comparing with the scenario #1. The average electricity payment of the HAs that own an EV was $1.05 and the average reduction was 17.5%. They had the maximum payment of $1.37 and the maximum reduction of 21.9%. The minimum payment was $0.76 and the minimum reduction was 12.3%. The HAs without an EV also benefited from the decreased bills of $0.39 (average), $0.78 (maximum) and $0.17 (minimum). The average, maximum and minimum percentage of decrease was 17.4%, 24.3% and 12.3% respectively.

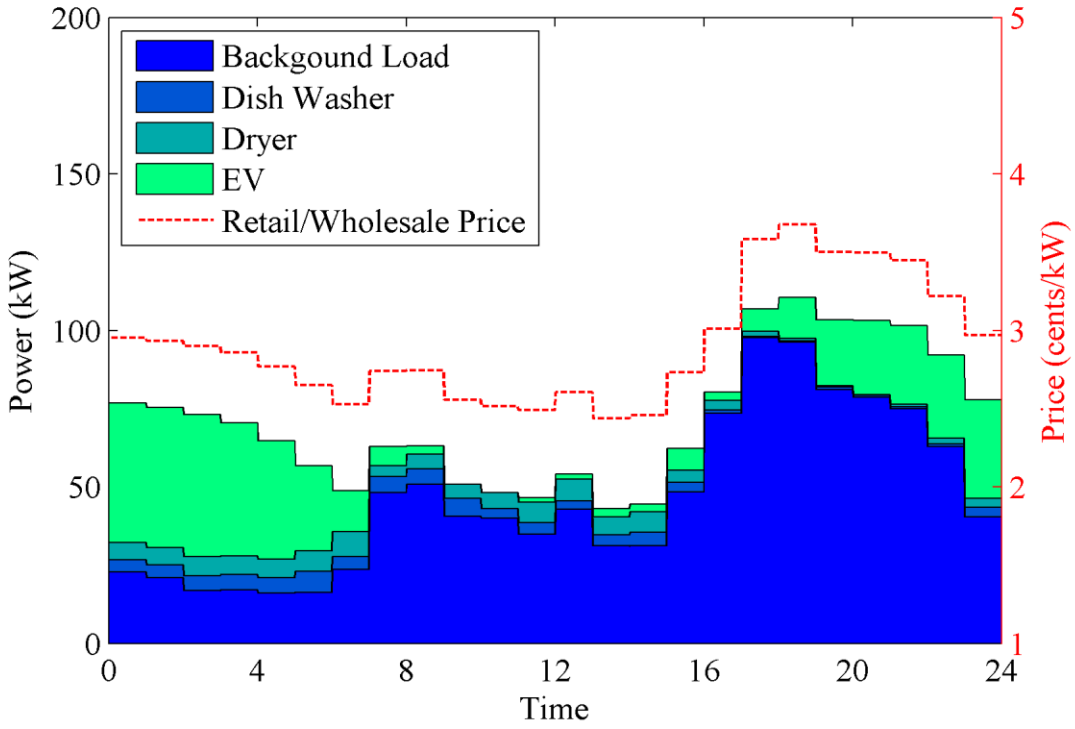

FIGURE 5-8 Load profile of aggregation of 100 HAs, retail electricity prices and wholesale electricity prices in the Scenario #3

(Reprinted from our publication in [1] Copyright © 2015, IEEE)

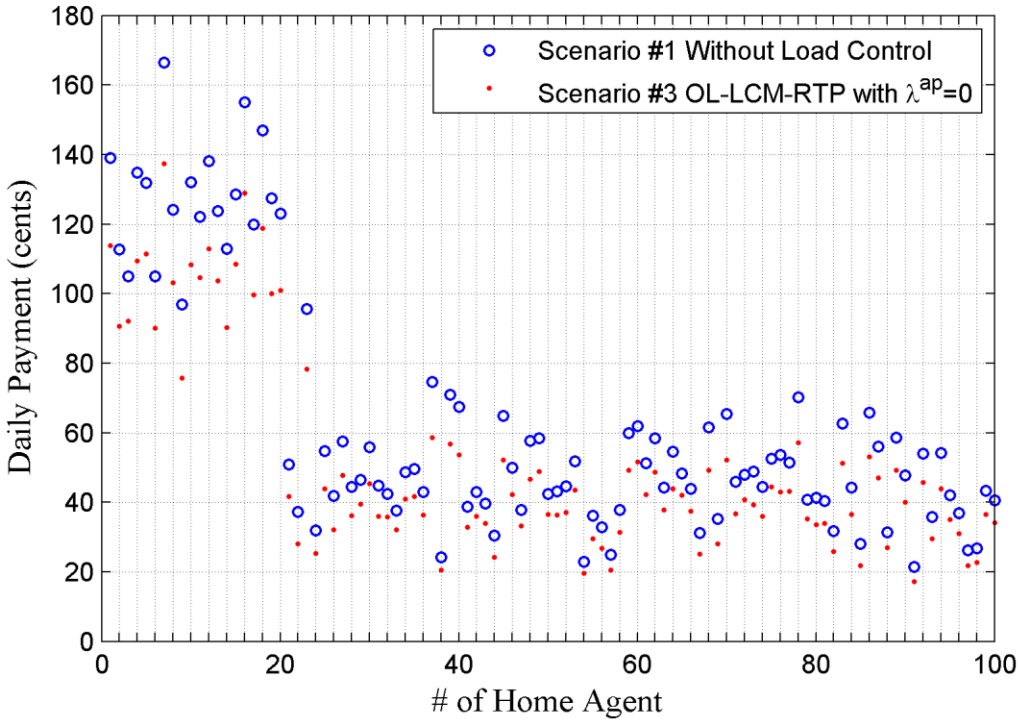

FIGURE 5-9 Electricity payment (100 HAs) in the Scenario #1 and #3

(Reprinted from our publication in [1] Copyright © 2015, IEEE)

5.4.5 Scenario #4: Open-Loop Load Control under RTP with $\lambda^{ap} > 0$

This scenario evaluates the impact of dissatisfaction factor on the load schedule. We first use a single EV of a HA as an example of the controllable load and consider other loads as background loads to emphasize the impact of the dissatisfaction factor for an individual load. Secondly, we study the impact of the dissatisfaction factor to the whole load control model.

5.4.5.1 The Impact of λ^{ap} on a Single EV

The plug-in time and must completed time of the EV was assumed at 17pm and 7am respectively. The initial SOC was 20%, which means the EV requires 4 hours to be fully charged. The background load profile is shown in the previous scenarios.

FIGURE 5-10 shows scheduled EV load using different dissatisfaction factors of 0, 0.4 and 0.8. From FIGURE 5-10 (a), we can see that the load is scheduled to the off-peak demand period to minimize the electricity payment without consideration of waiting time since the dissatisfaction factor is 0. By contrast, with dissatisfaction factor of 0.8, the EV load could not be scheduled shown in FIGURE 5-10 (c) since this high dissatisfaction factor represents the user preference to charge the EV immediately. FIGURE 5-10 (b) shows the situation where the dissatisfaction factor was 0.4, in which, the solution is a trade-off between electricity payment and waiting time.

FIGURE 5-11 shows the daily electricity payment versus waiting time using different dissatisfaction factors for a single EV. With increasing λ^{ap} from 0 to 0.8, the daily electricity payment for a single EV increases from 74 cents to 94 cents while the waiting time decreases from 10 hours to 0 hour. The waiting time is calculated as follows:

$$waiting\ time\ =\ completion\ time - plugin\ time - required\ charging\ time.$$

For instance, if the plugin time is 17hr; the fully charged time is 21hr; and required charging-up time is 4 hours (i.e., it requires 4 hours to fully charge the EV), the waiting time is zero.

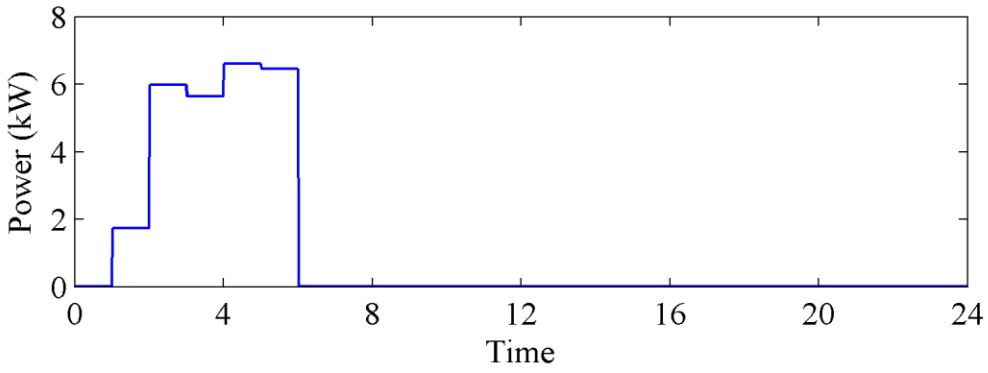

(a) $\lambda^{ap} = 0$

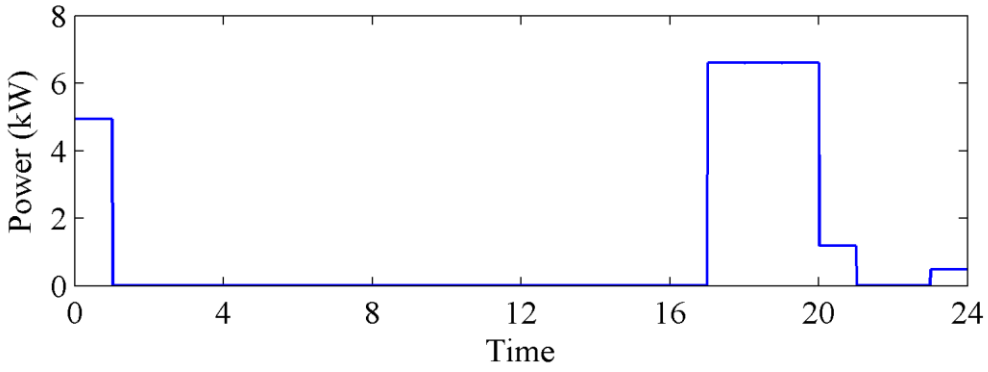

(b) $\lambda^{ap} = 0.4$

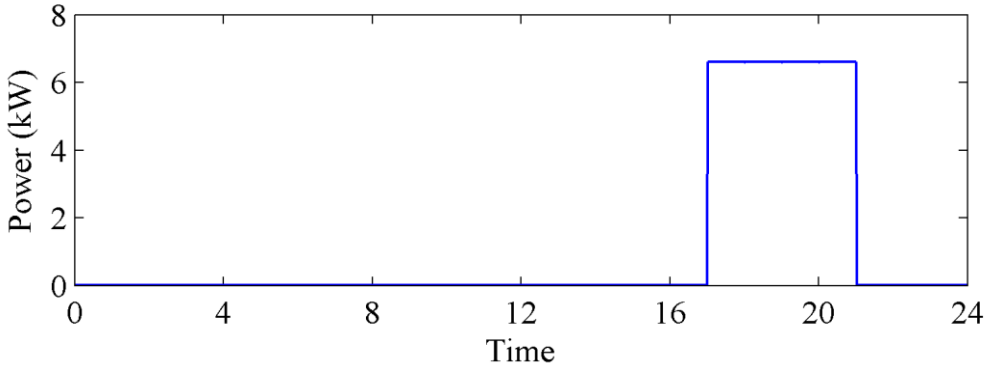

(c) $\lambda^{ap} = 0.8$

FIGURE 5-10 Scheduled EV load with different dissatisfaction factors. (a) $\lambda^{ap} = 0$, (b) $\lambda^{ap} = 0.4$, (c) $\lambda^{ap} = 0.8$

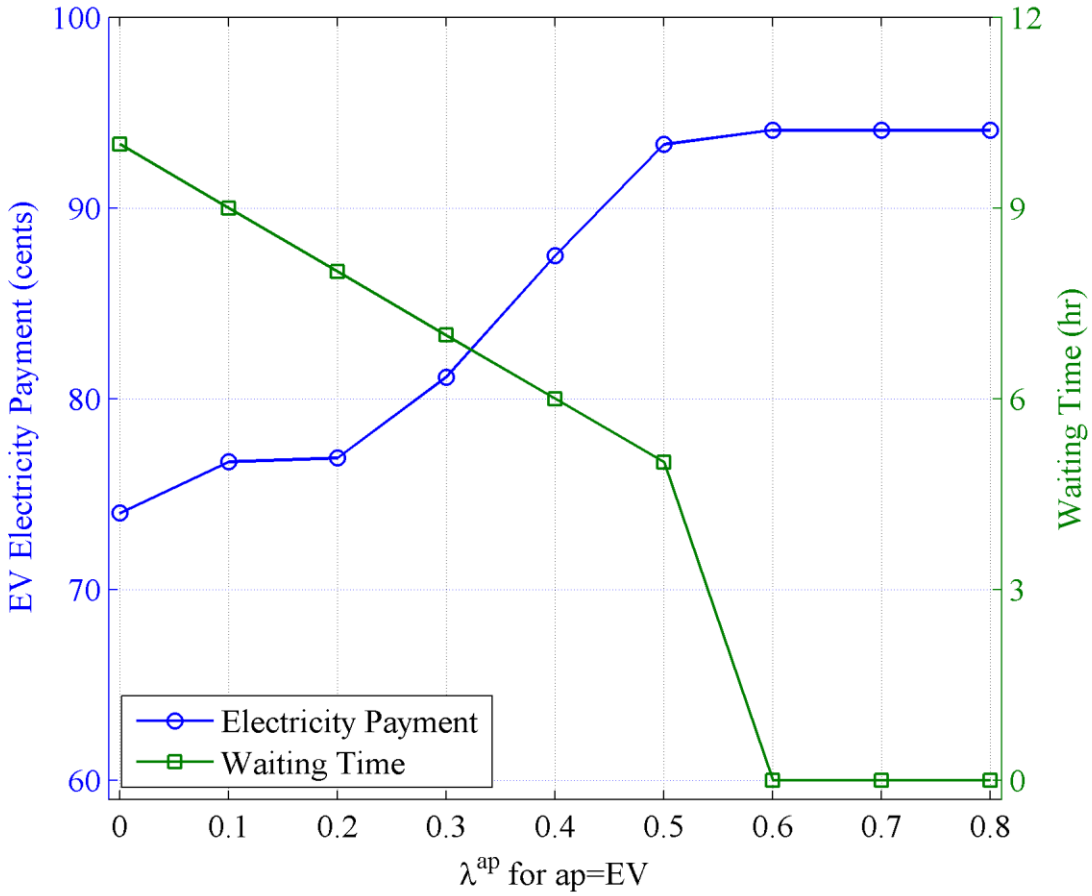

FIGURE 5-11 Electricity payment V.S. waiting time using different dissatisfaction factors for a single EV

(Reprinted from our publication in [1] Copyright © 2015, IEEE)

5.4.5.2 The Impact of λ^{ap} on the Load Control Model

We now discuss the impact of λ^{ap} on the OL-LCM-RTP. TABLE 5-3 shows the observation of the PAPR, the standard deviation, the electricity payment from the HAs and the cost for the RA to buy the electricity with respect to different λ^{ap} from 0 to infinity. The electricity payment from the HAs and the cost for the RA are essential the same since the RA charged the HAs by the wholesale electricity price. FIGURE 5-12 shows the plot of the observations of the standard deviation and the electricity payment from the HAs and the cost for the RA. A higher value of λ^{ap} represents a greater level of dissatisfaction. We can see that with increasing the value of λ^{ap}, both the electricity payment and the standard deviation increased. More exactly, the electricity payment climbed from \$51.82 to \$62.77. The PAPR and the standard deviation increased from 1.54 and 21.60 kW to 2.32 and 47.74 kW respectively. $\lambda^{ap} = \infty$ represents that the HAs did not schedule the load at all, which is the same as the reference scenario #1.

FIGURE 5-13 shows the load profile and the electricity price with $\lambda^{ap} = 0.1$. In this case, the PAPR and the standard deviation was 1.72 and 25.69 kW respectively. The total electricity payment from the HAs was \$53.23. The average electricity payment of the HAs that own an EV was \$1.07, which was reduced by 15.4% compared with the reference scenario #1. They had the maximum payment of \$1.42 with a reduction of 23.8% and the minimum payment of \$0.73 with a reduction of 10.2%. The HAs without an EV also benefited from the decreased bills of \$0.40 (average), \$0.80 (maximum) and \$0.17 (minimum). The average, maximum and minimum percentage of decrease was 15.1%, 25.6% and 8.3% respectively.

TABLE 5-3 The impact of different λ^{ap} on the OL-LCM-RTP in the scenarios of #4

λ^{ap}	PAPR	Standard Deviation (kW)	Payment from HAs and Cost for RA ($)
0	1.54	21.60	51.82
0.01	1.56	22.54	52.15
0.1	1.72	25.69	53.23
0.3	1.97	33.99	56.18
0.5	2.09	37.18	57.55
1	2.16	38.72	58.26
10	2.25	41.90	59.93
∞	2.32	47.74	62.77

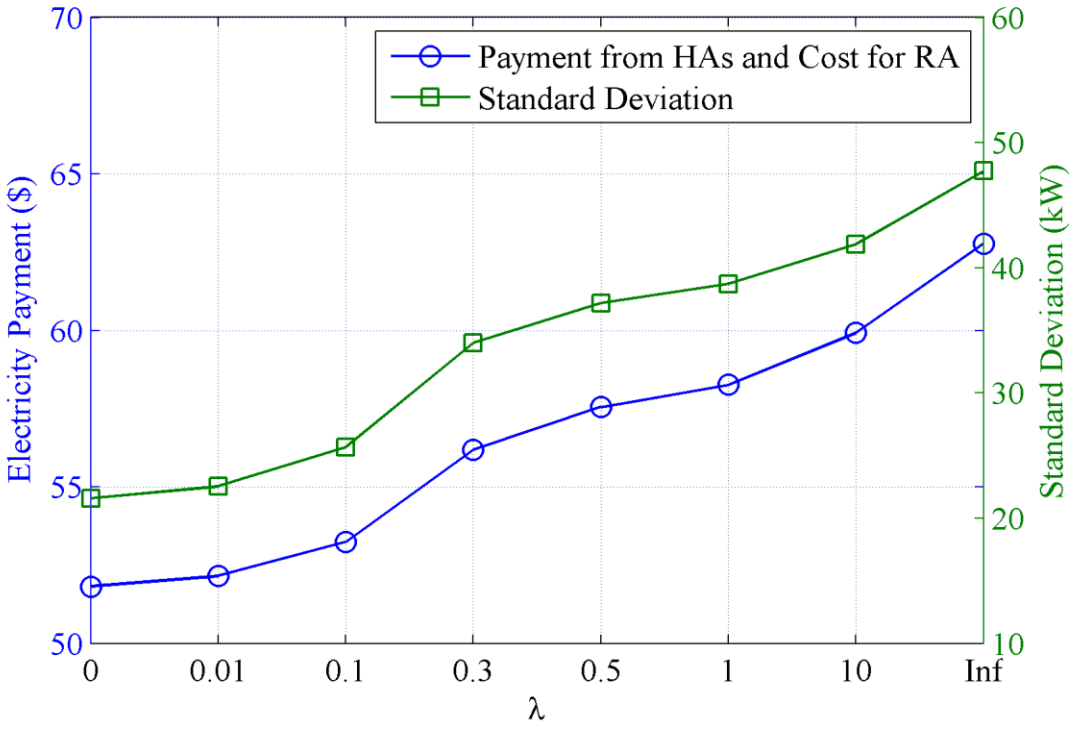

FIGURE 5-12 The observations with different λ^{ap} in the scenarios of #4

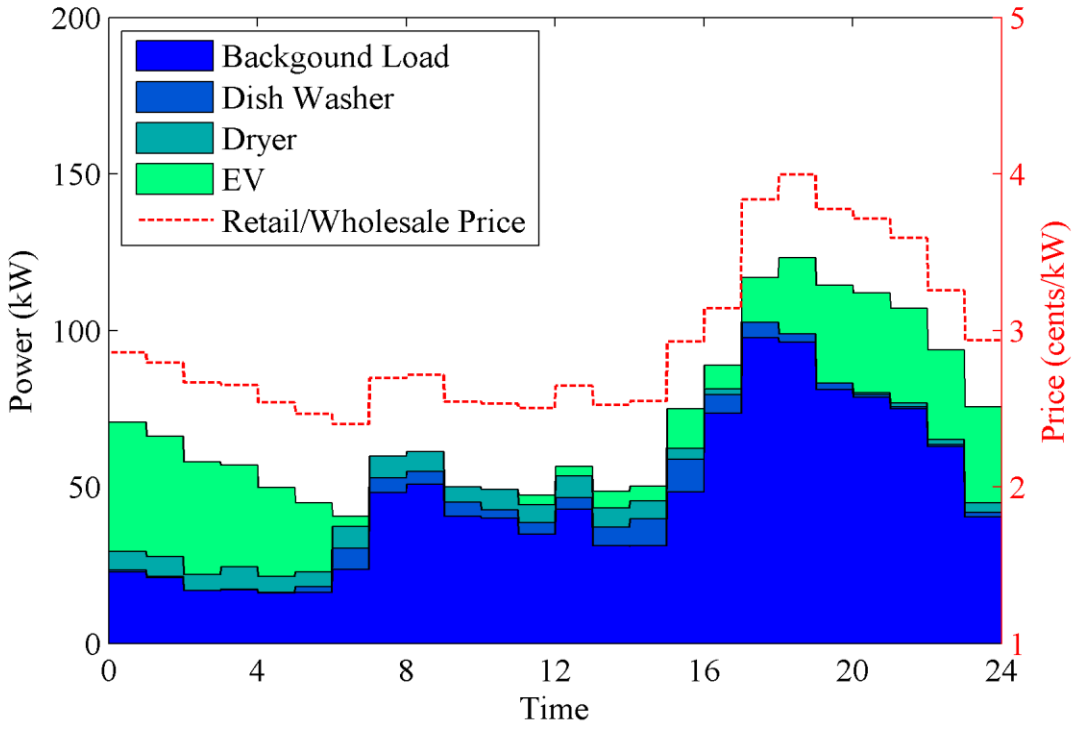

FIGURE 5-13 Load profile of aggregation of 100 HAs, retail electricity prices and wholesale electricity prices with $\lambda^{ap} = 0.1$ in the Scenario #4

5.4.6 Scenario #5: Closed-Loop Load Control under RTP with $\lambda^{ap} = 0.1$

This scenario evaluates the CL-LCM-RTP and discusses how the feedback in terms of coordination and communication among the HAs help to reduce the PAPR, the standard deviation and the electricity payment. The impacts of EV penetration levels and flexible charging periods are evaluated as well. The HAs schedule their controllable loads based on global information. The new background load becomes the sum of the background load of the HA itself and the aggregated total load of the other HAs. The RA informs a HA with the other HAs' load information, which is collected for billing purpose anyways.

We assume $\lambda^{ap} = 0.1$ in this scenario. The reason why we have picked $\lambda^{ap} = 0.1$ is because this value represents some levels of dissatisfaction for HAs to schedule the load while it is not very large to significantly affect the schedule of the controllable loads. It is not reasonable to pick a big value since scheduling the controllable loads in this study does not significantly affect users' comfortable levels.

This closed-loop load scheduling is a round process. In the first round there were 45 HAs who scheduled their controllable loads and in the second round only 4 HAs rescheduled their controllable loads. There were no HAs rescheduling the load in the third round; therefore, the system can quickly converge at the second round.

FIGURE 5-14 shows the load profile and the electricity price using CL-LCM-RTP in this scenario. The PAPR and the standard deviation was 1.41 and 13.03 kW. FIGURE 5-15 shows daily electricity bills comparing with the scenario #1. The electricity payment and cost was \$50.46. The average electricity payment of the HAs that own an EV was \$1.03, which was reduced by 18.8%. They had the maximum payment of \$1.33 with a reduction of 24.5% and the minimum payment of \$0.79 with a reduction of 17.5%. The HAs without

an EV also benefited from the decreased bills of $0.37 (average), $0.77 (maximum) and $0.17 (minimum). The average, maximum and minimum percentage of decrease was 20.2%, 26.1% and 16.6% respectively.

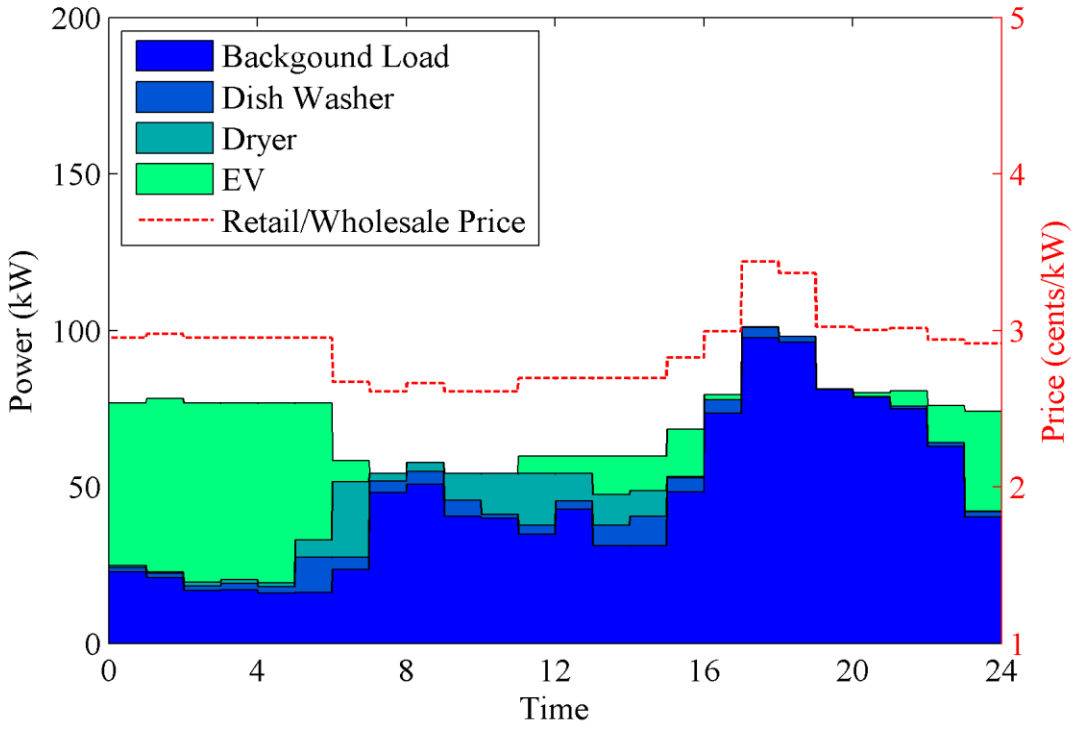

FIGURE 5-14 Load profile of aggregation of 100 HAs, retail electricity prices and wholesale electricity prices with $\lambda^{ap} = 0.1$ in the Scenario #5 (CL-LCM-RTP)

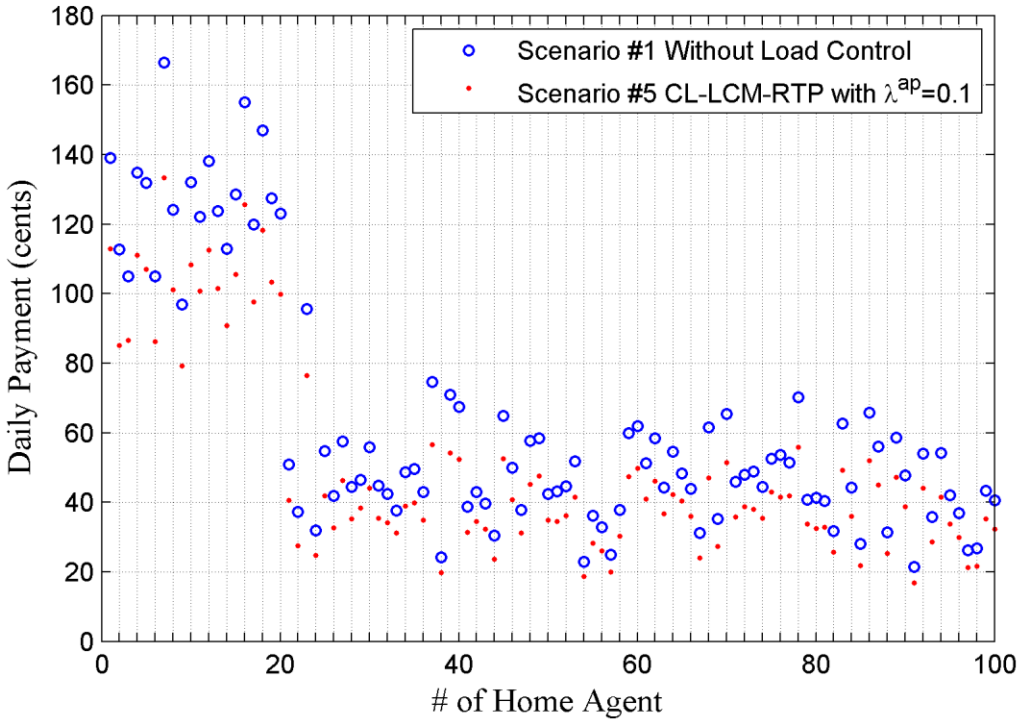

FIGURE 5-15 Electricity payment (100 HAs) in the scenario #1 and #5

5.4.6.1 The Impact of EV Penetration Levels

In this subsection, we evaluate the impact of EV penetration levels on the system. We observe a normalized standard deviation of the load profile to remove the inherently influence from the increasing electricity EV charging demand. For the same reason, we do not observe the electricity payment because it is not comparable with the previous scenarios.

TABLE 5-4 shows the PAPR, the normalized standard deviation and the energy consumption with EV penetration levels of 20%, 30%, 40% and 50%. The PAPR was 1.41, 1.22, 1.21 and 1.19 respectively. The normalized standard deviation was 0.0366, 0.0309, 0.0451 and 0.0492 respectively. The energy consumption continuously increased from 1.72×10^3 kWh with 20% EV penetration to 2.36×10^3 kWh with 50% EV penetration.

FIGURE 5-16 shows a plot of the PAPR and the normalized standard deviation. We can see that the PAPR continuously decreases with more and more EV penetration. This is because that the increase of the peak demand is slower than the increase of average demand. However, the normalized standard deviation decreased to 0.0309 at 30% of EV penetration and then started to increase with more and more EV penetration since the charging period was restricted from home-arrival time to home-departure time. Therefore, the restricted EV charging period in the residential sector can be a bottleneck when EV penetration is beyond a certain level. This can be alleviated by considering charging EV in the working place, which is beyond the scope of this study. However, if we allow some EVs having a flexible charging period, the problem could be eased. For instance, if some customers do not drive the EV in the next day, the charging period can be any time in the following day. This is studied in the next subsection. FIGURE 5-17 and FIGURE 5-18 shows the aggregated load profile with EV penetration levels of 30% and 50% respectively.

TABLE 5-4 The PAPR and the normalized standard deviation of the load profile with EV penetration levels of 20%, 30%, 40% and 50%

EV Penetration Level	20%	30%	40%	50%
PAPR	1.41	1.22	1.21	1.19
Normalized Standard Deviation	0.0366	0.0309	0.0451	0.0492
Energy Consumption ($\times 10^3$ kWh)	1.72	1.93	2.15	2.36

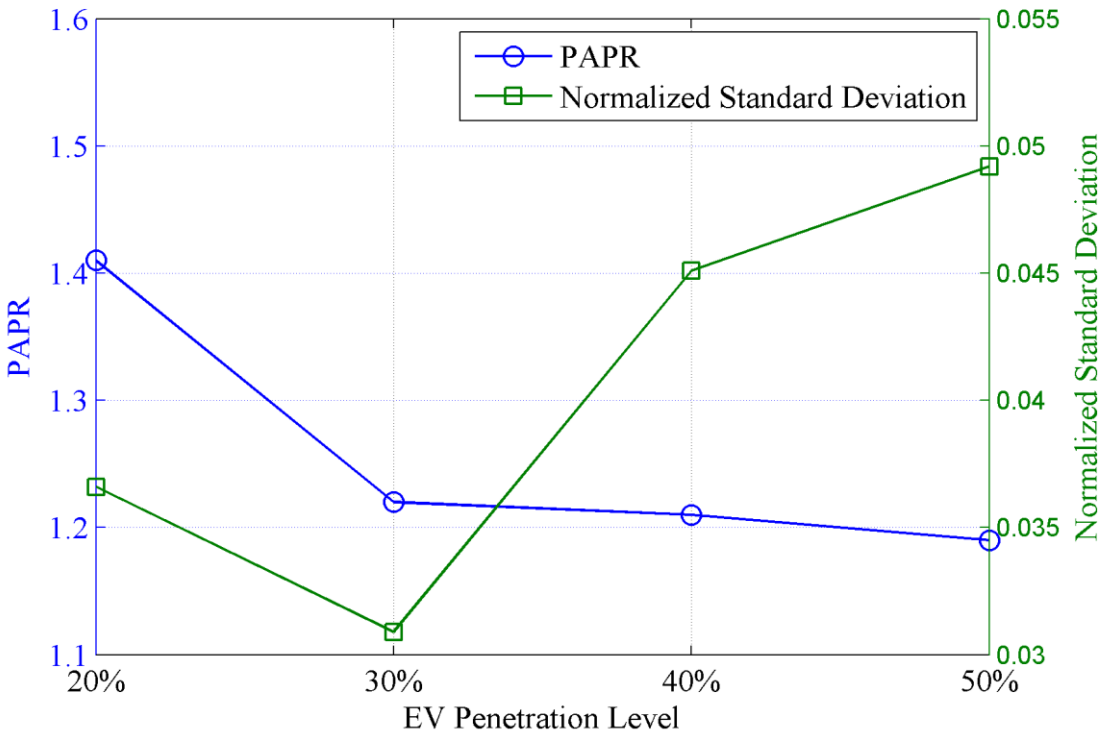

FIGURE 5-16 The PAPR and the normalized standard deviation of the load profile with EV penetration levels of 20%, 30%, 40% and 50%

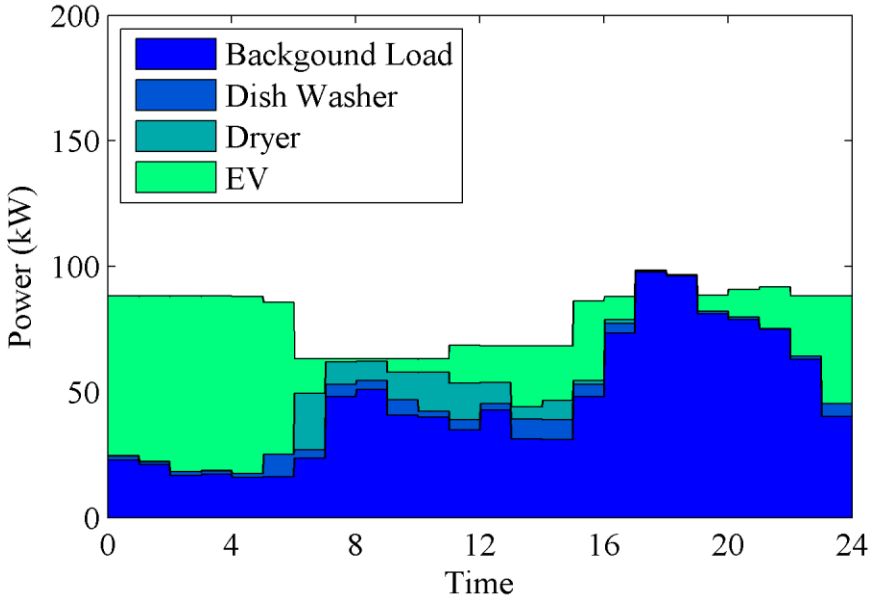

FIGURE 5-17 Load profile aggregated from 100 HAs with EV penetration levels of 30%

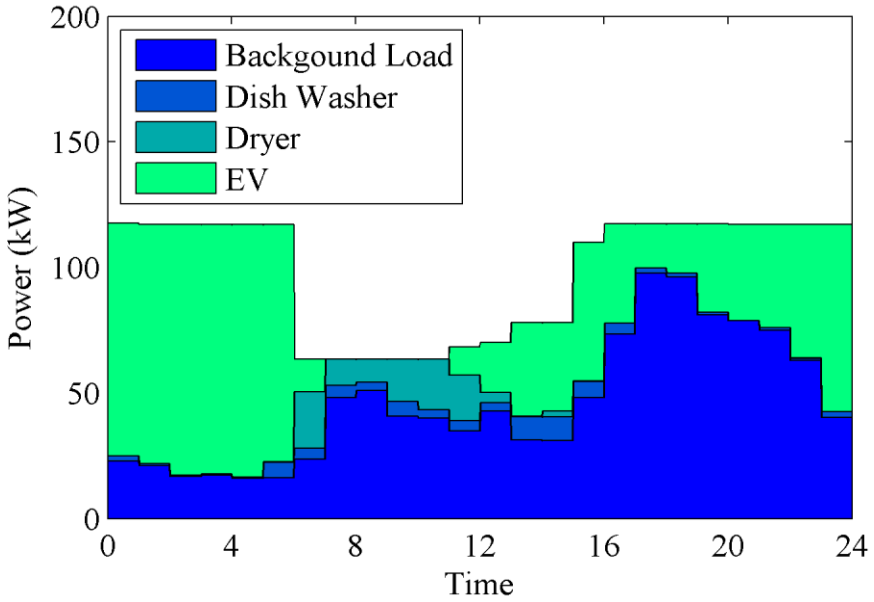

FIGURE 5-18 Load profile aggregated from 100 HAs with EV penetration levels of 50%

5.4.6.2 The Impact of EVs with a Flexible Charging Period

In this subsection, we evaluated the impacts of the flexible charging period in the case of 50% EV penetration (50 EVs). TABLE 5-5 summarizes the PAPR and the normalized standard deviation with different numbers of EVs having the flexible charging period. FIGURE 5-19 shows a plot of these observations. We can see that the normalized standard deviation continuously dropped from 0.0364 to 0. 0017 with more and more EV (from 5 to 25) that could be charged any time in a day. The PAPR also decreased with subtle variations. FIGURE 5-20 and FIGURE 5-21 shows the load profiles with 5 and 15 flexibly charged EVs respectively. FIGURE 5-21 shows an almost perfect flat overall load profile if 15 of 50 EVs can have a flexible charging period.

TABLE 5-5 The PAPR and the normalized standard deviation of the load profile with different number of flexible charged EVs at a 50% EV penetration level

The number of flexible EV	5	10	15	20	25
PAPR	1.16	1.11	1.03	1.06	1.04
Normalized Standard Deviation	0.0364	0.0185	0.0043	0.0034	0.0017

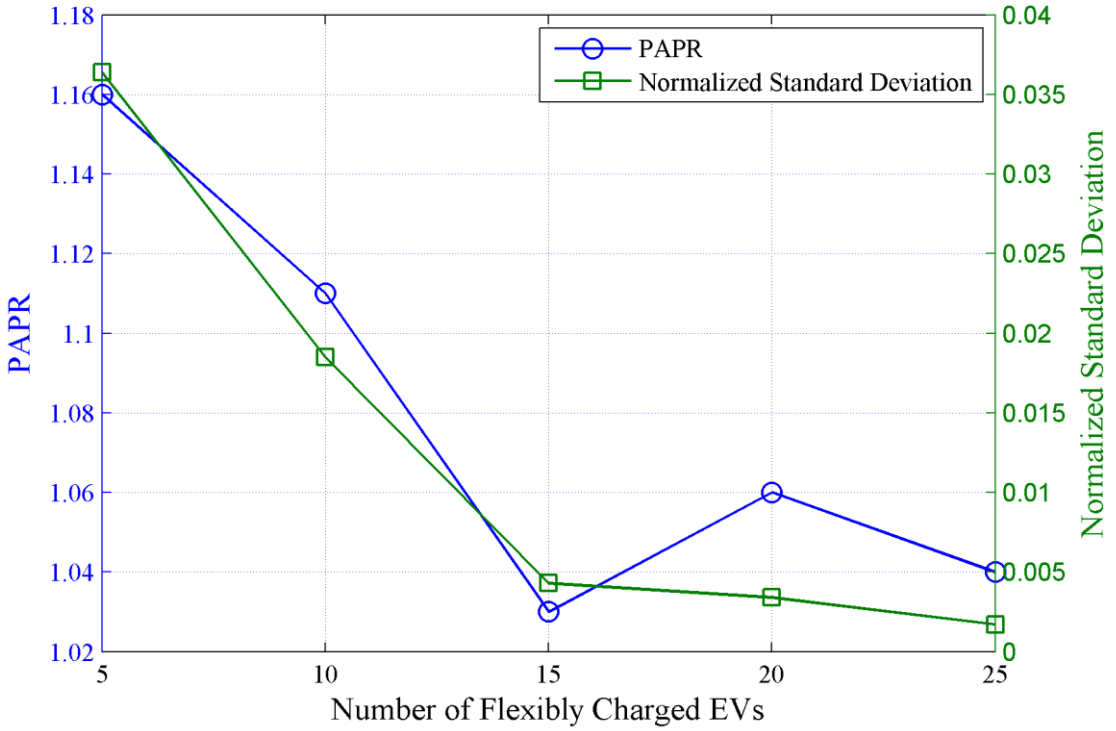

FIGURE 5-19 The PAPR and the normalized standard deviation of the load profile with different number of flexibly charged EVs at a 50% EV penetration level

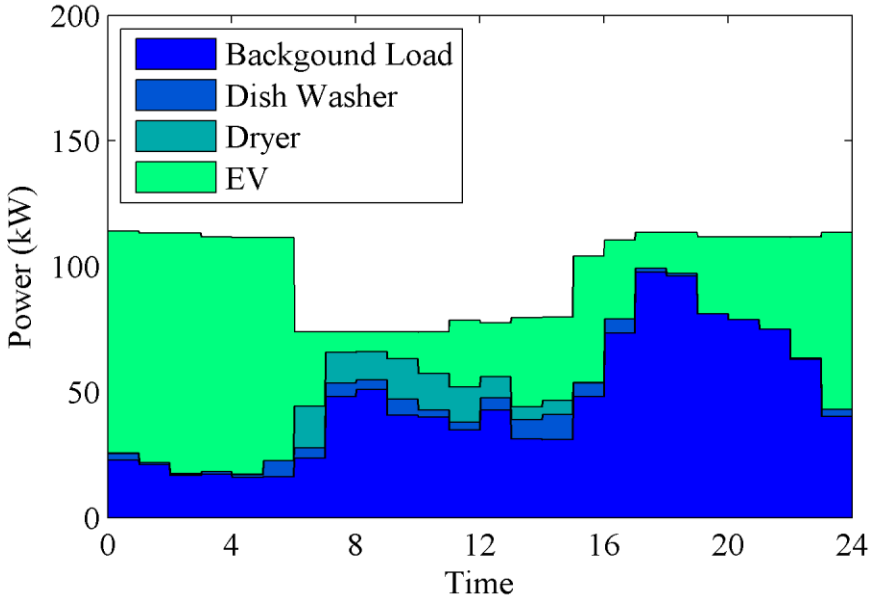

FIGURE 5-20 Load profile aggregated from 100 HAs with EV penetration levels of 50%

(5 EVs have flexible charging time)

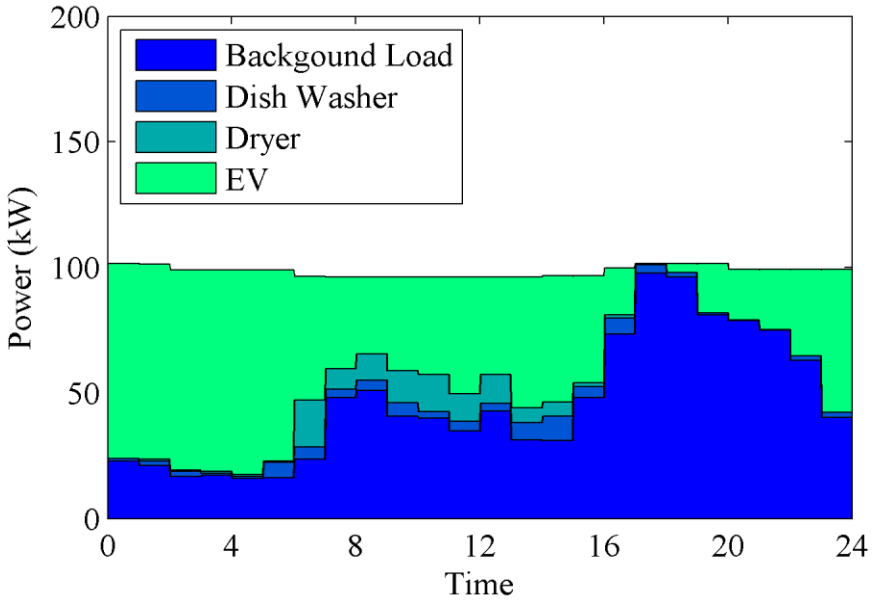

FIGURE 5-21 Load profile aggregated from 100 Has with EV penetration levels of 50%

(15 EVs have flexible charging time)

5.5 Discussion

This section discusses the five scenarios and actual RTP programs. For the observations of the PAPR, the standard deviation and the total electricity payment, lower values are preferable. We discuss the scenario #2 first. The total electricity payment from the HAs is $51.56. However, the RA spends $64.25 on purchasing the electricity energy. Apparently, the market cannot be budget-balanced. In general, although a customer's individual electricity payment can be reduced using day-ahead RTP, it is not a feasible plan if the customers are able to schedule the load accordingly.

TABLE 5-6 summarizes the observations of the PAPR, the standard deviation and the total electricity payment in the scenarios #1 (without load control), #3 (OL-LCM-RTP with $\boldsymbol{\lambda^{ap} = 0}$), #4 (OL-LCM-RTP with $\boldsymbol{\lambda^{ap} = 0.1}$) and #5 (CL-LCM-RTP with $\boldsymbol{\lambda^{ap} = 0.1}$). We can see that compared with the scenario #1, the PAPR, standard deviation and electricity payment decrease in the other scenarios. The value of observations in the scenario #3 are lower than the scenario #4 because the effect of dissatisfaction factor is assumed to zero ($\lambda^{ap} = 0$) in the scenario #3 while $\lambda^{ap} = 0.1$ in the scenario #4. Using the CL-LCM-RTP mechanism in the scenario #5 ($\lambda^{ap} = 0.1$), the quality of observations is the best among others because of the effect of the coordination and the communication. The electricity payment reduction using the OL-LCM-RTP and CL-LCM-RTP is 17.4% and 19.6% respectively. FIGURE 5-22 shows the load profiles simulated in these four scenarios.

The first large-scale residential RTP program in the U.S. was the Community Energy Cooperative's Energy-Smart Pricing Plan (ESPP) [101]. The program was conducted in the service area of Commonwealth Edison in northern Illinois between 2003 (750

participants) and 2006 (1,500 participants), in which the peak demand was reduced by 15%. The Olympic Peninsula Project in Washington (2005) showed a peak demand reduction of 18% [101]. It is noted that the latter program equipped with DR-enabling technology, which shows usefulness.

TABLE 5-6 Comparison of the observations in the scenarios #1 (without load control), #3 (OL-LCM-RTP with $\lambda^{ap} = 0$), #4 (OL-LCM-RTP with $\lambda^{ap} = 0.1$) and #5 (CL-LCM-RTP with $\lambda^{ap} = 0.1$)

Observations / Scenario	PAPR (% Reduction)	Standard Deviation (kW) (% Reduction)	Total Payment ($) (% Reduction)
Scenario #1 Without load control	2.32	47.74	62.77
#3 OL-LCM-RTP $\boldsymbol{\lambda^{ap} = 0}$	1.54 (33.6%)	21.60 (54.8%)	51.82 (17.4%)
#4 OL-LCM-RTP $\boldsymbol{\lambda^{ap} = 0.1}$	1.72 (25.9%)	25.69 (46.2%)	53.23 (15.2%)
#5 CL-LCM-RTP $\boldsymbol{\lambda^{ap} = 0.1}$	1.41 (39.2%)	13.03 (72.7%)	50.46 (19.6%)

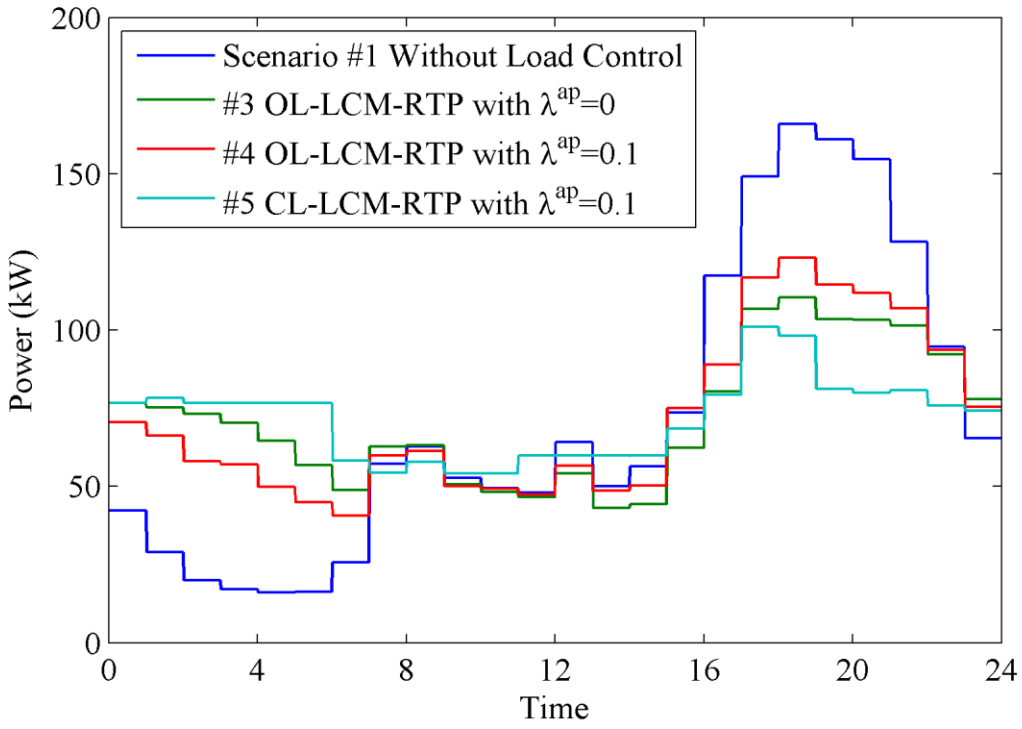

FIGURE 5-22 Load profiles in the scenarios #1 (without load control), #3 (OL-LCM-RTP with $\lambda^{ap} = 0$), #4 (OL-LCM-RTP with $\lambda^{ap} = 0.1$) and #5 (CL-LCM-RTP with $\lambda^{ap} = 0.1$)

TABLE 5-7 illustrates the individual electricity payment from the HAs in the scenarios #1 (without load control), #3 (OL-LCM-RTP with $\boldsymbol{\lambda^{ap} = 0}$), #4 (OL-LCM-RTP with $\boldsymbol{\lambda^{ap} = 0.1}$) and #5 (CL-LCM-RTP with $\boldsymbol{\lambda^{ap} = 0.1}$). In all the scenarios, the electricity payment of the HAs with an EV is higher than the HAs without an EV since EV charging represents a significant electricity demand. However, we can see that all HAs benefit from a reduced electricity payment with DR using the proposed mechanism regardless of controllable load usage, amount of energy consumed or EV ownership in the scenarios #3, #4 and #5. It is noted that, in the experiments, there were 24 HAs who did not use controllable loads in the simulation day and 80% of homes do not own an EV. FIGURE 5-23 shows the individual electricity payments in these scenarios.

TABLE 5-7 The summary of the individual electricity payment in the scenarios #1 (without load control), #3 (OL-LCM-RTP with $\lambda^{ap} = 0$), #4 (OL-LCM-RTP with $\lambda^{ap} = 0.1$) and #5 (CL-LCM-RTP with $\lambda^{ap} = 0.1$)

	Have EVS	Electricity Payment ($)			Payment Reduction (%)		
		Average	Max	Min	Average	Max	Min
Scenario #1	Yes	1.27	1.66	0.97	-	-	-
Without load control	No	0.47	0.96	0.21	-	-	-
#3 OL-LCM-RTP	Yes	1.05	1.37	0.76	17.5	21.9	12.3
$\boldsymbol{\lambda^{ap} = 0}$	No	0.39	0.78	0.17	17.4	24.3	12.3
#4 OL-LCM-RTP	Yes	1.07	1.42	0.73	15.4	23.8	10.2
$\boldsymbol{\lambda^{ap} = 0.1}$	No	0.40	0.80	0.17	15.1	25.6	8.3
#5 CL-LCM-RTP	Yes	1.03	1.33	0.79	18.8	24.5	17.5
$\boldsymbol{\lambda^{ap} = 0.1}$	No	0.37	0.77	0.17	20.2	26.1	16.6

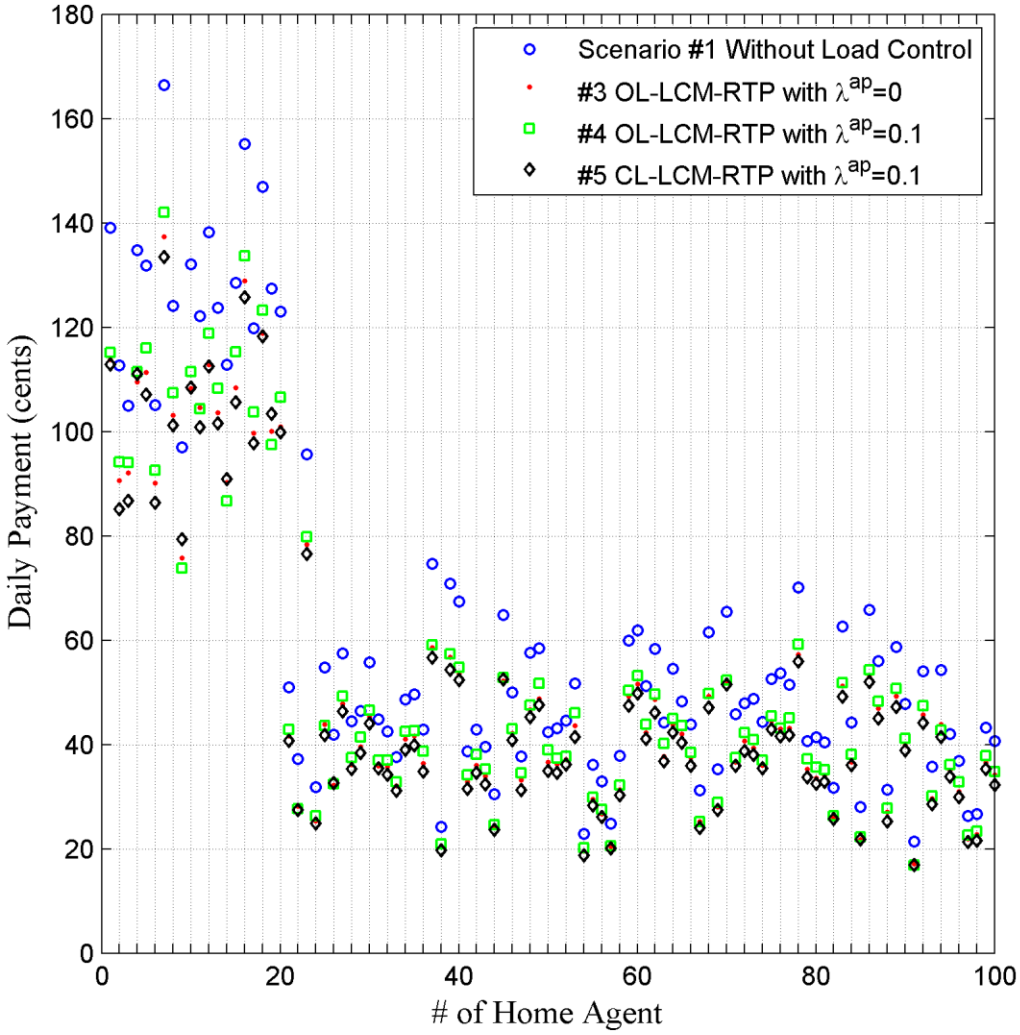

FIGURE 5-23. The individual electricity payments of the HAs in the scenarios #1 (without load control), #3 (OL-LCM-RTP with $\lambda^{ap} = 0$), #4 (OL-LCM-RTP with $\lambda^{ap} = 0.1$) and #5 (CL-LCM-RTP with $\lambda^{ap} = 0.1$)

5.6 Summary

RTP as a DR policy has great potential to reduce electricity payments and improve the stability of the power system with DR implementation, and responding to RTP requires DR enabling technologies. Several models including the heterogeneous load prediction model, the real-time price model, the OL-LCM-RTP and the CL-LCM-RTP are developed to associate with the proposed MAS. Simulation results show that the PAPR, the standard deviation and electricity payments are significantly reduced using the proposed mechanisms.

Day-ahead RTP can cause peak demand rebound in the scenario #2; therefore, it is considered as an infeasible plan without coordination among homes. In the scenario #3, the HAs solve the proposed OL-LCM-RTP problem to minimize the electricity payment based the predicted electricity price. The scheduled electricity load is significantly better than without load control. In addition, the HAs do not expose the electricity usage to the other HAs. Furthermore, it does not requires coordination among HAs. In the scenario #4, we study the impact of the dissatisfaction factor in the OL-LCM-RTP on the system. We can see that the electricity payment increases while the waiting time decreases with increasing the dissatisfaction factor. Users can determine a "best" value for the dissatisfaction factor to find a trade-off between electricity payment and waiting time.

The scenario #5 evaluates the proposed CL-LCM-RTP, which appears the best case among others since it incorporates the feedback from the RA with the communication and the cooperation among the HAs. One of the significant advantages is that the solution is globally optimal while the disadvantage is the requirement of a certain level of communication. The utility or the society needs to value the trade-off to determine a "best"

mechanism to apply. We also evaluated the impacts of different levels of EV penetration to the system. The study shows the increasing opportunities to flatten the load profile and improve the reliability of the power system via scheduling more and more EV charging demand. However, the restricted charging period at the residential sector can be a bottleneck when the EV penetration exceed a certain level. This can be alleviated by allowing the EV being charged at working place or being charged in a more flexible time period.

The optimal control of electricity consumption is evaluated in a simulation environment in this study. It can also be extended into a real-time environment, where the load prediction of the HA is replaced by real-time actual electricity consumption and the CP problem is solved hourly. The wholesale electricity prediction of the RA can be also replaced by actual prices by incorporation of bidding from multiple generators.

CHAPTER 6

OPTIMAL DR IMPLEMENTATION UNDER TOU

6.1 Load Control Model under TOU

The LCM-TOU is modelled by a LP problem enabling HAs to make intelligent decisions to minimize electricity payments. Except for the price structure, the difference of this model from the load control models under RTP (OL-LCM-RTP and CL-LCM-RTP) is the objective function. More precisely, the TOU is a sequence of predetermined prices with time; therefore the electricity payment is a linear function. In addition, a random weighted sequence/set is deployed in the penalty function. The constraints remain the same; however, they are duplicated here for audiences' convenience.

$minimize$

$$\sum_{t\in\mathcal{T}}\left(p_{TOU}\sum_{ap\in\mathcal{AP}} l_t^{ap}\right)+\sum_{t\in\mathcal{T}}\sum_{ap\in\mathcal{CAP}}\lambda^{ap}\,w^{ap}w_{rand}^{ap}l_t^{ap} \tag{o3}$$

$subject\ to$:

$$0\le l_t^{ap}\le q_{rated}^{ap},\forall\ ap\in\mathcal{CAP},t\in[t_0^{ap},t_1^{ap}] \tag{c1}$$

$$l_t^{ap}=\ 0,\forall\ ap\in\mathcal{CAP},t\in\mathcal{T}\backslash[t_0^{ap},t_1^{ap}] \tag{c2}$$

$$\sum_{ap}\sum_{t} l_t^{ap}=\ \widehat{E_C^{ap}},\forall\ ap\in\mathcal{CAP},t\in[t_0^{ap},t_1^{ap}] \tag{c3}$$

$$\sum_{ap\in\mathcal{CAP}} l_t^{ap}+\sum_{ap\in\mathcal{BAP}}\widehat{l_t^{ap}}\ \le\ Q_{HA}^{max},\forall\ t\in\mathcal{T} \tag{c4}$$

In the objective function, the electricity price p_{TOU} is defined as follows.

$$p_{TOU} = \begin{cases} p_{off-peak} & \forall\, t_{off\_peak} \\ p_{mid-peak} & \forall\, t_{mid\_peak} \\ p_{on-peak} & \forall\, t_{on\_peak} \end{cases} \tag{13}$$

The electricity payment $\sum_{t\in\mathcal{T}}(p_{TOU}\sum_{ap\in\mathcal{AP}} l_t^{ap})$ is a linear function since the price p_{TOU} is independent on the decision variable l_t^{ap}. The second term is a linear function of load l_t^{ap}, where w_{rand}^{ap} is a set of random number following a uniform distribution. The w_{rand}^{ap} is designed to avoid peak demand rebound at the start time of the lowest price period (see the scenario #7). The parameters of λ^{ap} and w^{ap} are discussed in section 5.2. The term $\sum_{t\in\mathcal{T}}\sum_{ap\in\mathcal{CAP}}\lambda^{ap}\, w^{ap} w_{rand}^{ap} l_t^{ap}$ penalizes the scheduling levels to find a trade-off among three factors: 1) the minimum electricity payment; 2) comfort levels with waiting time; and 3) to avoid the peak demand rebound, existing a little of unpredictable load scheduling behaviours, but still, without affecting the next usage.

6.2 Experiments and Numerical Analysis

This section presents simulation results and the numerical analysis for three scenarios and we continually number the scenarios from CHAPTER 5.

#6: Without load control under TOU. The HAs do not take actions to control load. This is the reference scenario in the study under TOU.

#7: LCM-TOU without w_{rand}^{ap}. The RA announces TOU and will charge the HAs with the announced prices. We also evaluates the impacts of dissatisfaction factor λ^{ap}.

#8: LCM-TOU with w_{rand}^{ap}. This scenario evaluates the impacts of w_{rand}^{ap} and the TOU program participation levels as well.

The experimental configurations are the same as discussed in section 5.4.1 or we state otherwise. The LP problem is solved by the CVX, a package for specifying and solving convex programs [99, 100].

6.2.1 Scenario #6: Without Load Control under TOU

This scenario is the reference in the study under TOU. The HAs do not take any actions to control load. FIGURE 6-1 shows the simulation results in this scenario. The wholesale electricity price is shown by the red dash line. The blue dash-dot line shows the TOU rate in the retail market assuming a budget-balanced market.

The TOU rate is calculated as follows. The energy consumption was 1,716.9 kWh. To purchase this amount of energy from the wholesale market, the retailer spent \$62.77 based on the wholesale price. The HAs are charged by the TOU. The off-peak demand period is defined from 23hr to 6hr; the mid-peak demand period is from 7hr to 16hr; and the on-peak demand period is from 17hr to 22hr. Assuming $p_{on\_peak} = 2 \times p_{off\_peak}$ and $p_{mid\_peak} = 1.5 \times p_{off\_peak}$, then to keep a budget-balanced market, we have $p_{off\_peak} \times t_{off\_period} + 1.5 \times p_{off\_peak} \times t_{mid\_period} + 2 \times p_{off\_peak} \times t_{on\_period} = \$62.77$. By solving this equation, we have $p_{off\_peak} = 2.1747\ cents/kWh$ and hence $p_{mid\_peak} = 3.2621\ cents/kWh$ and $p_{on\_peak} = 4.3494\ cents/kWh$.

The individual HA's electricity bills are shown by the blue circles in FIGURE 6-11 in section 6.3. The average electricity payments of the HAs that own an EV was \$1.32. The maximum and minimum electricity bill was \$1.83 and \$0.78 respectively. The electricity payment of the HAs without an EV was \$0.45 (average), \$0.86 (maximum) and \$0.19 (minimum).

The PAPR was 2.32 and the standard deviation of the load profile was 47.74 kW. The usages of controllable loads are as follows: 25 usages of Dish Washer, 33 usages of Dryers, and 20 usages of EVs. In addition, there were 24 HAs who did not use controllable loads in the simulation day.

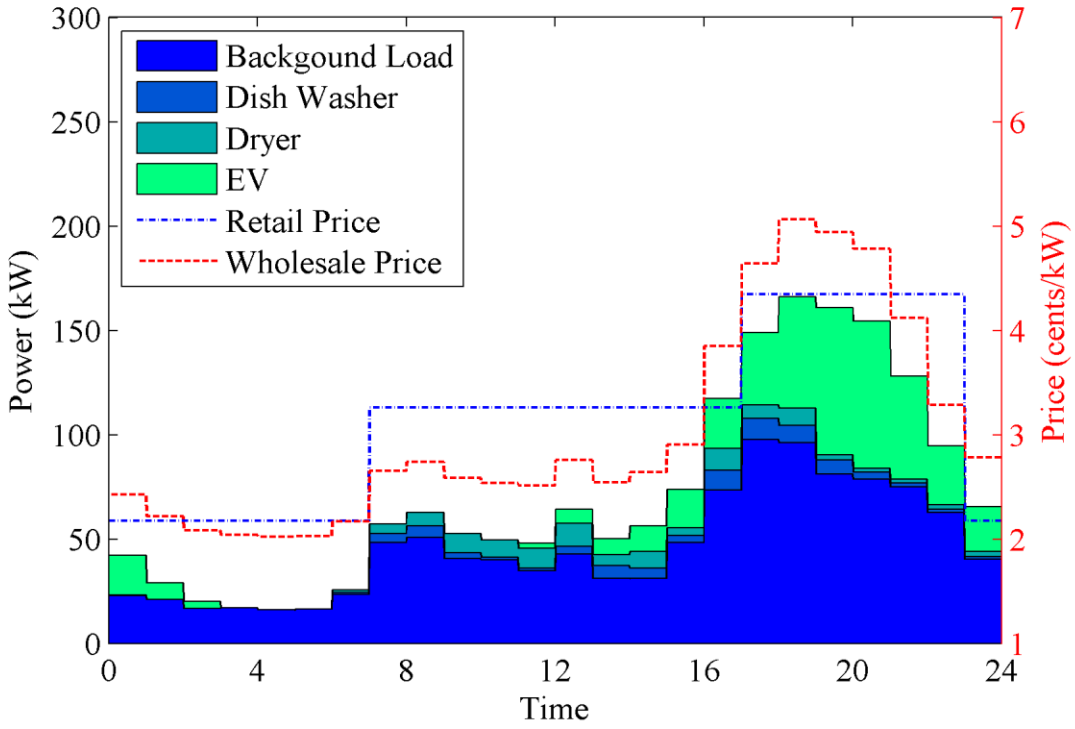

FIGURE 6-1. Load profile of aggregation of 100 HAs, retail electricity prices and wholesale electricity prices in the Scenario #6

6.2.2 Scenario #7: Load Control Model under TOU without w_{rand}^{ap}

The HAs scheduled the controllable loads based upon TOU by solving the LP problem shown in section 6.1. In this scenario, we assume $w_{rand}^{ap} = \mathbf{1}$, i.e., it does not play any roles in the penalty function. Since the prices are constant in each period, an earlier time in each period is strictly better than later; therefore, even though scheduling the controllable loads (e.g., EV) does not significantly affect significantly users' comfortable levels, it is not reasonable to assume that λ^{ap} is zero. This is unlike the situation under RTP. We assume that the controllable loads (dish washer, clothes dryer and EV) have the same $\lambda^{ap}, \forall ap \in \mathcal{CAP}$.

FIGURE 6-2 shows the simulation results with $\lambda^{ap} = 0.01$. The blue dash-dot line shows the TOU. Since an earlier time in each period is strictly better than later, even with a small dissatisfaction factor (e.g., $\lambda^{ap} = 0.01$), the controllable loads were shifted to the lowest price period and hence generated a higher new peak demand in the lowest price period. The red dash line shows the actual wholesale electricity price based on the scheduled load profile. Apparently, the HAs can benefit with lower bills from shifting load to low price periods. However, the total electricity payment from the HAs in the case of $\lambda^{ap} = 0.01$ was \$53.10 while to purchase the electricity energy from the wholesale market using the actual wholesale price, the retailer needs \$65.63. In addition, the PAPR and the standard deviation with $\lambda^{ap} = 0.01$ was increased to 3.56 and 53.05 kW respectively.

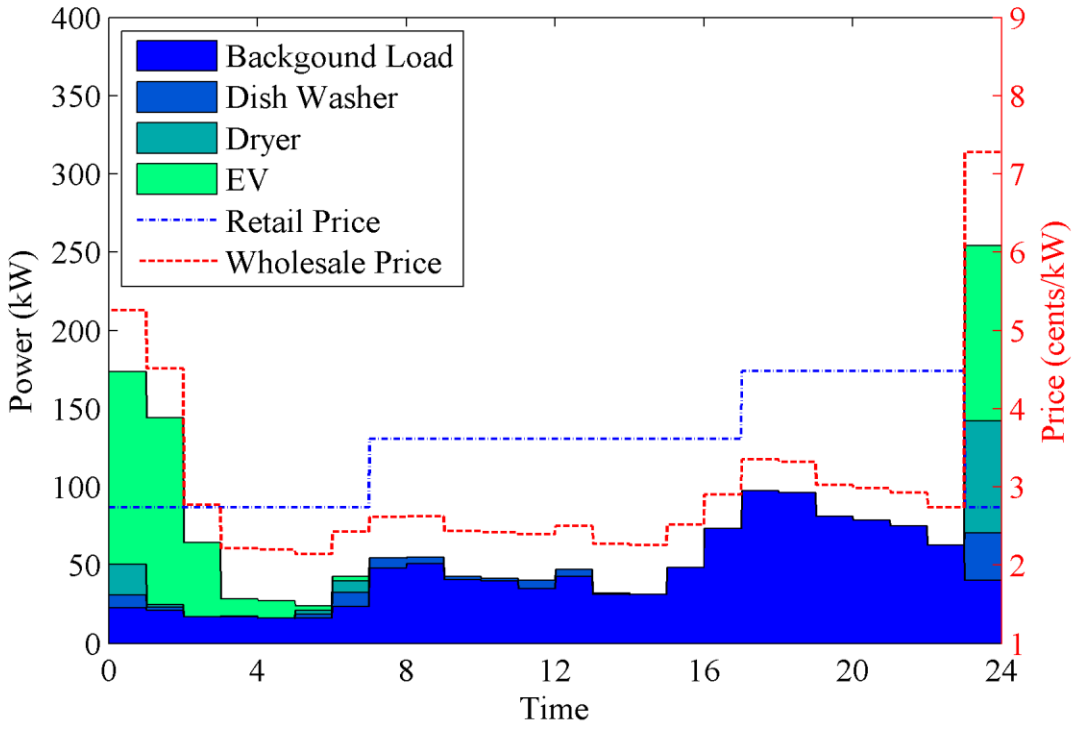

FIGURE 6-2. Load profile of aggregation of 100 HAs, retail electricity prices and wholesale electricity prices in the Scenario #6 with $\lambda^{ap} = 0.01$

We now evaluate the impact of λ^{ap}. TABLE 6-1 shows the observation of the PAPR, the standard deviation, the electricity payment from the HAs and the cost for the RA to buy the electricity with respect to different λ^{ap} from 0.001 to infinity. FIGURE 6-3 shows the plot of these observations. A higher value of λ^{ap} represents a greater level of dissatisfaction to schedule the controllable load. As mentioned earlier, even with a small dissatisfaction factor, the controllable loads can be shifted to the lowest price period. The electricity payment from the HAs gradually increased from \$53.10 ($\lambda^{ap} = 0.001$) to \$62.77 at $\lambda^{ap} = \infty$ where the HAs did not participate the TOU program. A high standard deviation was shown at low $\lambda^{ap} = 0.001$. With λ^{ap} increasing, the standard deviation decreased and reached the bottom (30.75 kW) at $\lambda^{ap} = 0.2$, after that, it gradually climbed to 47.74 kW when λ^{ap} went to infinity, which was the same as the reference scenario #6. The cost for the RA and the PAPR showed the same pattern as the standard deviation.

Similar to the scenario #2, if the HAs are willing to shift the controllable with low dissatisfaction factor, it can cause peak demand rebound at the start time of low price periods. It appears that the best case occurs when $\lambda^{ap} = 0.2$. The load profile and electricity prices at $\lambda^{ap} = 0.2$ is shown in FIGURE 6-4. Even this best case appears unacceptable. Although, the PAPR and the standard deviation is reduce, we can also see a peak rise at the start time of the lowest price period. In addition, the HAs' dissatisfaction factor are not easy to observe and also not controllable.

TABLE 6-1. The observations with different λ^{ap} in the scenarios of #6

λ^{ap}	PAPR	Standard Deviation (kW)	Payment from HAs ($)	Cost for RA ($)
0.001	3.56	51.96	53.10	65.64
0.01	3.56	51.95	53.10	65.63
0.03	3.56	52.45	53.10	65.92
0.05	3.56	52.15	53.10	65.73
0.07	3.47	51.13	53.23	65.05
0.09	3.14	45.45	53.68	61.76
0.11	2.80	37.64	54.46	57.81
0.13	2.62	34.87	54.70	56.56
0.15	2.39	32.29	55.03	55.32
0.17	2.22	31.24	55.16	54.91
0.2	2.22	30.75	55.16	54.75
0.3	2.22	33.18	55.97	55.68
0.5	2.25	38.97	59.39	58.37
0.7	2.25	40.59	60.21	59.15
1	2.25	42.18	61.17	59.97
2	2.25	42.94	61.70	60.42
3	2.25	43.16	61.92	60.49
∞	2.32	47.74	62.77	62.77

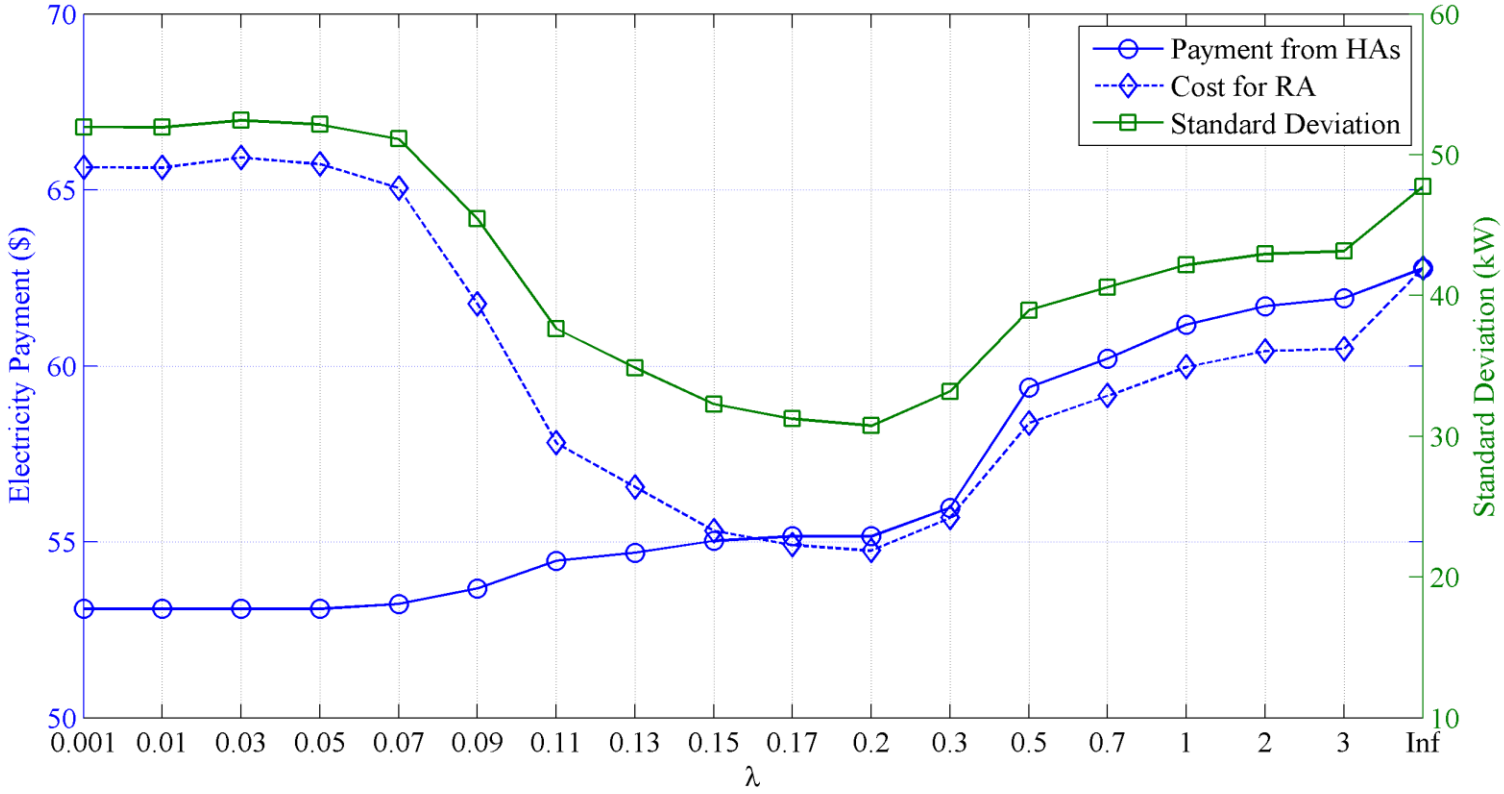

FIGURE 6-3. The observations with different λ^{ap} in the scenario #7

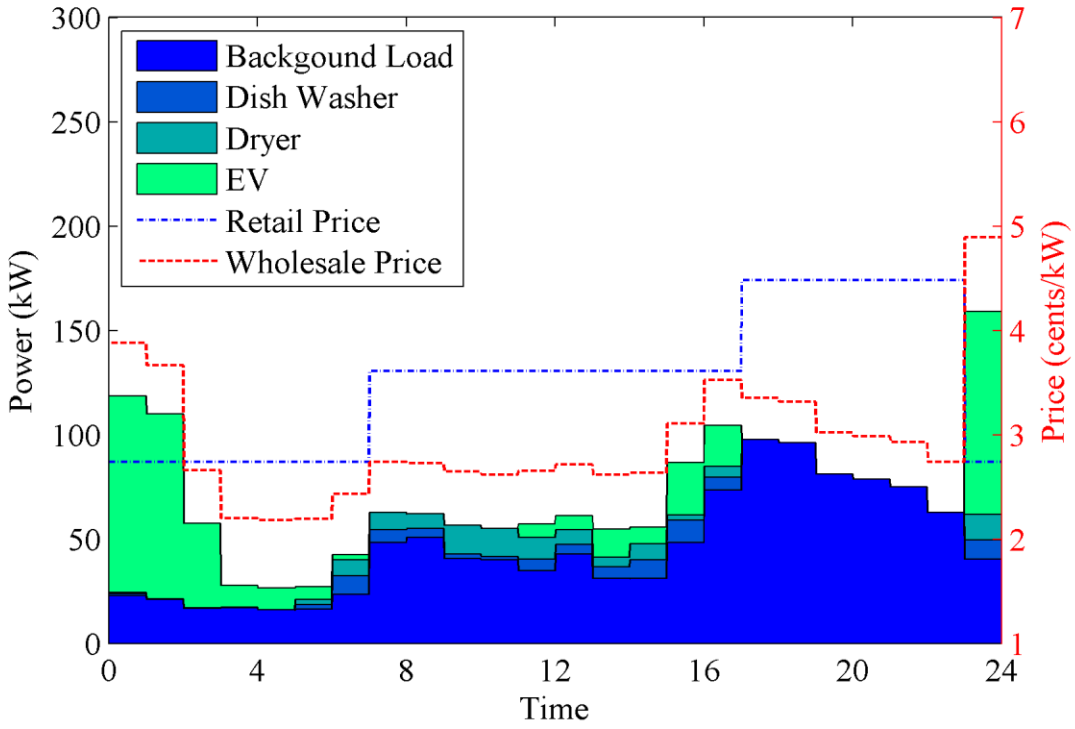

FIGURE 6-4. Load profile of aggregation of 100 HAs, retail electricity prices and wholesale electricity prices in the Scenario #7 with $\lambda^{ap} = 0.2$

6.2.3 Scenario #8: Load Control Model under TOU with w_{rand}^{ap}

In this scenario, we evaluate w_{rand}^{ap} and study the impact of different levels of TOU participation as well.

6.2.3.1 The Impact of w_{rand}^{ap}

The uniform random weights w_{rand}^{ap} provides variations for the flat price in certain periods. In the objective function, the term $\sum_{t\in\mathcal{T}}\sum_{ap\in\mathcal{C}_{\mathcal{AP}}}\lambda^{ap}\ w^{ap}w_{rand}^{ap}l_t^{ap}$ penalizes the scheduling levels to find the trade-off among three factors: 1) the minimum electricity payment; 2) comfort levels with waiting time; and 3) to avoid peak demand rebound, existing a little of unpredictable load scheduling behaviours, but still, without affecting the next usage. We assume $\lambda^{ap}=0.01$. w_{rand}^{ap} is a set of uniformly distributed random numbers with 24 elements in it. In this subsection, we assume that 100% of HAs are willing to participate the TOU program for evaluation of w_{rand}^{ap}.

It is noted that since the w_{rand}^{ap} follows a uniform distribution, the schedule level do not depend on the norm of this set as long as it is big enough to influence the dissatisfaction factor λ^{ap} in the penalty function while is small enough not to dominate the whole objective function. FIGURE 6-5 shows the plot of the observations of the standard deviation, the electricity payment from the HAs and the cost for the RA with different norm-1 values $\left|w_{rand}^{ap}\right|_1$ (i.e., average value), from 0.1 to 100. We can see that the observations are greatly stable for $1\le\left|w_{rand}^{ap}\right|_1\le 10$.

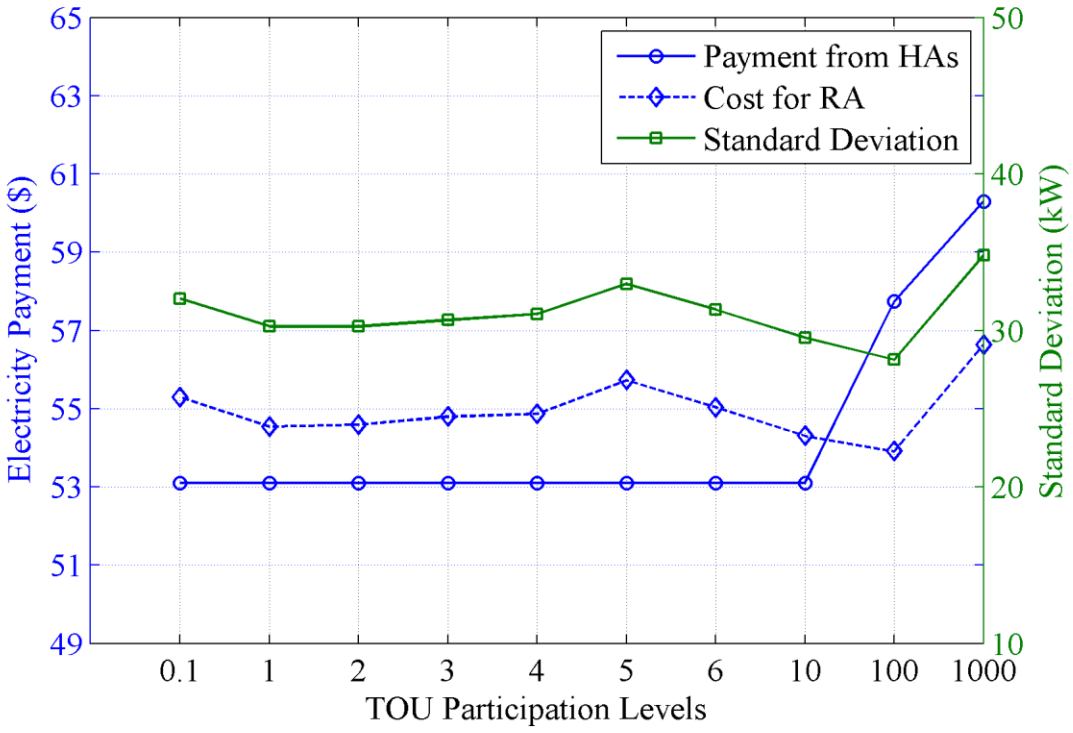

FIGURE 6-5. The observations with different $\left|w_{rand}^{ap}\right|_1$ in the scenario #8

FIGURE 6-6 shows the simulation results with $\left|w_{rand}^{ap}\right|_1 = 2$, which is selected from the stable range. The PAPR and standard deviation of the load profile was 1.96 and 30.25 kW respectively. The total electricity payment from the 100 HAs was $53.10 and the electricity cost for the RA was $54.59. Although, there is a small mismatch between electricity payment from HAs and the cost for the RA, the quality of all the observations are improved. This mismatch can be leveled by increasing the TOU rate. The observations in the reference scenario #6 are duplicated as follows for a quick comparison. The PAPR was 2.32 and the standard deviation was 47.74 kW. Both the electricity payment from the HAs and the cost for the RA was $62.77.

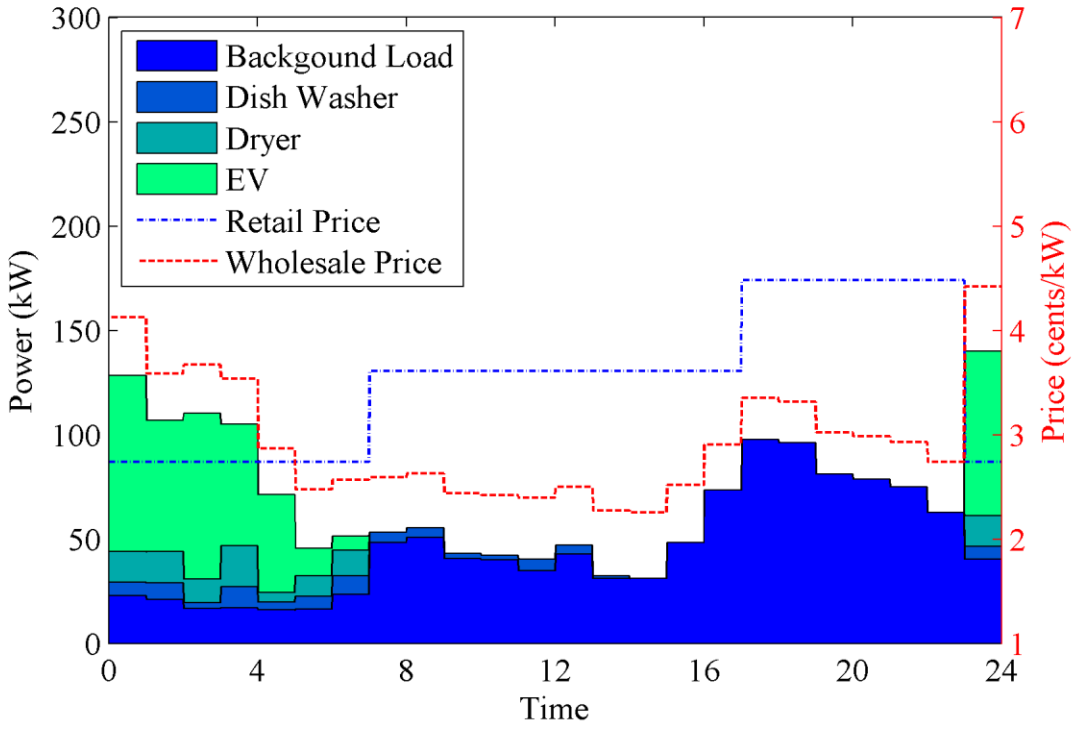

FIGURE 6-6. Load profile of aggregation of 100 HAs, retail electricity prices and wholesale electricity prices in the Scenario #8 with λ^{ap}=0.01, $\left|w_{rand}^{ap}\right|_1 = 2$, and TOU participation percentage = 100%

6.2.3.2 The Impact of TOU Participation Levels

By incorporating w_{rand}^{ap}, the simulation results show the promising application of TOU. We now study how the participation levels can affect the DR implementation. We continuous to assume $\lambda^{ap} = 0.01$ and $\left|w_{rand}^{ap}\right|_1 = 2$.

There are two ways to interpret the participation levels. 1) the percentage of HAs who sign a contract with the RA to participate the TOU; 2) the HAs only have some fraction of ability to participate the TOU due to lack of DR enable technologies (e.g., smart meter). In this study, we use the first interpretation.

TABLE 6-2 and FIGURE 6-7 show the observations with different levels of TOU participation. From the zero level to the 50% participation level, we can see that the standard deviation decreased from 47.74 kW to 28.59 kW, while if the participation level is greater than 50%, the standard deviation slightly increased and stayed at an approximate level of 30 kW till 100% participation. The PAPR had a similar pattern as the standard deviation. The electricity payment from the HAs continuously decreased from \$62.77 (no participation) to \$53.10 (100% participation). Apparently, the more the HAs participate the TOU program the more savings they can have. The cost to buy the electricity energy for the RA also dropped from \$62.77 with no HAs participating the TOU to \$54.16 at the participation level of 50%. After that, the incremental interests were subtle and the cost hovered at about \$54.6.

In terms of the quality of the PAPR, the standard deviation and the electricity cost for the RA, the 50% participation level appears to be the best case. FIGURE 6-8 shows the simulation results for the 50% participation level. In terms of the electricity payments for

the HAs, the best case occurred at the participation level of 80%. FIGURE 6-9 show the simulation results for the 80% participation level.

TABLE 6-2. The observations with different levels of TOU participation in the scenarios of #8 (λ^{ap}=0.01 and $\left|w_{rand}^{ap}\right|_1 = 2$)

Percentage Participation	PAPR	Standard Deviation (kW)	Payment from HAs ($)	Cost for RA ($)
0%	2.32	47.74	62.77	62.77
10%	2.31	44.58	61.87	61.25
20%	2.16	39.43	60.72	58.50
30%	2.02	36.88	59.97	57.50
40%	1.84	33.71	58.66	56.03
50%	1.84	28.59	58.00	54.16
60%	1.76	29.71	56.62	54.32
70%	1.78	30.47	55.77	54.61
80%	2.11	30.52	54.47	54.69
90%	2.12	30.45	53.54	54.66
100%	1.96	30.25	53.10	54.59

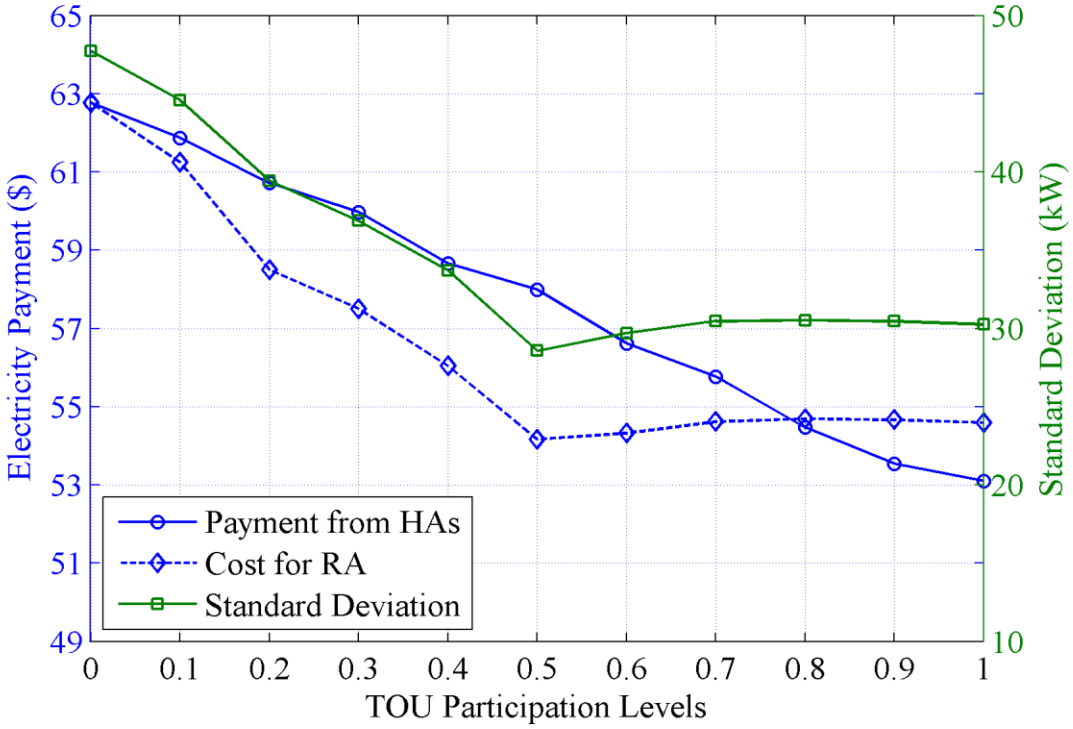

FIGURE 6-7. The observations with different TOU participation levels in the scenario #8

(λ^{ap}=0.01 and $\left|w_{rand}^{ap}\right|_1 = 2$)

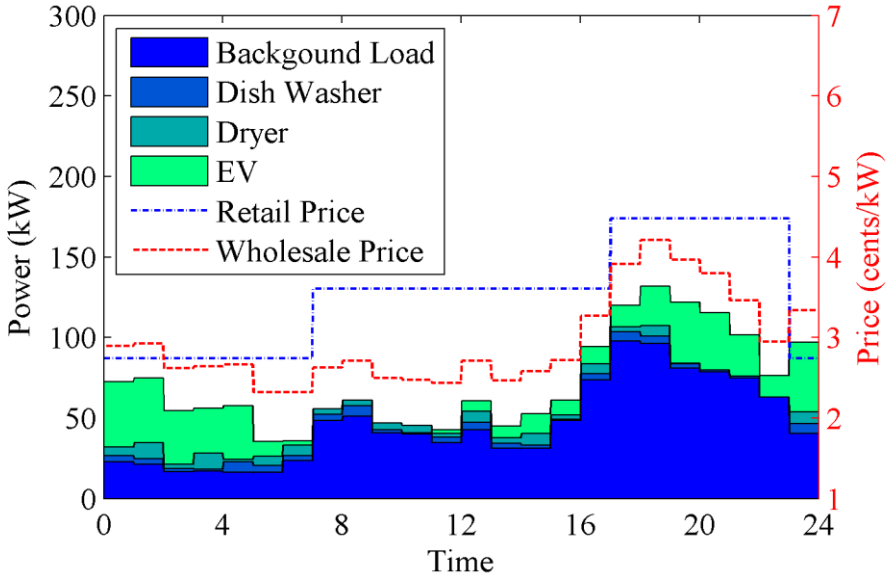

FIGURE 6-8. Load profile of aggregation of 100 HAs, retail electricity prices and wholesale electricity prices in the Scenario #8 with λ=0.01, $\left|w_{rand}^{ap}\right|_1 = 2$, and TOU participation percentage = 50%

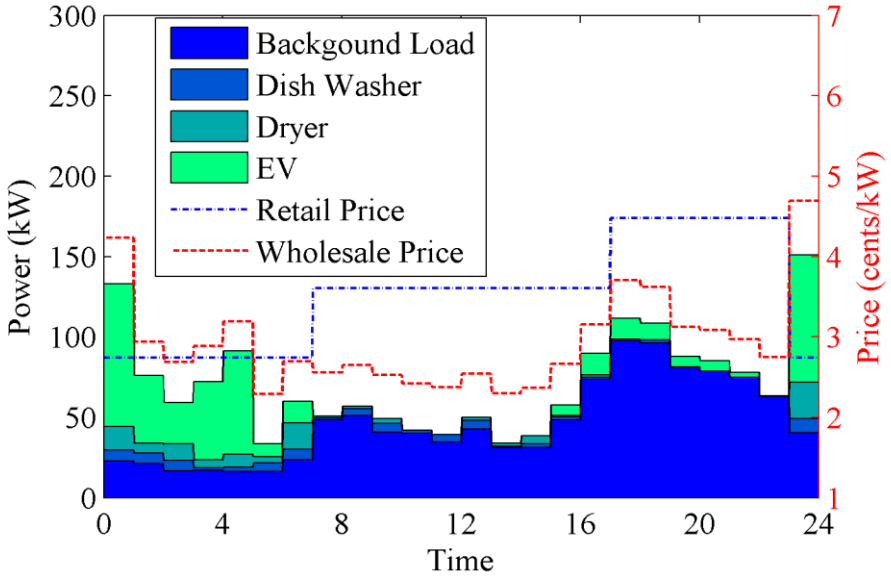

FIGURE 6-9. Load profile of aggregation of 100 HAs, retail electricity prices and wholesale electricity prices in the Scenario #9 with λ=0.01, $\left|w_{rand}^{ap}\right|_1 = 2$, and TOU participation percentage = 80%

6.3 Discussion

We discuss and evaluate the scenarios #6 ~ #8 in this section. The scenario #6 is the reference for evaluating the LCM-TOU.

The scenario #7 shows a peak demand rebound at the start time of the lowest price period if all the HAs are willing to participate the TOU program using the LCM-TOU without w_{rand}^{ap}. In addition, the impacts of the different dissatisfaction factor λ^{ap} on load scheduling is studied as well. If some customers are frustrated to schedule the controllable load, the peak demand rebound can be alleviated. The best case happens at $\lambda^{ap} = 0.2$, in which the standard deviation and electricity cost reaches the bottom value of 30.75 kW and \$54.75 respectively. However, it is very difficult to observe and control users' dissatisfaction factor of scheduling load. Furthermore, the observations are still not satisfied.

The scenario #8 shows the promising applicability of the LCM-TOU with w_{rand}^{ap}. This scenario assume a reasonable small dissatisfaction factor $\lambda^{ap} = 0.01$ and evaluates the impact of TOU participation levels. In the case of 100% participation level, the PAPR and standard deviation of the load profile is reduced to 1.96 and 30.25 kW respectively. The total electricity payment from the 100 HAs is \$53.10 and the electricity cost for the RA was \$54.59. Although, there is small mismatch between electricity payment from HAs and the cost for the RA, the quality of all the observations are improved.

In term of the quality of the PAPR, the standard deviation and the electricity cost for the RA, the 50% participation level appears the best case. In terms of the electricity payments for the HAs, the best case occurs at the participation level of 80%. TABLE 6-3 summarizes the observations in the scenario #6 (without load control), the scenario #7

without w_{rand}^{ap} and $\lambda^{ap} = 0.2$, and the scenario #8 with w_{rand}^{ap}, 50% & 80% participation level. FIGURE 6-10 shows the load profiles among these cases.

At the participation level of 50%, the standard deviation is the minimum of 28.59 kW. The cost for the RA to buy the electricity energy is also at the minimum ($54.16) and the electricity payment from the HAs is $58.00; therefor the RA has $3.84 profit. At the participation level of 80%, the cost for the RA and the electricity payment from the HAs are almost balanced, in which the cost is $54.69 and the electricity payment from the HAs is $54.47. The TOU participation level is easy to control or at least easy to know for the RA and it is suitable to control the participation level between 50% and 80%. In this range, the incremental interests for the RA is subtle, in which the cost stays around $54.6.

TABLE 6-4 summarizes the statistical information of the electricity payment for the 80% participants. FIGURE 6-11 shows electricity payment for the individual HAs in the scenario #6 and the scenario #8 with the 80% TOU participation level. Interestingly, we can see that the #20 HA who is not a participant, has a great reduced electricity payment. The reason is because that the HA happens to come home late and charging its EV immediately when is the lowest price period.

TABLE 6-3 The observations in the scenario #6 (without load control under TOU), the scenario #7 (without w_{rand}^{ap} and $\lambda^{ap} = 0.2$) and the scenario #8 (with w_{rand}^{ap}, 50% & 80% participation level).

	PAPR (% Reduction)	Standard Deviation (kW) (% Reduction)	Payment from HAs ($) (% Reduction)	Cost for RA ($) (% Reduction)
Scenario #6	2.32	47.74	62.77	62.77
#7 without w_{rand}^{ap} and $\lambda^{ap} = 0.2$	2.22 (4.3%)	30.75 (35.6%)	55.16 (12.1%)	54.75 (12.8%)
#8 with w_{rand}^{ap} participation level = 50%	1.84 (20.7%)	28.59 (40.1%)	58.00 (7.6%)	54.16 (13.7%)
#8 with w_{rand}^{ap} participation level = 80%	2.11 (9.1%)	30.52 (36.1%)	54.47 (13.2%)	54.69 (12.9%)

TABLE 6-4 The summary of the individual electricity payment in the scenarios #6, #8 with the 80% TOU participation level

	Have EVS	Electricity Payment ($)			Payment Reduction (%)		
		Average	Max	Min	Average	Max	Min
Scenario #6 without w_{rand}^{ap}	Yes	1.32	1.83	0.78	-	-	-
	No	0.45	0.86	0.19	-	-	-
Scenario #8 with w_{rand}^{ap} Participants	Yes	0.92	1.24	0.68	30.2	39.3	13.5
	No	0.44	0.86	0.22	5.1	19.2	0

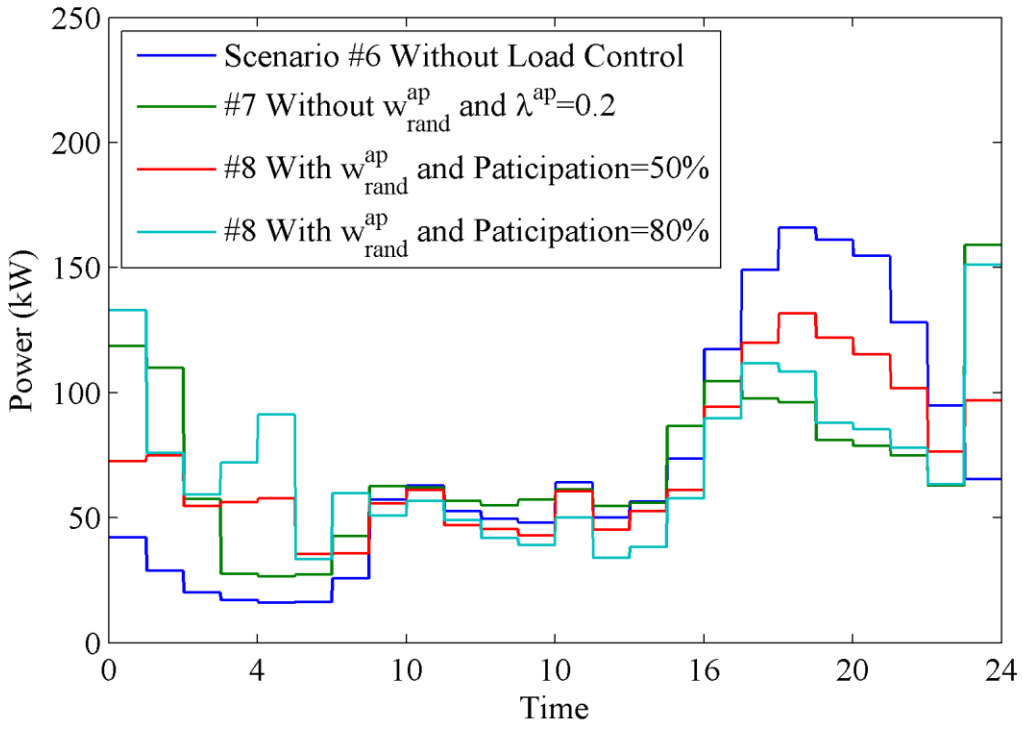

FIGURE 6-10 Load profiles of the scenarios #6 (without load control), #7 (without w_{rand}^{ap} and $\lambda^{ap} = 0.2$) and #8 (with w_{rand}^{ap}, participation level of 50% & 80%)

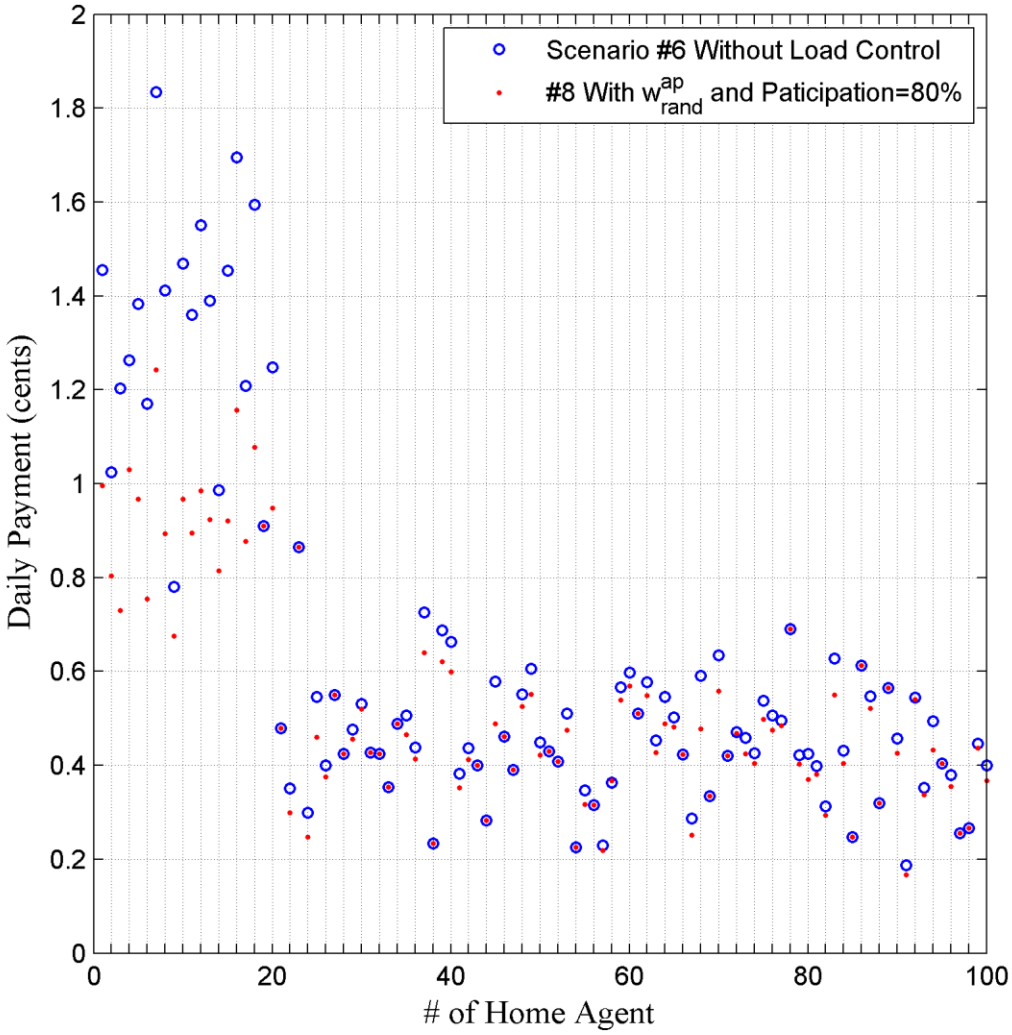

FIGURE 6-11 The individual electricity payments of the HAs in the scenarios #6 (without load control) and #8 (with w_{rand}^{ap} and participation level of 80%)

Several TOU programs were run in the period from 2001 to 2007. The TOU programs without DR-enabling technology supporting include the California statewide pricing pilot (2003-2004), the Ontario Energy Board smart price pilot (2006-2007) and the Puget Sound Energy's TOU program (2001-2002) and the TOU programs with DR-enabling technology have the California automated DR system pilot (2004-2005), the Gulf power select program (2000-2001), and the Public Service Electric and Gas residential pilot program (200-2007). The peak demand reduction in these programs are summarized in TABLE 6-5 [101]. We can see that the DR-enabling technologies are greatly effective.

TABLE 6-5 Peak demand reduction in TOU programs

Programs	DR-Enabling Technology	Peak Demand Reduction (%)
California state wide pricing pilot (2003-2004)	NO	5%
Ontario Energy Board smart price pilot (2006-2007)	NO	5%
Puget Sound Energy's TOU program (2001-2002)	NO	5%
California automated DR system pilot (2004-2005)	YES	28%
Gulf power select program (2000-2001)	YES	22%
Public Service Electric and Gas residential pilot program (200-2007)	YES	21%

6.4 Summary

The LCM-TOU is proposed for DR implementing based on the TOU. Experiments are conducted in three scenarios using numerical analysis.

We can see that the DR implementation can cause higher peak demand rebound in the start time of the lowest price period in the scenario #7 (LCM-TOU without w_{rand}^{ap}). Although, this peak demand rebound can be eased if there are HAs who are frustrated (incorporated by the dissatisfaction factor) to schedule their controllable load, the simulation results are not satisfactory even in the best case where $\lambda^{ap} = 0.2$. Furthermore, the dissatisfaction factor is difficult to observe and control.

The LCM-TOU with w_{rand}^{ap} is evaluated in the scenario #8. The simulation results show that the peak demand rebound is avoided and the PAPR and standard deviation are both reduced by 15.5% and 36.6% respectively at the participation level of 100%; however, in this case the cost for the RA is greater than the electricity payment from the HAs. The range from 50% to 80% of participation levels appear to be "best cases" for the welfare of the society, in which the PAPR and standard deviation are approximately reduced by 14% and 39% respectively, and the electricity payments from the HAs and the cost for the RA can be balanced in this range. More exactly, the electricity payments from the HAs are greater than or almost equal to the cost for RA. To keep the budget-balanced market, the RA should propose some mechanism to pay back the earnings to the HAs. If the participation level is greater than 80%, the RA needs to raise the TOU rate. Furthermore, at the participation level of 50% (the load profile is shown by the red line in FIGURE 6-10) can be identified as the best case for the welfare of the society, in which the standard deviation and the cost for the RA is the lowest among all the cases under TOU.

CHAPTER 7

CONCLUSIONS AND RECOMMENDATIONS

DR as an essential component of the smart grid plays a key role to reduce peak demand and improve the energy efficiency and the stability of the power system. A successful DR implementation requires both the DR enable technologies and the DR policies. This thesis proposes a MAS to evaluate both these aspects considering a general wholesale electricity market, and focuses on the power and information flow in the distribution network in a residential sector. The residential users are modeled by the heterogeneous HAs and the power provider (retailer/utility) is captured by the RA. We assume the end-users are equipped with a home EMS and a smart meter. Two popular price-based DR policies are evaluated, namely RTP and TOU.

A residential load prediction model is proposed to forecast the electricity load profile for heterogeneous HAs. This load prediction model simulates the benchmark based on statistical information of how people use their appliances including EVs. Each HA has a unique load profile depending on its heterogeneous local configurations.

Under the RTP, the OL-LCM-RTP and the CL-LCM-RTP are formulated to CP problems to minimize both the electricity payment and the penalty function associated with the dissatisfaction factor λ^{ap} in order to find a trade-off between the minimum electricity payment and comfort levels with waiting time. The electricity price prediction model is proposed to forecast RTP and is incorporated into the objective function of the CP problems. The proposed MAS incorporating these models are evaluated in five scenarios. The scenario #1 is the reference, in which no load control action is taken. The scenario #2

shows that the day-ahead announced RTP can cause peak demand rebound in the lowest price time since all the HAs synchronize their controllable loads accordingly.

The OL-LCM-RTP with $\lambda^{ap} = 0$ is examined in the scenario #3. The simulation results show that the PAPR, the standard deviation and the electricity payment is reduced by 33.6%, 54.8% and 17.4% respectively. The PAPR and the standard deviation can both describe the stability of the power system and small values represent high stability. In this scenario, the HAs schedule their controllable loads based on local information; therefore, it is called an open-loop control model and it only requires a minimum of communication between the utility/retailer and multiple homes. This is greatly useful because the infrastructure for communication is still under development. Since HAs minimize electricity payments locally, the privacy of users is not sacrificed.

The scenario #4 evaluates the OL-LCM-RTP with $\lambda^{ap} > 0$. The simulation results show that a high dissatisfaction factor can reduce the waiting time to use the controllable loads however it increases the PAPR, the standard deviation and the electricity payment. The simulation results can provide end-users with a method to determine an appropriate dissatisfaction factor for the controllable loads based on their own preferences. A utility can also consults these simulation results for a better plan with different dissatisfaction factors.

The CL-LCM-RTP as a closed-loop control mechanism is evaluated in the scenario #5. In this scenario, we assume that the dissatisfaction factor $\lambda^{ap} = 0.1$ and the load control is not only based on the local information but also the feedback from the RA. The feedback is the electricity consumption of the other HAs collected by the RA. Load scheduling is conducted in a round process. The HAs schedule their controllable loads by

solving the CP problem in a random order and send the scheduled load profile to the RA. The RA updates the global load information and feedback to the next HA. The RA has increasingly precise global load information inside a round, i.e., the earlier HA has less precise global load information. However, all the HAs can reschedule their load in the next round. The experiments show that the schedule process can quickly converge at the second round. The PAPR, the standard deviation and the electricity payment is reduced by 39.2%, 72.7% and 19.6% respectively, which is the best scenario in terms of the quality of the observations. The trade-off is a certain level of communication and coordination.

Under the TOU, the LCM-TOU is formulated to a LP problem. The model minimizes the objective function to find a trade-off among three factors: 1) the minimum electricity payment; 2) comfort levels with waiting time; and 3) to avoid peak demand rebound, but still, without affecting the total usage. The DR implementation under TOU is evaluated in three scenarios. The scenario #6 is the reference scenario. The scenario #7 examines the LCM-TOU without w_{rand}^{ap}. Since an earlier time in each period is strictly better than later, even with a small dissatisfaction factor (e.g., $\lambda^{ap} = 0.01$), the controllable loads can be shifted to the lowest price period and hence generate a significantly higher new peak demand. This scenario also evaluates the impact of different values of λ^{ap}. The standard deviation and electricity cost reaches the minimum at $\lambda^{ap} = 0.2$; however the observations are still not satisfied. Furthermore, it is very difficult to observe and control users' dissatisfaction factor.

The scenario #8 evaluates the LCM-TOU with w_{rand}^{ap} and the TOU participation levels as well. The simulation results show a reduced PAPR (by 15.5%), the standard deviation (36.6%), and the electricity payments from the HAs (by 15.4%) at a 100% participation

level. However, the cost for the RA to buy the electricity energy is greater than the electricity payments collected from the HAs by $1.49. In the range from 50% to 80% of participation levels appear to be the "best cases" for the welfare of the society, in which the PAPR and standard deviation are approximately reduced by 14% and 39% respectively. In addition, the electricity payments from the HAs and the cost for the RA can be balanced in this range. To keep a budget-balanced market, the RA should propose some mechanism to pay back the earnings to the HAs. If the participation level is greater than 80%, the RA needs to raise the TOU. Furthermore, a participation level of 50% can be identified as the best case for the welfare of the society, in which the standard deviation and the cost for the RA is the lowest among all the cases under TOU.

This study proposes several optimal DR mechanisms in an agent-based framework for multiple heterogeneous homes to respond to dynamic pricing of RTP and TOU automatically. The proposed simulation model can be a test-bed to evaluate various DR enabling technologies and policies. The HA, with the optimal control algorithms, can also be implemented in a home EMS to minimize the electricity payment.

This study can be extended in the following aspects. 1) EV electricity flow can be bidirectional, i.e., charge/discharge a battery. Mathematically, the decision variables can have both positive and negative values. This would further improve the power system stability and the energy efficiency; 2) small power generation units, such as small turbines and solar panels, and electricity storage facilities, such as, batteries and compressed air energy storage, can be incorporated; 3) stochastic behaviours of the HAs need to be studied. For instance, the HAs change behaviours after a commitment; 4) the proposed MAS can be readily extended to incorporate DLC.

CHAPTER 8

REFERENCES

[1] Z. Wang and R. Paranjape, "Optimal Residential Demand Response for Multiple Heterogeneous Homes with Real-Time Price Prediction in a Multi-Agent Framework " *IEEE Trans. Smart Grid,* Oct. 2015.

[2] Z. Wang, R. Paranjape, A. Sadanand, and Z. Chen, "Residential demand response: An overview of recent simulation and modeling applications," in *Proc. 2013 IEEE Canadian Electrical and Computer Engineering Conf.*, Regina, SK, Canada, pp. 1-6.

[3] H. Chao, "Price-responsive demand management for a smart grid world," *The Electricity Journal,* vol. 23, pp. 7-20, Feb. 2010.

[4] A. Conchado and P. Linares, "The Economic Impact of Demand-Response Programs on Power Systems. A Survey of the State of the Art," in *Handbook of Networks in Power Systems I*, 2012, pp. 281-301.

[5] Q. QDR, "Benefits of demand response in electricity markets and recommendations for achieving them," U. S. Department of Energy, Feb. 2006.

[6] BC Hydro. (2015, February 3). *Residential Rates*. Available: https://www.bchydro.com/accounts-billing/customer-service-residential/residential-rates.html

[7] N. R. Canada, "Comprehensive Energy Use Database, 1990 to 2010," 2013.

[8] P. Du and N. Lu, "Appliance commitment for household load scheduling," *Smart Grid, IEEE Transactions on,* vol. 2, pp. 411-419, 2011.

[9] P. Vrba *et al.*, "A Review of Agent and Service-Oriented Concepts Applied to Intelligent Energy Systems," *IEEE Trans. Ind. Informat.,* vol. 10, pp. 1890-1903, Aug. 2014.

[10] H. Farhangi, "The path of the smart grid," *IEEE Power Energy Mag.,* vol. 8, pp. 18-28, 2010.

[11] R. Wiser, "Renewable portfolio standards in the United States-a status report with data through 2007," *Lawrence Berkeley National Laboratory,* 2008.

[12] GE Energy, "New England wind integration study," ed: Holyoke, Massachusetts: ISO New England Inc, 2010.

[13] L. G. Swan and V. I. Ugursal, "Modeling of end-use energy consumption in the residential sector: A review of modeling techniques," *Renewable and Sustainable Energy Reviews,* vol. 13, pp. 1819-1835, Jan. 2009.

[14] A. Grandjean, J. Adnot, and G. Binet, "A review and an analysis of the residential electric load curve models," *Renewable and Sustainable Energy Reviews,* vol. 16, pp. 6539-6565, Oct. 2012.

[15] A. Grandjean, J. Adnot, and G. Binet, "A review and an analysis of the residential electric load curve models," *Renewable and Sustainable Energy Reviews,* vol. 16, pp. 6539-6565, 2012.

[16] S. Shao, M. Pipattanasomporn, and S. Rahman, "Development of Physical-Based Demand Response-Enabled Residential Load Models," *IEEE Trans. Power Syst.,* vol. 28, pp. 607-614, May 2013.

[17] W. Zhang, J. Lian, C. Y. Chang, and K. Kalsi, "Aggregated Modeling and Control of Air Conditioning Loads for Demand Response," *IEEE Trans. Power Syst.*, vol. 28, pp. 4655-4664, Nov. 2013.

[18] J. Kondoh, L. Ning, and D. J. Hammerstrom, "An Evaluation of the Water Heater Load Potential for Providing Regulation Service," *IEEE Trans. Power Syst.*, vol. 26, pp. 1309-1316, Aug. 2011.

[19] M. M. Armstrong, M. C. Swinton, H. Ribberink, I. Beausoleil-Morrison, and J. Millette, "Synthetically derived profiles for representing occupant-driven electric loads in Canadian housing," *Journal of Building Performance Simulation*, vol. 2, pp. 15-30, 2009.

[20] Natrual Resources Canada, *Energy use data handbook, 1990 and 1997 to 2003. Gatineau, QC, Canada: NRCan Office of Energy Efficiency.*

[21] Natrual Resources Canada. (2002, September 9). *Photovoltaic systems – a buyer's guide. Appendix B.* Available: http://www.canren.gc.ca/prod_serv/index.asp?CaID101&PgId551

[22] R. Pratt, *Description of Electric Energy Use in Single-family Residences in the Pacific Northwest: End-use Load and Consumer Assessment Program (ELCAP)*: Bonneville Power Administration, 1989.

[23] J. Widén and E. Wäckelgård, "A high-resolution stochastic model of domestic activity patterns and electricity demand," *Applied Energy*, vol. 87, pp. 1880-1892, 2010.

[24] I. Richardson, M. Thomson, D. Infield, and C. Clifford, "Domestic electricity use: A high-resolution energy demand model," *Energy and Buildings*, vol. 42, pp. 1878-1887, 2010.

[25] N. Venkatesan, J. Solanki, and S. K. Solanki, "Residential Demand Response model and impact on voltage profile and losses of an electric distribution network," *Applied energy*, vol. 96, pp. 84-91, Jan. 2012.

[26] J. Vardakas, N. Zorba, and C. Verikoukis, "A Survey on Demand Response Programs in Smart Grids: Pricing Methods and Optimization Algorithms," *IEEE Commun. Surveys Tuts.*, July 2014.

[27] A.-H. Mohsenian-Rad and A. Leon-Garcia, "Optimal residential load control with price prediction in real-time electricity pricing environments," *IEEE Trans. Smart Grid*, vol. 1, pp. 120-133, Sep. 2010.

[28] Ontario Energy Board. (May 13, 2014). *Electricity Prices*. Available: http://www.ontarioenergyboard.ca/OEB/Consumers/Electricity/Electricity+Prices

[29] Z. Wang and R. Paranjape, "Agent-Based Simulation of Home Energy Management System in Residential Demand Response," in *Proc. 2014 IEEE Canadian Electrical and Computer Engineering Conf.*, Toronto, ON, Canada, pp. 1-6.

[30] Z. Wang and R. Paranjape, "Optimal Scheduling Algorithm for Charging Electric Vehicle in a Residential Sector Under Demand Response," in *Proc. 2015 IEEE Electrical Power & Energy Conf.*, London, ON, Canada, pp. 1-5.

[31] PJM. (2015, February 3). *Real-Time Energy Market*. Available: http://www.pjm.com/markets-and-operations/energy/real-time.aspx

[32] P. Cappers, C. Goldman, and D. Kathan, "Demand response in US electricity markets: Empirical evidence," *Energy,* vol. 35, pp. 1526-1535, July 2010.

[33] M. Doostizadeh and H. Ghasemi, "A day-ahead electricity pricing model based on smart metering and demand-side management," *Energy,* vol. 46, pp. 221-230, Sep. 2012.

[34] K. M. Tsui and S.-C. Chan, "Demand response optimization for smart home scheduling under real-time pricing," *IEEE Trans. Smart Grid,* vol. 3, pp. 1812-1821, Dec. 2012.

[35] L. P. Qian, Y. J. A. Zhang, J. Huang, and Y. Wu, "Demand response management via real-time electricity price control in smart grids," *IEEE J. Sel. Areas Commun.,* vol. 31, pp. 1268-1280, 2013.

[36] N. Gudi, L. Wang, and V. Devabhaktuni, "A demand side management based simulation platform incorporating heuristic optimization for management of household appliances," *International Journal of Electrical Power & Energy Systems,* vol. 43, pp. 185-193, 2012.

[37] Y. Guo, M. Pan, and Y. Fang, "Optimal power management of residential customers in the smart grid," *IEEE Trans. Parallel Distrib. Syst.,* vol. 23, pp. 1593-1606, 2012.

[38] T. Logenthiran, D. Srinivasan, and T. Z. Shun, "Demand side management in smart grid using heuristic optimization," *IEEE Trans. Smart Grid,* vol. 3, pp. 1244-1252, 2012.

[39] P. Samadi, H. Mohsenian-Rad, R. Schober, and V. W. Wong, "Advanced demand side management for the future smart grid using mechanism design," *IEEE Trans. Smart Grid*, vol. 3, pp. 1170-1180, 2012.

[40] M. A. A. Pedrasa, T. D. Spooner, and I. F. MacGill, "Coordinated scheduling of residential distributed energy resources to optimize smart home energy services," *IEEE Trans. Smart Grid*, vol. 1, pp. 134-143, 2010.

[41] N. Li, L. Chen, and S. H. Low, "Optimal demand response based on utility maximization in power networks," in *Proc. 2011 IEEE Power Energy Soc. Gen. Meet.*, pp. 1-8.

[42] S. Boyd and L. Vandenberghe, *Convex optimization*: Cambridge university press, 2004.

[43] T.-H. Chang, M. Alizadeh, and A. Scaglione, "Real-time power balancing via decentralized coordinated home energy scheduling," *IEEE Trans. Smart Grid*, vol. 4, pp. 1490-1504, Sep. 2013.

[44] A. Safdarian, M. Fotuhi-Firuzabad, and M. Lehtonen, "A distributed algorithm for managing residential demand response in smart grids," *IEEE Trans. Ind. Informat.*, vol. 10, pp. 2385-2393, Nov. 2014.

[45] M. Muratori and G. Rizzoni, "Residential Demand Response: Dynamic Energy Management and Time-Varying Electricity Pricing," *IEEE Trans. Smart Grid*, pp. 1-10, Apr. 2015.

[46] D. Senthilkumar, S. Kumar, Y. Ozturk, and G. Lee, "An Intelligent Home Energy Management System to. Improve Demand Response," *IEEE Trans. Smart Grid*, vol. 4, Jun. 2013.

[47] H.-T. Roh and J.-W. Lee, "Residential Demand Response Scheduling With Multiclass Appliances in the Smart Grid," *IEEE Trans. Smart Grid*, 2015.

[48] R. de Sá Ferreira, L. A. Barroso, P. Rochinha Lino, M. M. Carvalho, and P. Valenzuela, "Time-of-use tariff design under uncertainty in price-elasticities of electricity demand: A stochastic optimization approach," *IEEE Trans. Smart Grid*, vol. 4, pp. 2285-2295, Dec. 2013.

[49] B. M. Davis and T. H. Bradley, "The efficacy of electric vehicle time-of-use rates in guiding plug-in hybrid electric vehicle charging behavior," *IEEE Trans. Smart Grid*, vol. 3, pp. 1679-1686, Dec. 2012.

[50] Y. Shoham and K. Leyton-Brown, *Multiagent systems: Algorithmic, game-theoretic, and logical foundations*: Cambridge University Press, 2008.

[51] W. Wei, L. Feng, and M. Shengwei, "Energy Pricing and Dispatch for Smart Grid Retailers Under Demand Response and Market Price Uncertainty," *IEEE Trans. Smart Grid*, vol. 6, pp. 1364-1374, May 2015.

[52] O. Kilkki, A. Alahaivala, and I. Seilonen, "Optimized Control of Price-Based Demand Response With Electric Storage Space Heating," *IEEE Trans. Ind. Informat.*, vol. 11, pp. 281-288, Feb. 2015.

[53] A.-H. Mohsenian-Rad, V. W. Wong, J. Jatskevich, R. Schober, and A. Leon-Garcia, "Autonomous demand-side management based on game-theoretic energy consumption scheduling for the future smart grid," *IEEE Trans. Smart Grid*, vol. 1, pp. 320-331, Dec. 2010.

[54] P. Yang, G. Tang, and A. Nehorai, "A game-theoretic approach for optimal time-of-use electricity pricing," *IEEE Trans. Power Syst.*, vol. 28, pp. 884-892, May 2013.

[55] Z. Baharlouei, M. Hashemi, H. Narimani, and H. Mohsenian-Rad, "Achieving optimality and fairness in autonomous demand response: Benchmarks and billing mechanisms," *IEEE Trans. Smart Grid,* vol. 4, pp. 968-975, May 2013.

[56] H. S. Nwana, "Software agents: An overview," *Knowledge Engineering Review,* vol. 11, pp. 205-244, 1996.

[57] C. Hewitt, "Viewing control structures as patterns of passing messages," *Artificial intelligence,* vol. 8, pp. 323-364, 1977.

[58] M. Wooldridge and N. R. Jennings, "Intelligent agents: Theory and practice," *Knowledge Engineering Review,* vol. 10, pp. 115-152, 1995.

[59] S. Gill and R. Paranjape, "A Review of Recent Contribution in Agent-Based Healthcare Modeling," in *Multi-agent Systems for Healthcare Simulation and Modeling: Applications for System Improvement*, R. Paranjape and A. Sadanand, ed: Information Science Reference-Imprint of: IGI Publishing, 2009, pp. 26-44.

[60] C. Castelfranchi, "Guarantees for autonomy in cognitive agent architecture," *Intelligent Agents,* pp. 56-70, 1995.

[61] M. R. Genesereth and S. P. Ketchpel, "Software agents," *Commun. ACM,* vol. 37, pp. 48-53, 147, 1994.

[62] J. Ferber, "Simulating with reactive agents," *Many Agent Simulation and Artificial Life,* vol. 36, pp. 8-28, 1994.

[63] P. Maes, "Intelligent software," in *Proc. of the 2nd international conference on Intelligent user interfaces, 1997*, pp. 41-43.

[64] L. N. Foner, "What's an agent, anyway? a sociological case study," *FTP Report MIT Media Lab,* vol. 1, 1993.

[65] M. J. Wooldridge, *An introduction to multiagent systems*: Wiley, 2002.

[66] E. Oliveira, K. Fischer, and O. Stepankova, "Multi-agent systems: which research for which applications," *Robotics and Autonomous Systems,* vol. 27, pp. 91-106, 1999.

[67] K. P. Sycara, "Multiagent systems," *AI magazine,* vol. 19, pp. 79, 1998.

[68] S. D. McArthur, *et al.*, "Multi-agent systems for power engineering applications—Part I: Concepts, approaches, and technical challenges," *IEEE Trans. Power Syst.,* vol. 22, pp. 1743-1752, Nov. 2007.

[69] H. S. V. S. Kumar Nunna and S. Doolla, "Energy Management in Microgrids Using Demand Response and Distributed Storage—A Multiagent Approach " *IEEE Trans. Power Delivery,* vol. 28, pp. 939-947, Apr. 2013.

[70] J. Bingnan and F. Yunsi, "Smart Home in Smart Microgrid: A Cost-Effective Energy Ecosystem With Intelligent Hierarchical Agents," *IEEE Trans. Smart Grid,* vol. 6, pp. 3-13, Jan. 2015.

[71] S. Kahrobaee, R. A. Rajabzadeh, L.-K. Soh, and S. Asgarpoor, "A multiagent modeling and investigation of smart homes with power generation, storage, and trading features," *IEEE Trans. Smart Grid,* vol. 4, pp. 659-668, June 2013.

[72] P. Papadopoulos, N. Jenkins, L. M. Cipcigan, I. Grau, and E. Zabala, "Coordination of the charging of electric vehicles using a multi-agent system," *IEEE Trans. Smart Grid*, vol. 4, pp. 1802-1809, Nov. 2013.

[73] E. L. Karfopoulos and N. D. Hatziargyriou, "A multi-agent system for controlled charging of a large population of electric vehicles," *IEEE Trans. Power Syst.*, vol. 28, pp. 1196-1204, May 2013.

[74] C.-X. Dou and B. Liu, "Multi-agent based hierarchical hybrid control for smart microgrid," *IEEE Trans. Smart Grid*, vol. 4, pp. 771-778, June 2013.

[75] Y. S. Foo Eddy, H. Gooi, and S. Chen, "Multi-Agent System for Distributed Management of Microgrids," *IEEE Trans. Power Syst.*, vol. 30, pp. 24-34, Jan. 2015.

[76] H. Nunna and S. Doolla, "Demand Response in Smart Distribution System With Multiple Microgrids," *IEEE Trans. Smart Grid*, vol. 3, pp. 1641-1649, Dec. 2012.

[77] S. Kahrobaee, R. A. Rajabzadeh, L. K. Soh, and S. Asgarpoor, "A Multiagent Modeling and Investigation of Smart Homes With Power Generation, Storage, and Trading Features."

[78] J. Wu, F. Gao, and Z. Kang, "A multi-agent system for households response to dynamic pricing," in *Proc. 2012 Innovative Smart Grid Technologies-Asia (ISGT Asia), 2012 IEEE*, pp. 1-5.

[79] R. Fazal, J. Solanki, and S. K. Solanki, "Demand response using multi-agent system," in *Proc. 2012 North American Power Symposium (NAPS), 2012*, pp. 1-6.

[80] H. Nunna and S. Doolla, "Demand Response in Smart Distribution System With Multiple Microgrids," *IEEE Transactions on Smart Grid,* vol. 3, pp. 1641-1649, 2012.

[81] F. Ren, M. Zhang, and D. Sutanto, "A Multi-Agent Solution to Distribution System Management by Considering Distributed Generators," *IEEE Transactions on Power Systems,* pp. 1-10, 2012.

[82] E. Guerci, M. A. Rastegar, and S. Cincotti, "Agent-based modeling and simulation of competitive wholesale electricity markets," *Handbook of Power Systems II,* pp. 241-286, 2010.

[83] J. Valenzuela, P. R. Thimmapuram, and J. Kim, "Modeling and simulation of consumer response to dynamic pricing with enabled technologies," *Applied Energy,* 2011.

[84] P. R. Thimmapuram, J. Kim, A. Botterud, and Y. Nam, "Modeling and simulation of price elasticity of demand using an agent-based model," in *Proc. 2010 Innovative Smart Grid Technologies (ISGT), 2010,* pp. 1-8.

[85] M. Wooldridge, *An introduction to multiagent systems*: John Wiley & Sons, 2009.

[86] F. Bellifemine, F. Bergenti, G. Caire, and A. Poggi, "JADE—a java agent development framework," in *Multi-Agent Programming,* ed: Springer, 2005, pp. 125-147.

[87] Z. Wang and R. Paranjape, "The self-aware diabetic patient software agent model," *Computers in Biology and Medicine,* vol. 43, pp. 1900-1909, Sep. 2013.

[88] Z. Wang and R. Paranjape, "A Signal Processing Application for Evaluating Self-Monitoring Blood Glucose Strategies in a Software Agent Model," *Computer Methods and Programs in Biomedicine,* vol. 120, pp. 77-87, Jul. 2015.

[89] C. Gibbs, "TEEMA Reference Guide, Version 1.0," 2000.

[90] Z. Wang and R. Paranjape, "An Evaluation of Electric Vehicle Penetration under Demand Response in a Multi-Agent Based Simulation," in *Proc. 2014 IEEE Electrical Power & Energy Conf.*, Calgary, AB, Canada, pp. 1-6.

[91] I. Richardson and M. Thomson. (2010, 20 February). *Domestic electricity demand model - simulation example*. Available: https://dspace.lboro.ac.uk/2134/5786

[92] I. Richardson, M. Thomson, D. Infield, and C. Clifford, "Domestic electricity use: A high-resolution energy demand model," *Energy and Buildings,* vol. 42, pp. 1878-1887, June 2010.

[93] J. Taylor, A. Maitra, M. Alexander, D. Brooks, and M. Duvall, "Evaluations of plug-in electric vehicle distribution system impacts," in *Proc. 2010 IEEE Power Energy Soc. Gen. Meet.*, pp. 1-6.

[94] K. Young, C. Wang, L. Y. Wang, and K. Strunz, "Electric Vehicle Battery Technologies," in *Electric Vehicle Integration into Modern Power Networks*, ed: Springer, 2013, pp. 15-56.

[95] C. Madrid, J. Argueta, and J. Smith, "Performance characterization—1999 Nissan Altra-EV with lithium-ion battery," Sep. 1999.

[96] A. Santos, N. McGuckin, H. Y. Nakamoto, D. Gray, and S. Liss, "Summary of travel trends: 2009 national household travel survey," 2011.

[97] A. Mendoza and J. Argueta, "Performance characterization—GM EV1 Panasonic lead acid battery," *Southern California EDISON*, 2000.

[98] "POWER GENERATION in CANADA," Canadian Electricity Association, Ottawa, Ontario, 2006.

[99] M. Grant and S. Boyd, CVX: Matlab software for disciplined convex programming, version 2.0 beta. http://cvxr.com/cvx, Sep. 2013.

[100] M. Grant and S. Boyd, Graph implementations for nonsmooth convex programs, Recent Advances in Learning and Control (a tribute to M. Vidyasagar), V. Blondel, S. Boyd, and H. Kimura, editors, pages 95-110, Lecture Notes in Control and Information Sciences, Springer, 2008. http://stanford.edu/~boyd/graph_dcp.html.

[101] A. Faruqui and S. Sergici, "Household response to dynamic pricing of electricity: a survey of 15 experiments," *Journal of Regulatory Economics*, vol. 38, pp. 193-225, 2010.